POPX2 phosphatase regulates cell polarity and centrosome placement

Hoon, Jing Ling

2014

Hoon, J. L. (2014). POPX2 phosphatase regulates cell polarity and centrosome placement. Doctoral thesis, Nanyang Technological University, Singapore.

https://hdl.handle.net/10356/62211

https://doi.org/10.32657/10356/62211

POPX2 PHOSPHATASE REGULATES CELL POLARITY AND CENTROSOME PLACEMENT

Hoon Jing Ling
SCHOOL OF BIOLOGICAL SCIENCES
2014

POPX2 PHOSPHATASE REGULATES CELL POLARITY AND CENTROSOME PLACEMENT

HOON JING LING

SCHOOL OF BIOLOGICAL SCIENCES

A thesis submitted to the Nanyang Technological University in partial fulfillment of the requirement for the degree of Doctor of Philosophy

2014

Acknowledgements

First and foremost, I would like to thank my Lord and Savior Jesus Christ for his grace and salvation. He has watched over me and blessed me in many ways, and I wouldn't be where I am today without Him.

I thank God for the wonderful family He has given me. They have done their best to provide me with a good environment to grow up in, and have supported me at each and every step of my life. I sincerely thank them for all the love and care that they have shown me and for all the sacrifices that they have made throughout these years. I'd like to especially thank my husband Lester, for his support and company through good times and bad. His encouragement has always provided me hope and strength, especially in rough times.

I am deeply grateful to my supervisor, Dr Koh Cheng Gee, for her advice and guidance over these past years. I truly appreciate the trust and freedom she has given me in planning my experiments and determining the direction of my project, while providing me with constructive criticism and advice. It was been a wonderful experience working in her lab, and I have learned so much during my time here.

I would also like to extend my thanks to the members of my thesis advisory committee, Dr Thirumaran Thanabalu and Dr Su I-Hsin for all the advice they have given me as I developed my project.

I truly appreciate the friends and mentors I have met in this lab: Yiwen, Elynn, Meihua, Andrew, Anna, Pritpal, Songjing, Sirong, Weng Ting, Ishani, Xue Ling, Kelvin and Soak Kuan. They are the ones that have spent the most time with me as we worked on our projects, and I am thankful for all the things that they have taught me; for the listening ear that they have lent; for their constant encouragement and for all the fun and laughter that we had.

Last but not least, I am grateful for the opportunity and financial support granted to me by Nanyang Technological University to make this PhD study possible.

Table of contents

List of figures

List of tables

Abbreviations

APC	Adenomatous Polypopsis Coli
ATP	Adenosine triphosphate
BSA	Bovine Serum Albumin
CaMKII	Calcium/calmodulin-dependent protein kinase II
Cdc42	Cell division cycle 42
CDK5	Cyclin-dependent kinase 5
C/EBP	CCAAT-enhancer-binding protein
CKII	Casein kinase II
DMEM	Dulbecco's modified Eagle's medium
DTT	Dithiothreitol
EB1	End binding 1
ECM	Extracellular matrix
EDTA	Ethylenediaminetetraacetic acid
EGFR	Epidermal growth factor receptor
FAK	Focal adhesion kinase
FBS	Fetal Bovine Serum
GEF	Guanine nucleotide exchange factor
GFP	Green fluorescent protein
GSK3	Glycogen synthase kinase 3
GST	Glutathion S-transferase
HA	Haemagglutinin
HRP	Horseradish peroxidase
HSF	Heat shock factor
INSR	Insulin receptor
KAP3	Kinesin-associated protein 3
LIC	Light intermediate chain
LPA	Lysophosphatidic acid
MAPK	Mitogen-activated protein kinase
MRCK	Myotonic dystrophy kinase-related CDC42-binding kinase
MZF-1	Myeloid zinc finger 1
PAK	P21-activated kinase
PIX	PAK-interacting exchange protein
PI3K	Phosphoinositide 3-kinase

PKA	Protein kinase A
PKB	Protein kinase B
PKC	Protein kinase C
PLK1	Polo-like kinase 1
POPX	Partner of PIX
RSK	Ribosomal S6 kinase
SRF	Serum response factor
SRY	Sex-determining region Y
VASP	Vasodilator-stimulated phosphoprotein
YY1	Yin Yang 1

Abstract

The wound healing process involves fibroblasts orienting their centrosomes towards the wound edge, such that they are able to migrate into the wound to close it. There are two currently known pathways that regulate centrosome positioning. The first pathway lies under the control of Cdc42, and another pathway involves the localization of N-cadherin to cell-cell contacts as well as the activation of integrin signaling at the leading edge. It is currently unknown whether these pathways function in an independent or cooperative manner. Thus, it is of interest to study how these signaling pathways might function to regulate centrosome positioning, as well as identify other proteins that might regulate these pathways to control the position of the centrosome.

In this study, we investigated how centrosome orientation is regulated in mouse fibroblasts, NIH3T3 cells, and have identified a serine-threonine phosphatase, POPX2, as a regulator of centrosome orientation. By measuring the positions of the centrosome and nucleus, we show that POPX2 negatively regulates multiple proteins that control centrosome positioning to inhibit centrosome centration, but not rearward nuclear movement. N-cadherin localization to cell-cell junctions is required for proper centrosome orientation. We observed that high POPX2 expression results in a reduced peripheral N-cadherin localization using immunofluorescence staining, and this is due to the inhibition of Kinesin-2 motor motility by POPX2. Consequently, this perturbs the localization of focal adhesions as well as Cdc42-Par6/PKCζ signaling, thus impairing proper centrosome orientation. Microtubule-based motors also play an important role in centrosome orientation by generating a force along the microtubules to position the centrosome, and this is perturbed in cells overexpressing POPX2. Overexpression of POPX2 results in reduced peripheral Par3 localization and reduced expression of LIC2 (cytoplasmic dynein 1 light intermediate chain 2), resulting in defects in microtubule tethering and perturbations in microtubule dynamics at cell-cell contacts. We thus propose that POPX2 modulates the position of centrosomes during wound healing by acting as an integrator and regulator of multiple signaling pathways.

1. Introduction

1.1 Cell polarity

The control of cell polarity is crucial in multiple cellular processes including cell division, differentiation and migration. Migratory polarization is induced when confluent cell monolayers are scratch-wounded, and this results in the repositioning of cellular structures such as the centrosome, Golgi apparatus and microtubules towards the wound edge (Etienne-Manneville and Hall, 2001; Gomes et al., 2005; Ridley et al., 2003).

1.1.1 The migration cycle

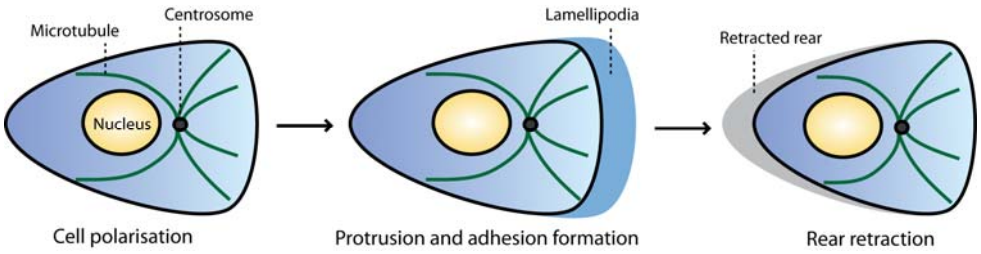

Figure 1. Steps involved in the cell migration cycle

Cell migration first begins with polarization of the cell. During cell polarization, the centrosome and Golgi apparatus reorient themselves towards the region that later forms the leading edge, while the nucleus remains towards the rear of the cell. Actin polymerization is also induced at the cell front, resulting in the formation of the lamellipodia. Adhesions are formed at the lamellipodia, allowing the cell to adhere to the extracellular matrix. As the cell translocates, adhesions at the rear of the cell disassemble and the rear retracts, allowing the cell to move forward.

There are many proteins and signaling pathways that are involved in cell migration. In response to migration-promoting agents, Cdc42 is activated at the region that will form the cell front. In cells such as fibroblasts, the centrosome reorients itself such that it lies between the leading edge and the nucleus, establishing cell polarity. Rac activation then occurs at the cell front, as a result of the activation of Rac guanine nucleotide exchange

factors (GEFs) by Phosphoinositide 3-kinases (PI3Ks) produced upon Cdc42 activation. This results in the formation of protrusions such as lamellipodia, which are stabilized by adhering to the extracellular matrix. As the cell moves over these adhesions, adhesions that have moved to the rear of the cell are disassembled as a result of Rho activity, and the rear retracts (Figure 1) (Raftopoulou and Hall, 2004; Ridley et al., 2003).

1.1.2 Centrosome positioning

The position of the centrosome plays a critical role in determining the direction of migration in cells such as fibroblasts and astrocytes. When cells are scratch-wounded, the nucleus moves towards the rear of the cell while the centrosome remains at the cell centroid, lying between the nucleus and the leading edge. Centrosome positioning is controlled by multiple pathways, and involves microtubules, Cdc42 signaling, Kinesin-2 transport and dynein activity (Dupin et al., 2009; Etienne-Manneville and Hall, 2001; Gomes et al., 2005; Laan et al., 2012; Schmoranzer et al., 2009).

1.1.3 Cdc42 signaling

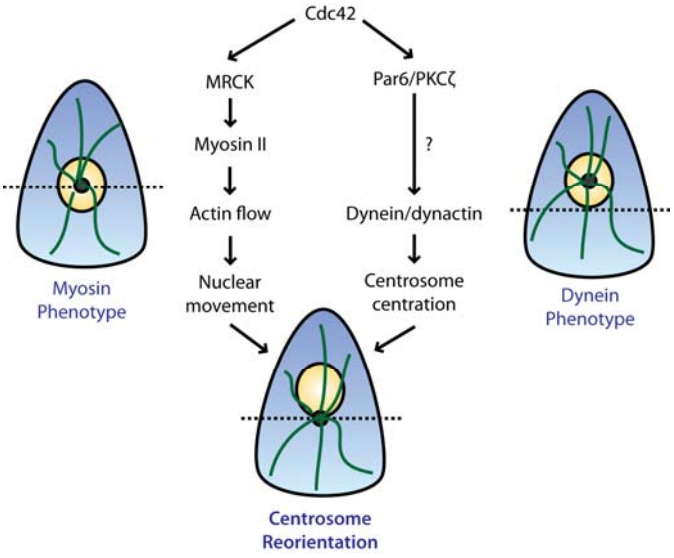

Figure 2. Cdc42-regulated pathways leading to centrosome reorientation
Cdc42 controls nuclear movement through MRCK and centrosome centration through Par6 and PKCζ. Dotted lines denote the approximate position of the cell center.

It is well-established that Cdc42 signaling regulates the process of centrosome orientation, and this is occurs through two different pathways, one controlling nuclear movement and the other controlling centrosome centration (Figure 2). Cdc42 acts through MRCK, which then activates myosin II by phosphorylating myosin light chain on Serine 19 (Leung et al., 1998). This triggers retrograde actin flow, which moves the nucleus rearward. Centrosome centration is controlled by Cdc42 activation of the Par6/PKCζ complex, which acts through the dynein/dynactin complex to position the centrosome (Etienne-Manneville and Hall, 2001; Gomes et al., 2005; Palazzo et al., 2001; Tzima et al., 2003).

The signaling pathway controlling centrosome centration is slightly different between fibroblasts and astrocytes. In astrocytes, Cdc42 activation at the leading edge results in the localized activation of Par6 and PKCζ. The active Par6/PKCζ complex then directly interacts with GSK3β and phosphorylates it on serine 9, leading to its inactivation. As a result, Adenomatous Polyposis Coli (APC) remains unphosphorylated, allowing it to interact with the plus ends of microtubules. APC can interact with the microtubule plus ends directly, or through binding to EB1, which interacts with the dynein-dynectin complex that is associated with microtubules. GSK3β plays an important role in centrosome positioning in astrocytes, as the phosphorylation status of the kinase directly influences its association with PKCζ, thus affecting signaling downstream through APC (Etienne-Manneville and Hall, 2003a; Iden and Collard, 2008).

In fibroblasts, however, while Cdc42 activation still leads to the localized activation of Par6 and PKCζ, GSK3β and APC do not appear to be directly involved (Eng et al., 2006; Wen et al., 2004). Both overexpression and inhibition of GSK3β do not affect centrosome positioning (Eng et al., 2006); Similarly, overexpression of APC does not affect the orientation process (Wen et al., 2004). Instead, both proteins appear to control microtubule stabilization in fibroblasts (Eng et al., 2006). Signaling downstream of GSK3β and APC is conserved however, with the stabilization of microtubule plus ends and the dynein-dynactin complex being required for centrosome orientation (Gomes et al., 2005; Schmoranzer et al., 2009).

1.1.4 Activation of Cdc42 signaling through N-cadherin and focal adhesions

Cdc42 signaling can be activated extracellularly through the addition of drugs such as lysophosphatidic acid (LPA), or intracellularly through various signaling pathways. One such pathway involves the localized activation of integrins, which is indirectly controlled by the localization of N-cadherin (Dupin et al., 2009; Osmani et al., 2010).

1.1.4.1 Structure and functions of N-cadherin

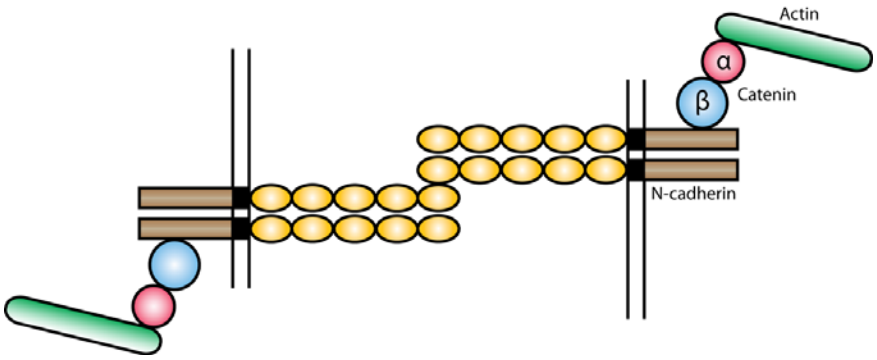

Figure 3. Architecture of adherens junction in fibroblasts
N-cadherin forms lateral homodimers, which interact with homodimers from neighbouring cells through the EC1 domain. N-cadherin links to the actin cytoskeleton through α-catenin and β-catenin.

N-cadherin belongs to the family of classical cadherins. It is a single-pass transmembrane glycoprotein that has an N-terminal extracellular domain, a transmembrane domain and a C-terminal cytoplasmic tail. The extracellular domain has 5 calcium-binding EC-repeats (Grunwald et al., 1982; Halbleib and Nelson, 2006; Hatta and Takeichi, 1986). The first extracellular domain, EC1, is required for homophilic adhesion in a calcium-dependent manner (Chen et al., 2005; Nose et al., 1988; Patel et al., 2006). The cytoplasmic domain binds several proteins, one of which is β-catenin. β-catenin, together with α-catenin, links N-cadherin homodimers to the actin cytoskeleton to form the adherens junction (Figure 3) (Halbleib and Nelson, 2006; Yap et al., 1997).

The adherens junctions serve as principal mediators of cell-cell adhesion, which stimulate cues that control multiple cellular functions such as cell survival, cell fate, migration and cell polarity (Gumbiner, 1996; Takeichi, 1991). Loss of cell-cell adhesion favors cell migration, giving rise to a more motile and invasive phenotype characteristic of cancer cells (Tamura et al., 1998; Teng et al., 2005).

1.1.4.2 Focal adhesions

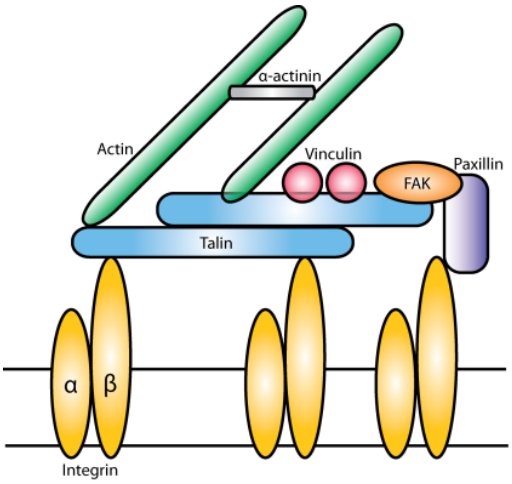

Figure 4. Schematic diagram of a focal adhesion complex.
The α/β integrin complex links the ECM to the cytoskeleton-signalling network. This is achieved through the interaction between the cytoplasmic tails of integrin with talin, which in turn interacts with actin.

The focal adhesion complex is a specialized attachment site where the cell contacts the extracellular matrix (ECM). Integrins are the major components in focal adhesions. There are 18 known α subunits and 8 β subunits, which combine to give 24 different adhesion receptors. The extracellular domains of these subunits recognize ECM proteins or other receptors, while the cytoplamic tails interact with the cytoskeleton-signalling network. The focal adhesion complex consists of many proteins. These include structural proteins such as filamin, α-actinin and vinculin, as well as regulatory proteins such as VASP, paxillin and FAK. The regulatory proteins function to control actin dynamics, serve as adaptor proteins or regulate integrin-mediated signaling (Figure 4) (Petit and Thiery, 2000).

Since focal adhesions are found at the end of actin stress fibers and link the cytoskeletal network to the ECM, they serve as mechanosensors to transmit forces generated by the ECM to the cytoskeletal network and vice versa. The amount of force sensed affects focal adhesion assembly and turnover, which involves structural rearrangement of the complex and affects downstream signaling pathways. This in turn affects cellular responses such as directional movement, cell growth, differentiation and survival (Legate et al., 2009; Wang and Suo, 2005; Zaidel-Bar et al., 2004). In stationary cells, focal adhesions form at the periphery and move inwards due to the contraction of associated actin fibers. On the other

hand, focal adhesions form at the leading edge of migrating cells and remain stationary as the cell migrates over them (Smilenov et al., 1999).

1.1.4.3 N-cadherin and focal adhesions in centrosome positioning

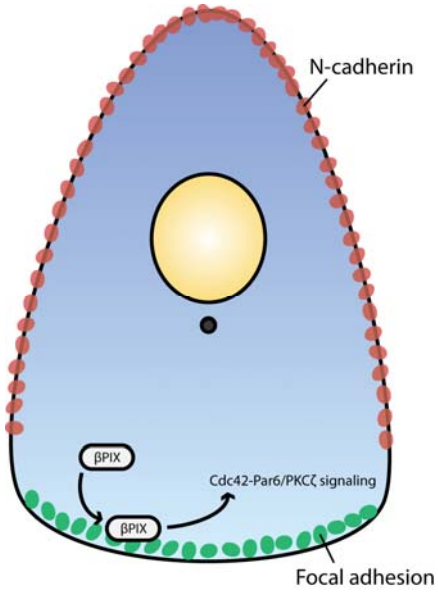

Figure 5. Spatial segregation of N-cadherin and focal adhesions is required for centrosome positioning.
N-cadherin localizes in a mutually exclusive manner with focal adhesions. N-cadherin localizes to cell-cell contacts while focal adhesions are found at the free edge. Focal adhesions are able to recruit βPIX, resulting the activation of Cdc42-Par6/PKCζ signaling, which plays a role in centrosome positioning.

Other than its well-characterized function in cell-cell adhesion, N-cadherin has recently been shown to regulate centrosome positioning. N-cadherin localizes to cell-cell contacts, and the centrosome positions itself away from these structures. Altering the geometry of N-cadherin-mediated interactions (or E-cadhein-mediated interactions in cells lacking N-cadherin) in turn alters the orientation of the centrosome-nucleus axis (Desai et al., 2009; Dupin et al., 2009). Primary rat astrocytes involved in intracellular interactions have been shown to preferentially position their centrosome in front of the nucleus and facing the free edge of the cell. On the other hand, both isolated cells and cells that were entirely surrounded and had no free edge had a randomly oriented nuclear-centrosome axis. Reduction of N-cadherin expression, or removal of calcium, which disrupts the adherens junctions, also results in a randomly orientated centrosome-nucleus axis (Dupin et al.,

2009). This demonstrates the requirement for an asymmetrical distribution of N-caherin for proper centrosome placement. A similar study carried out using kidney epithelial cells also demonstrated that N-cadherin is required for proper centrosome orientation. Cells lining a scrape wound were shown to orient their centrosomes such that they faced the wound edge, while removal of calcium from the cell culture media disrupted proper centrosome orientation (Desai et al., 2009). N-cadherin has been proposed to influence the direction of the nuclear-centrosome axis in a manner dependent on the actin cytoskeleton and Cdc42 signaling, while the microtubule network plays a role in positioning the centrosome (Desai et al., 2009; Dupin et al., 2009).

Spatial segregation occurs between cell-cell adhesions mediated through cadherins and cell-matrix adhesions mediated through focal adhesions as a result of negative feedback (Burute and Thery, 2012). Thus, in scratch-wounded monolayers, focal adhesions are restricted largely to the free edge of the cell. Focal adhesion complexes contain integrin, which activate Src-like kinase and recruit Scrib to the leading edge. Scrib recruits βPIX, which is phosphorylated by Src-like kinase. This promotes its GEF activity towards Cdc42, thus activating Cdc42 signaling at the leading edge (Figure 5) (Osmani et al., 2010; Osmani et al., 2006).

The asymmetrical distribution of N-cadherin and focal adhesions in scratch-wounded monolayers also influences directional cell migration. Adhesions and protrusions have been observed to form at the free edge of scratch-wounded monolayers (Desai et al., 2009; Dupin et al., 2009), and this indicates the direction of cell migration (Raftopoulou and Hall, 2004; Ridley et al., 2003). Analysis of ruffling activity in scratch-wounded kidney epithelial cells has demonstrated that membrane ruffling could be detected the free edge of the cell that is distal to cell-cell contacts, thus “priming” the cells to move away from these contacts and into the wound (Desai et al., 2009).

1.1.5 Kinesin-2-mediated transport

The kinesin-2 family consists of KIF3A, KIF3B, KIF3C and KIF17. KIF17 functions as a homodimer (Setou et al., 2000), while KIF3A functions as a heterodimeric complex containing either KIF3B or KIF3C and a non-motor subunit, KAP3 (Muresan et al., 1998; Yamazaki et al., 1995).

1.1.5.1 Structure and functions of the KIF3 heterotrimeric motor

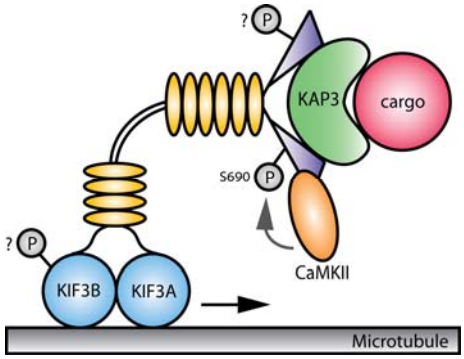

Figure 6. Schematic diagram of the KIF3 heterotrimeric motor
The heterodimer consisting of KIF3A and KIF3B interacts with KAP3, which is involved in cargo binding.

The KIF3 heterotrimeric motor has two globular motor domains formed by the N-termini of KIF3A and KIF3B. The stalk region is formed by dimerisation of KIF3A and KIF3B, and the C-termini of the heterodimer interact with KAP3 to form a heterotrimer (Figure 6) (Hoeng et al., 2008; Rashid et al., 1995). A putative hinge region has been predicted in the KIF3 heterotrimeric motor (Lupas et al., 1991), suggesting that folding may occur. This is supported by the experimental observation of both folded and extended forms of KIF3 (Wedaman et al., 1996). Other than these preliminary observations however, not much is known about how conformational changes occur within the motor and these different physiological states affect the motor and its functions.

The KIF3 motor transports organelles, viruses, RNA, as well as proteins within the cell. Proper intracellular transport is crucial for processes such as mitosis and cytokinesis, cell polarization, cell-cell adhesion and development (Scholey, 2013).

1.1.5.2 Cargoes of the KIF3 heterotrimeric motor

The KIF3 heterotrimeric motor transports many intracellular cargoes, which are listed in Table 1. Amongst the many proteins transported by the KIF3 motor, N-cadherin and Par3 are of particular interest in this study. N-cadherin forms a complex with the KIF3 motor complex, which allows it to be transported from the Golgi to the cell periphery (Teng et al., 2005), where it functions in cell-cell adhesion. The cell polarity protein Par3 interacts directly with the C-terminus of KIF3A, allowing for accumulation of Par3 in axon tips and the establishment of neuronal polarity (Nishimura et al., 2004). Par3 is also known to exist in a complex together with Par6 and aPKC, and controls epithelial cell polarity by regulating tight junction formation (Etienne-Manneville and Hall, 2003b; Yamanaka et al., 2001).

Cargo	Cargo type	Light chain involvement	Adaptor or scaffold proteins	Reference
APC	Vesicles	KAP3	Unknown	(Shi et al., 2004)
aPKC	Intraflagellar transport complex	KAP3	Unknown	(Cole et al., 1998; Ou et al., 2005)
β-catenin	Vesicles	KAP3	Unknown	(Teng et al., 2005)
Complex A	Intraflagellar transport complex	KAP3	Unknown	(Cole et al., 1998; Ou et al., 2005)
Crumbs 3	Intraflagellar transport complex	KAP3	Unknown	(Cole et al., 1998; Ou et al., 2005)
KDEL receptor	Golgi-ER vesicles	KAP3	Unknown	(Stauber et al., 2006)
N-cadherin	Vesicles	KAP3	Unknown	(Teng et al., 2005)
Par3	Vesicles	KAP3	Unknown	(Nishimura et al., 2004)
Par6	Intraflagellar transport complex	KAP3	Unknown	(Cole et al., 1998; Ou et al., 2005)
Rab4	Early and late endosomes	Unknown	Unknown	(Imamura et al., 2003)
Rab7	Early and late endosomes	Unknown	Unknown	(Bananis et al., 2004)
Rab11	Recycling endosomes	Unknown	RIP11	(Schonteich et al., 2008)
Unknown	Vesicles	KAP3	Fondrin	(Takeda et al., 2000)

Table 1. Cargo complexes transported by the Kinesin-2 motor complex

1.1.6 Physical forces acting on microtubules through dynein

1.1.6.1 Cytoplasmic dynein complex

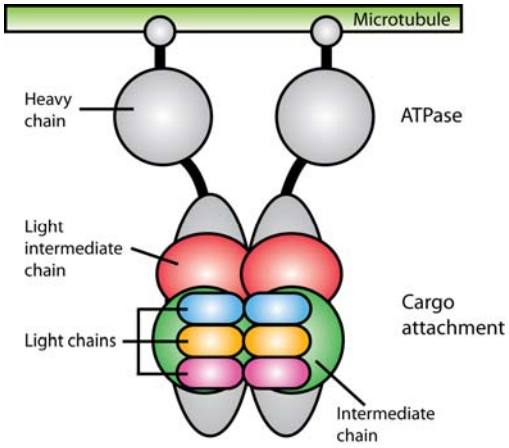

Figure 7. Schematic diagram of the cytoplasmic dynein complex
The cytoplasmic dynein complex consists of 2 heavy chains, 2 light intermediate chains, 2 light chains and 2 intermediate chains. The heavy chains contain the ATPase domain and the light intermediate chains, light chains and intermediate chains function in cargo attachment.

Cytoplasmic dynein is a minus-end directed motor protein (Paschal and Vallee, 1987). It consists of two subclasses: Dynein-1 and Dynein-2. Dynein-1 is found in all cells containing microtubules while Dynein-2 is found within and around the base of cilia and flagella (Höök and Vallee, 2006; Mikami et al., 2002). The dynein complex consists of two identical heavy chains, two intermediate chains, two light intermediate chains and several light chains (Figure 7). Reconstitution experiments have shown that the dynein heavy chain itself is mostly insoluble, and appears as aggregates. Addition of other subunits that are associated with the heavy chain, such as the intermediate and light intermediate chains, increase the solubility of the resulting complex. Reconstitution experiments carried out in the presence of the dynein light intermediate chains give rise to soluble dynein complexes where the dynein heavy chains exist as homodimers. This indicates that the subunits that are associated with the heavy chain are necessary and sufficient for correct complex formation. The light intermediate chains are the most structurally important, followed by the intermediate chains and light chains, as both the light intermediate chains and intermediate chains are required for full solubility of the dynein complex. The light chains are essential for complete folding to occur (Trokter et al., 2012). The cytoplasmic dynein complex is activated by binding to Dynactin, which functions to target the dynein complex to specific cellular

locations, link dynein to its cargo and increase the processivity of the motor. The dynein complex can also interact with other cofactors such as LIS1, NUDE and NUDEL, which regulate dynein function and localization (Kardon and Vale, 2009).

1.1.6.2 Cytoplasmic dynein heavy chain

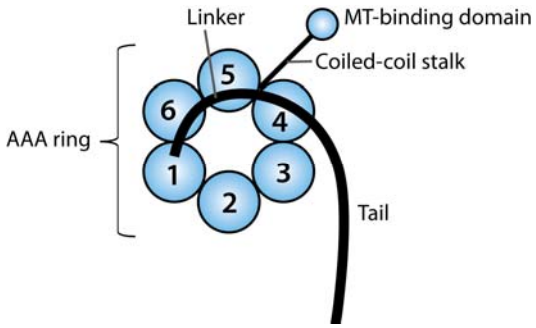

Figure 8. Schematic diagram of the cytoplasmic dynein heavy chain
The motor domain consists of 6 AAA ATPase domains arranged in a ring. The microtubule binding stalk projects from the AAA ring. The N-terminal tail is required for heavy chain dimerisation and also contains binding sites for the intermediate and light intermediate chains.

The cytoplasmic dynein heavy chain (*dync1h1*), which has a molecular weight of about 500kDa and exists as a homodimer, is the largest subunit of the dynein complex. Its main function is to generate mechanical force through ATP hydrolysis, and this is achieved through the AAA+ ATPase-like domains found within the C-terminal motor domain of the heavy chain. The heavy chain also contains a microtubule binding domain at the tip of an antiparallel coiled coil structure known as the stalk, whose affinity for microtubules changes depending on the ATP cycle (Carter et al., 2011; Höök and Vallee, 2006).

The heavy chain also contains a linker domain which stretches across the ring of AAA domains. The position of the linker changes as the motor domain is in different nucleotide states, and influences the powerstroke that generates motility (Burgess et al., 2003). Lastly, the N-terminal region of the heavy chain forms the tail, which is responsible for binding to other subunits (Figure 8) (Höök and Vallee, 2006).

1.1.6.3 Cytoplasmic dynein intermediate chains

The dynein intermediate chains are encoded by 2 genes in vertebrates (*dync1i1*, *dync1i2*). They have a molecular weight of approximately 74kDa and exist as dimers (Paschal and Vallee, 1987). The intermediate chains serve as an "interaction hub", as they are able to associate with the heavy chain, light chains as well as adaptor complexes. Multiple isoforms of intermediate chain 1 exist in mammals as a result of alternative splicing and phosphorylation (Dillman and Pfister, 1994; Pfister et al., 2006), and this gives rise to specificity in cargo binding and allows for regulation of cargo transport.

1.1.6.4 Cytoplasmic dynein light intermediate chains

There are 2 light intermediate chains (LICs) that interact with Cytoplasmic dynein 1 – LIC1 and LIC2 – and they are encoded by the *dync1li1* and *dync1li2* genes respectively. LIC1 and LIC2 share 65% similarity, and both contain an evolutionarily conserved P-loop region. Even though the P-loop shares homology with ATPase active ABC transporters and often indicates the presence of ATPase activity, it does not appear to be functional in the LICs. The LICs bind to amino acids 649-800 of the heavy chain in a mutually exclusive manner, creating 2 different subgroups of Cytoplasmic dynein (Tynan et al., 2000a) with different functions. LIC1 interacts with proteins such as pericentrin (Tynan et al., 2000b), Rab4a (Bielli et al., 2001) and FIB3 (Horgan et al., 2010) and functions in slow anterograde axonal transport (Susalka and Pfister, 2000) and Golgi and ER-to-Golgi trafficking (Palmer et al., 2009). LIC2, on the other hand, interacts with Par3 (Schmoranzer et al., 2009) and FIP3 (Horgan et al., 2010), and functions in both fast and slow anterograde axonal transport (Susalka and Pfister, 2000), endosomal trafficking (Palmer et al., 2009) and centrosome positioning (Schmoranzer et al., 2009).

1.1.6.5 Cytoplasmic dynein light chains

The cytoplasmic dynein 1 complex also contains 3 classes of light chains - TcTex, Roadblock, and LC8 - with two known isoforms for each class. They have a molecular weight of about 8kDa, and are incorporated into the dyenin complex through interaction with the intermediate chains. The light chains are thought to have a potential role in cargo binding. Additionally, some of the light chains have functions independent of their roles in the dynein complex (Pfister et al., 2006).

1.1.6.6 Centrosome positioning by dynein

The cytoplasmic dynein 1 complex has multiple functions in cells, one of which is centrosome positioning. Multiple experiments have shown that loss of dynein or inhibition of its motor activity results in centrosome off-centering, demonstrating the importance of dynein in the regulation of centrosome position (Gomes et al., 2005; Palazzo et al., 2001).

There are 2 models that predict how the centrosome can be positioned by dynein in stationary interphase cells. In the first model, dynein interacts with the tips of microtubules at the plus ends, thus giving rise to a relatively constant force per microtubule. In the second model, microtubules interact with cortical dynein along their length. This gives rise to a force that is proportional to the length of the microtubule (Vallee and Stehman, 2005).

The cytoplasmic dynein complex has been shown to accumulate at the leading edge of migrating cells (Dujardin et al., 2003; Levy and Holzbaur, 2008), and two other models have been proposed to explain how the centrosome is positioned in migrating cells. The first model suggests that passive redistribution of dynein occurs as the cell migrates. Dynein could be removed from cortical sites by moving along microtubules, but as the lamellipodium extends, microtubules become unable to reach the leading edge as a result of increased actin growth and/or rearward actomyosin forces. This disrupts dynein transport from the cortex, leading to their accumulation along the leading edge. As microtubules grow and reach the leading edge however, cortical dynein is now able to interact with these microtubules, pulling on them to center the centrosome. The second model, on the other hand, suggests that dynein is actively redistributed in migrating cells. Dynein accumulates at

the leading edge through an unknown mechanism, pulling on the microtubules to position the centrosome (Vallee and Stehman, 2005).

Dynein found at the cell cortex, also known as cortical dynein, has been shown to associate with Par3 through LIC2 (Schmoranzer et al., 2009). This interaction tethers microtubules to the cell cortex and generates a pulling force on the microtubules that helps to position the centrosome at the cell centroid (Laan et al., 2012; Schmoranzer et al., 2009).

1.2 POPX2

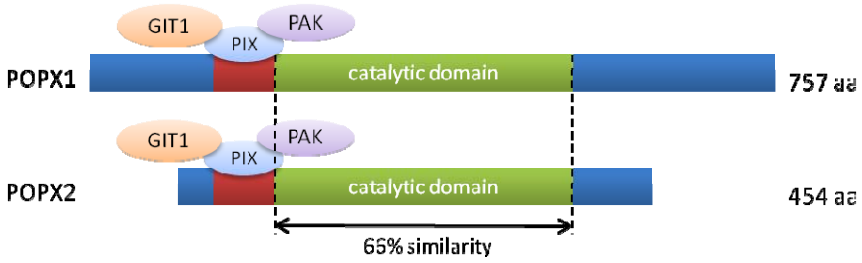

Figure 9. Domain architectures of POPX1/2 and their binding partners
Both proteins contain a core catalytic domain in the middle, flanked by other amino acid residues at the N- and C- termini. PIX binds to a region near the N-terminus of POPX1/2.

POPX1 and 2 are serine/threonine phosphatases that belong to the PP2C family. POPX1 is longer, and is expressed mainly in the brain, while POPX2 is ubiquitously expressed. POPX1 and 2 were identified as binding partners of PIX, and are known to form trimeric complexes with PIX and PAK1 (Figure 9). Within this complex, POPX is able to dephosphorylate PAK1 on T422, and other PAK auto-phosphorylated serines and threonines thus inactivating the kinase (Koh et al., 2002). This blocks the phenotypic effects of active PAK, preventing the loss of stress fibers and other morphological changes that occur as a result of PAK activation.

POPX2 is also known as PPM1F, Ca^{2+}/Calmodulin-dependent protein kinase II phosphatase (CaMKII phosphatase) and hFEM-2 (Koh et al., 2002). POPX2 is able to interact with CaMKII, and dephosphorylates it on Threonine 286. Threonine 286 is autophosphorylated in CaMKII, which activates it, and thus dephosphorylation by POPX2 inactivates CaMKII (Harvey et al., 2004). The phosphatase is implicated in stress fibre formation, serum response factor (SRF)-mediated transcription, apoptosis, dorsal ruffling, cell migration and intracellular transport (Harvey et al., 2004; Koh et al., 2002; Singh et al., 2011; Susila et al., 2010; Xie et al., 2008; Zhang et al., 2013).

POPX2 affects SRF-mediated transcription though its interaction with mDia1. SRF-mediated transcription is regulated by the ratio of monomeric G-actin to F-actin in cells; a high level of G-actin inhibits transcription from the SRE while a high level of F-actin promotes it. G-actin inhibits transcription from the SRE by binding to MalA, a transcriptional co-activator of SRF, and inhibiting it (Sotiropoulos et al., 1999). When RhoA is activated and binds to mDia1,

mDia1 is relieved from its autoinhibited state and is able to initiate actin nucleation and polymerization (Watanabe et al., 1997). This decreases the level of G-actin in the cell, thus initiating SRF-dependent transcription (Geneste et al., 2002; Tominaga et al., 2000). Binding of POPX2 to mDia1 inhibits SRF-dependent transcription in a manner independent of the phosphatase activity of POPX2 (Xie et al., 2008).

POPX2 has also been implicated in the regulation of cell motility in fibroblasts and cancer cells. NIH3T3 fibroblasts overexpressing POPX2 migrate at higher speeds as compared to control fibroblasts (Singh et al., 2011), while silencing of POPX2 in MDA-MB-231 breast cancer cells reduced their motility (Zhang et al., 2013). Identification of signaling pathways controlling cell motility that are perturbed in POPX2-overexpressing or silenced cells revealed that pathways involving MAP kinase (MAPK1/3) and glycogen synthase kinase 3 (GSK3α/β) are perturbed when there are changes in POPX2 levels. An increase in POPX2 expression in NIH3T3 cells appears to be correlated with an increase in GSK3 α and β phosphorylation on serine-21 and serine-9 respectively, which results in the inactivation of GSK3 (Singh et al., 2011). A high level of POPX2 is also correlated with an increased level of phosphorylation on MAPK1/3, which is known to promote cell migration (Singh et al., 2011; Zhang et al., 2013).

More recently, POPX2 has been shown to regulate Kinesin-2-mediated transport by affecting the phosphorylation status of KIF3A. A high level of POPX2 is correlated with a reduced phosphorylation on serine-690 of KIF3A, and this is due to both a direct dephosphorylation of KIF3A by POPX2 and the indirect effect of POPX2's activity on CaMKII . CaMKII is the kinase that phosphorylates KIF3A on serine-690. POPX2 interacts with CaMKII and dephosphorylates it on threonine 286. This inhibits the kinase activity of CaMKII, thus precluding phosphorylation of serine-690 of KIF3A. Loss of KIF3A phosphorylation on this residue results in a decrease in KIF3A motility and a reduction in Kinesin-2-mediated motor transport (Phang et al., 2014).

Overexpression of POPX2 also inhibits proper centrosome orientation post-wounding; however, how POPX2 affects this process is unknown. The aim of this work is to elucidate the pathway(s) that POPX2 acts on to inhibit proper centrosome positioning in response to scratch wounding.

1.3 Aim

A number of proteins have been identified to function in centrosome positioning in response to wound healing in recent years, and the identification of these proteins have led to the establishment of multiple signaling pathways that play a role in this process (see page 2 for details). However, it is not known whether these signaling pathways function independently or cooperatively, or whether they complement each other in the regulation of centrosome positioning. Preliminary experiments carried out by our group have shown that upon scratch wounding, cells overexpressing POPX2 are unable to migrate straight into the wound, and show defects in centrosome positioning, thus implicating POPX2 in the regulation of this process.

In this project, we aim to identify the role of POPX2 in centrosome positioning. POPX2 has previously been implicated in the regulation of KIF3A phosphorylation. KIF3A is a component of the Kinesin-2 motor, which is responsible for transporting N-cadherin, a protein that plays a role in the control of centrosome positioning. Thus, POPX2 could potentially regulate centrosome positioning through its effects on N-cadherin transport. Forces acting on the centrosome through microtubules are also known to play a role in centrosome positioning, and we would also like to investigate whether POPX2 could affect this process as well.

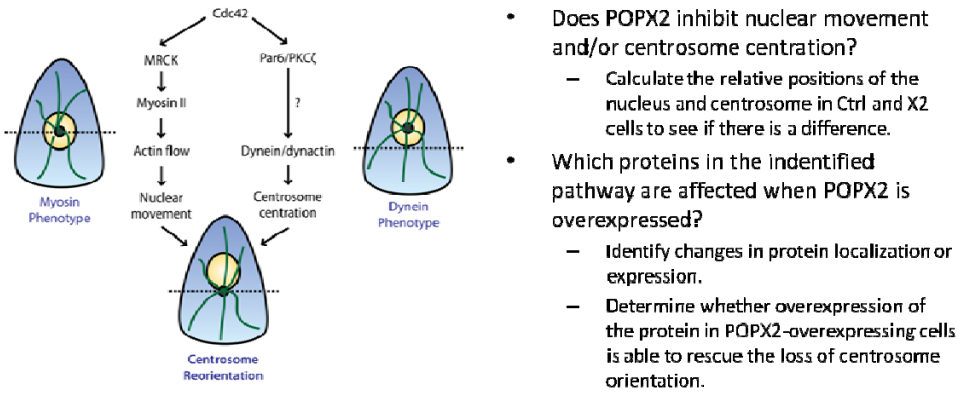

Figure 10. Brief description of the workflow used in investigating the role of POPX2 in centrosome positioning.

Specifically, we aim to:

1. Confirm that transport of N-cadherin and Par3, cargoes of the Kinesin-2 motor that are known to play a role in centrosome positioning, is impaired in POPX2-overexpressing cells.
2. Determine whether POPX2 regulates the two pathways controlling centrosome orientation separately or collectively.
3. Determine whether POPX2 inhibits proper centrosome positioning by inhibiting nuclear movement and/or inhibiting centrosome centration.
4. Determine whether POPX2 can also regulate centrosome positioning by affecting proteins that are involved in force generation, by specifically looking at proteins involved in anchoring microtubules to the cell cortex.

2. Materials and methods

2.1 Materials

2.1.1 General reagents

All chemicals and reagents used were purchased from the following companies:

Buffers and salts	Sigma-Aldrich (St. Louis, MO, USA)
	Merck (Darmstadt, Germany)
	USB (Sampscott, MA, USA)
	Bio-Rad (Hercules, CA, USA)
Restriction endonucleases, enzymes and protein markers	New England Biolabs (Ipswich, MA, USA)
	Takara Bio Inc. (Shiga, Japan)
	Fermentas (Burlington, CA, USA)
Cell culture and transfection reagents	Sigma-Aldrich (St. Louis, MO, USA)
	Gibco (Grand Island, NY, USA)
	PAA Laboratories (Buckinghamshire, UK)
	Invitrogen (Carlsbad, CA, USA)
SDS-PAGE and Western Blot reagents	Sigma-Aldrich (St. Louis, MO, USA)
	Bio-Rad (Hercules, CA, USA)

2.1.2 Commercial kits

QIAquick® Gel Extraction Kit	Qiagen (Valencia, CA, USA)
QIAquick® PCR Purification Kit	
QIAquick® Spin Maxiprep Kit	
RNeasy Mini Kit	
AxyPrep Plasmid Miniprep Kit	Axygen (Union City, CA, USA)
SuperScript® *VILO*™ *cDNA* Synthesis Kit	Life Technologies (Carlsbad, CA, USA)
QuikChange Site-Directed Mutagenesis Kit	Stratagene (La Jolla, CA, USA)
Amersham ECL Plus	GE healthcare (Buckinghamshire, UK)

2.1.3 Media

LB medium	1% (w/v) Bacto-tryptone, 0.5% (w/v) yeast extract, 1% (w/v) NaCl
LB agar	LB medium plus 1.5% (w/v) bacto-agar
Ampicillin broth	LB medium containing 60 µg/mL ampicillin
Ampicillin plate	LB agar plate containing 60 µg/mL ampicillin
Kanamycin broth	LB medium containing 30 µg/mL kanamycin
Kanamycin plate	LB agar plate containing 30 µg/mL kanamycin
Cell culture media	Dulbecco's Modified Eagle's Medium with 4500mg/L glucose
Cell freezing medium	10% (v/v) DMSO in FBS

2.1.4 Buffers

GST purification buffer	376ml PBS
	20ml 1M Tris pH8
	4ml 10% Triton-X
	0.2ml 1M $MgCl_2$
TAE buffer, 50×	24.2g Tris base
	57.1ml acetic acid
	100ml 0.5M EDTA, pH8
	Top up to 1L with water
Mammalian cell lysis buffer	10ml 1M Hepes, pH7.5
	24ml 5M NaCl
	400µl 1M $MgCl_2$
	0.8ml 0.5M EGTA
	8ml 1M β-glycerol phosphate
	4ml 0.1M sodium orthovanadate
	8ml 0.5M sodium fluoride
	2ml glycerol (neat)
	10ml 20% Triton-X
	Top up to 400ml with water
	Add 1× protease inhibitor and 1× DTT before use
SDS-PAGE running buffer, 10×	30.2g Tris base
	144g glycine
	10g SDS

	1000ml water
PBS (phosphate buffered saline), 10×	80g NaCl
	2g KCl
	14.4g Na_2HPO_4
	2.4 g KH_2PO_4
	1L water, pH 7.4
TBS, 10×	24.2g Tris base
	80g NaCl
	1L water, pH 7.6
Nitrocellulose transfer buffer, 10×	30.3g Tris base
	144g glycine
	1L water
Nitrocellulose transfer buffer, 1×	50ml 10× nitrocellulose transfer buffer
	50ml methanol
	400ml water

2.1.5 Bacterial strains and mammalian cell lines

DH5α	Chemically competent bacterial strain	Invitrogen
COS-7	African green monkey kidney fibroblast	ATCC-CRL-1651
NIH3T3	Mouse embryonic fibroblast	ATCC-CRL-1658
NIH3T3-GFP	Stable line overexpressing GFP. Puromycin resistant.	
NIH3T3-POPX2	Stable line overexpressing GFP-POPX2. Puromycin resistant.	
NIH3T3-POPX2m	Stable line overexpressing GFP-POPX2m. Puromycin resistant.	
NIH3T3-KIF3A	Stable line overexpressing GFP-KIF3A. Puromycin resistant.	
NIH3T3-KIF3A S690A	Stable line overexpressing GFP-KIF3A S690A. Puromycin resistant.	
NIH3T3-KIF3A S690D	Stable line overexpressing GFP-KIF3A S690D. Puromycin resistant.	

2.1.6 Primary antibodies

Antibody	Species	Clonal	Source	Catalog #
Actin	mouse	monoclonal	Millipore	MAB1501R
β-catenin	rabbit	polyclonal	Sigma	C2206
βPIX	rabbit	polyclonal	Chemicon	AB3829
Cdc42	mouse	monoclonal	BD Transduction Labs	610928
Dynein LIC1	rabbit	polyclonal	GeneTex	GTX120114
Dynein LIC2	rabbit	polyclonal	Proteintech	18885-1-AP
Dynein LIC2	rabbit	polyclonal	Abcam	Ab118082
Flag	mouse	monoclonal	Sigma	F3165
Flag	rabbit	polyclonal	Sigma	F7425
α-tubulin	mouse	monoclonal	Sigma	T9026
γ-tubulin	rabbit	polyclonal	Sigma	T5192
GFP	rabbit	polyclonal	Invitrogen	11122
GST	rabbit	polyclonal	Bethyl Laboratories	A190-122A
HA	rabbit	polyclonal	Zymed	71-5500
KAP3A	mouse	monoclonal	BD Transduction Labs	610637
KIF3A	mouse	monoclonal	BD Transduction Labs	611508
N-cadherin	mouse	monoclonal	BD Transduction Labs	610920
p150 (Glued)	mouse	monoclonal	BD Transduction Labs	610473
Par3	rabbit	polyclonal	Millipore	07-330
Par6	rabbit	polyclonal	Santa Cruz Biotechnology	Sc-25525
Paxillin	mouse	monoclonal	Upstate	#05-417
Pericentrin	rabbit	polyclonal	Abcam	Ab4448
PKCζ	rabbit	polyclonal	Santa Cruz Biotechnology	Sc-216
POPX2	rabbit	antisera	Self-raised	

2.1.7 Secondary antibodies

Antibody	Company
Goat anti-mouse IgG, HRP conjugated	Dako Cytomation
Goat anti-rabbit IgG, HRP conjugated	Dako Cytomation
Goat anti-mouse IgG, Alexa Fluor 488	Molecular Probes
Goat anti-mouse IgG, Alexa Fluor 546	Molecular Probes
Goat anti-rabbit IgG, Alexa Fluor 488	Molecular Probes
Goat anti-rabbit IgG, Alexa Fluor 546	Molecular Probes

2.1.8 siRNAs

siRNA	Sequence (5'->3')
Control	ACAUCACGUACGCGGAAUACUUCGA
Cdc42 #1	ACAGCUGGUGUUGUCGUCAUACUAA
Cdc42 #2	CCCUCUUUCUAGGAUGCACUCUAUA
LIC2 #1	CGACAUGUCUCGACCUUGGACGAUA
LIC2 #2	CCACUUUACCAUACCCGCCUUAGUU
N-Cadherin #1	CCGGUUUCACUUGAGAGCACAUGCA
N-Cadherin #2	CCAACAUUUCCAUCCUGCGUGUGAA
Par3 #1	GACCCAGCUUUAACUGGCCUUUCCA
Par3 #2	CCACCCAAGGGAAAUGAAUGCUGAA
POPX2	ACCGCGCCUACUUUGCUGUGUUUGA

2.1.9 qPCR primers

Primer name		Sequence (5'->3')
TBP	Forward	CCCCACAACTCTTCCATTCT
	Reverse	GCAGGAGTGATAGGGGTCAT
LIC2 #1	Forward	CGGCGACCTGACAAGTGAA
	Reverse	TGCAGCGTGTGTGATCGTC
LIC2 #2	Forward	CTCAGGCTCAGACGAAGACAG
	Reverse	TCATGGCATCACACTTTGTGC

2.1.10 Plasmids

Plasmid	Insert		Accession Number	
pBABE-mCherry				
pBABE-mCherry-LIC2	Cytoplasmic dynein 1 light intermediate chain 2	Full length	NM_001013380	
pBABE-mCherry-LIC2^{S194A}	Cytoplasmic dynein 1 light intermediate chain 2	Full length; S194A		
pBABE-mCherry-LIC2^{S194D}	Cytoplasmic dynein 1 light intermediate chain 2	Full length; S194A		
pBOS-mCherry-tubulin	β-tubulin	Full length	NM_001197181	
pCMV-Neo-Bam APC	Adenomatous polyposis coli protein	Full length	NM_000038	Addgene plasmid 16507
pEGFP-N1				
pEGFP-N1-N-cadherin	N-cadherin	Full length	NM_007664	Addgene plasmid 18870
pXJ-Flag				
pXJ-Flag-Cdc42 V12	Cell division control protein 42 homolog	Full length; G12V		
pXJ-Flag-Cdc42 N17	Cell division control protein 42 homolog	Full length; T17N		
pXJ-Flag-KIF3A	Kinesin-like protein KIF3A	Full length	BC045542	
pXJ-Flag-KIF3A S690A	Kinesin-like protein KIF3A	Full length; S690A		
pXJ-Flag-KIF3A S690D	Kinesin-like protein KIF3A	Full length; S690D		
pXJ-Flag-LIC1	Cytoplasmic dynein 1 light intermediate chain 1	Full length	NM_146229	
pXJ-Flag-LIC2	Cytoplasmic dynein 1 light intermediate chain 2	Full length	NM_001013380	
pXJ-Flag-LIC2^{S194A}	Cytoplasmic dynein 1 light intermediate chain 2	Full length; S194A		
pXJ-Flag-LIC2^{S194D}	Cytoplasmic dynein 1 light intermediate chain 2	Full length; S194D		
pXJ-Flag-Par3b	Partitioning defective 3 homolog beta	Full length	NM_001081050	

pXJ-Flag-Par6	Partitioning defective 6 homolog	Full length	NM_001047435
pXJ-Flag-PKCζ	Protein kinase C zeta type	Full length	NM_001033581
pXJ-Flag-POPX2	Protein phosphatase 1F/ Partner of PIX 2	Full length	NM_014634
pXJ-GFP			
pXJ-GFP-POPX2	Protein phosphatase 1F	Full length	
pXJ-GFP-POPX2m	Protein phosphatase 1F	Full length; R362A, I338A	
pXJ-GST			
pXJ-GST-KIF3A Tail	Kinesin-like protein KIF3A	Amino acids 601-702	
pXJ-GST-POPX2	Protein phosphatase 1F	Full length	
pXJ-HA			
pXJ-HA-β-catenin	Catenin beta-1	Full length	NM_001165902

2.2 Methods

2.2.1 Plasmid purification

Plasmids were amplified in DH5α cells and purified from an overnight culture in LB medium supplemented with Ampicillin or Kanamycin using AxyPrep Plasmid Miniprep Kit according to the manufacturer's protocol.

2.2.2 Cell culture

NIH3T3 and COS-7 cells were cultured in DMEM containing 4500mg/L glucose, supplemented with 3.7g/L sodium bicarbonate and 10% fetal bovine serum (FBS) at 37^{o}C in 5% CO_2. Cells were seeded at 35000 cells/cm^2 on fibronectin-coated surfaces and allowed to grow to confluence overnight for experiments involving analysis of migration paths, nucleus and centrosome orientation as well as for immunofluorescence staining. Cells were not synchronized prior to these assays. NIH3T3 cells were used for all experiments except for pull-down assays, where Cos-7 cells were used.

2.2.3 Transfection

NIH3T3 and COS-7 cells were grown to 80-90% confluence and transiently transfected with 1-3µg plasmid DNA using LipofectAMINE^{TM} 2000 according to manufacturer's instructions. Cells were used for experiments 24h post-transfection.

2.2.4 RNAi

NIH3T3 cells were seeded at 80% confluence. Stealth siRNA (Invitrogen) was reverse transfected into cells using LipofectAMINE^{TM} 2000 according to manufacturer's instructions. Experiments were carried out 48h post-transfection.

2.2.5 Western blot

Protein lysates were harvested from NIH3T3 or COS-7 cells, and the concentration determined with the Bio-Rad protein assay kit. 50µg of sample was boiled in 1x SDS loading buffer and loaded into each well on an 8-12% polyacrylamide gel. The proteins were then transferred to nitrocellulose membranes. Blocking was carried out for 1h at room temperature in 5% non-fat milk. Immunoblotting with primary antibody was carried out at 4^{o}C overnight and secondary antibody for 1h at room temperature. The chemiluminesent signals were detected on film with Novex® ECL (Invitrogen) or Lumigen® TMA-6 (GE Healthcare).

2.2.6 qPCR

NIH3T3 cells were lysed and total RNA extracted using the RNeasy Mini Kit (Qiagen). First strand cDNA synthesis was carried out using SuperScript® *VILO™ cDNA* Synthesis Kit (Life Technologies). qPCR was carried out in triplicates for each sample, using a StepOne Plus real time PCR machine (Applied Biosystems). No-template controls (NTC) and no reverse transcription (RT) controls were included to check for DNA contamination. Gene expression levels were calculated using the ΔΔCT method and normalized using TBP as an endogenous control. Melting curve analysis and gel electrophoresis were performed on the qPCR end products to check for primer specificity and contamination.

2.2.7 Analysis of cell migration paths

NIH3T3 cells were seeded at 35000 cells/cm^2 and allowed to grow to confluence overnight. The monolayer was scratched with a p200 pipette tip, and cells were imaged for 15h at 15min/frame using a Zeiss Axiovert 200M inverted microscope at 37°. Cell nuclei were manually tracked using the Manual Tracking plugin in ImageJ. Cells were tracked unless they underwent cell division, and their paths were traced and aligned using Ibidi chemotaxis and migration tool 2.0 (Ibidi) such that their start points lie at the origin.

2.2.8 Centrosome orientation assay

NIH3T3 cells were seeded at 35000 cells/cm^2 on fibronectin-coated coverslips and allowed to grow to confluence overnight. Individual wounds were made across the monolayer using a 200ul pipette tip. Cells were fixed in paraformaldehyde containing 0.2% Triton-X 4 hours post-wounding and stained with γ-tubulin and DAPI. Centrosomes were determined to be correctly oriented if they were positioned within a 120° sector defined by the nucleus and leading edge (Palazzo et al., 2001). At least 100 cells from 3 independent experiments were analyzed for each condition. Error bars represent the standard deviation.

2.2.9 Analysis of nucleus and centrosome position

Scratch-wounded cells were fixed in fixed in paraformaldehyde containing 0.2% Triton-X 4 hours post-wounding and stained with γ-tubulin and DAPI. Images were aligned such that the wound was parallel to the x-axis. ImageJ was used to trace the parameters of the whole cell, the nucleus and the centrosome, and to determine the position of their centroids. The distance between the nucleus and centrosome to the cell centroid was calculated, and the values normalized to cell size. At least 100 cells from 2 independent experiments were analyzed for each condition. Error bars represent SEM.

2.2.10 Immunofluorescence staining

Cells were fixed with either 4% paraformaldehyde or cold methanol. Cells were permerabilized in 0.2% Triton X-100 and blocked with BSA, and incubated with primary antibody at 4°C overnight. Incubation with secondary antibody was carried out at room temperature for 1 hour. Coverslips were mounted using Vectorshield with DAPI and images were obtained using a Carl Zeiss axiovert microscope using Plan-Apochromat 40X/1.25 or Plan-Apochromat 63X/1.4 objectives and recorded on a Roper Scientific CoolSNAP CCD camera.

2.2.11 Time-lapse imaging of MT dynamics

NIH3T3 cells were transfected with mCherry-tubulin and either GFP-POPX2, control siRNA or siRNA against LIC2 or Par3. Cells were imaged using the Zeiss Plan Neo-fluar 100X/1.3 oil objective on a Carl Zeiss axiovert microscope equipped with a humid chamber at 37°C and 5% CO_2. Images were captured with Axiovision software using a Roper Scientific CoolSNAP CCD camera. MTs present at cell-cell contacts were imaged at 5s/frame for a total of 3 minutes, and those that could be clearly observed for at least 2 minutes were used for tracking analysis. 95-100 MTs from at least 2 independent experiments were analyzed using ImageJ. The error bars represent SEM.

2.2.12 Site-directed mutagenesis

LIC2 mutants were generated using QuikChange Site-Directed Mutagenesis Kit (Stratagene) according to manufacturer's protocol.

The following primers were used:

Name	**Sequence (5'->3')**
LIC2 S194A sense	CCTGAAGAAGGTTGTCAGGGTGCCCCACAGAGA
LIC2 S194A antisense	TCTCTGTGGGGCACCCTGACAACCTTCTTCAGG
LIC2 S194D sense	AGCCTGAAGAAGGTTGTCAGGGTGACCCACAGAGAAG
LIC2 S194D antisense	CTTCTCTGTGGGTCACCCTGACAACCTTCTTCAGGCT

2.2.13 Pull-down assay

Protein lysates were prepared by homogenization in 300µl protein lysis buffer 24h post-transfection, and centrifuged at 14,000rpm for 10min at 4°C to clarify them. The clarified supernatant was added to 50µl Glutathione Sepharose™ 4B (Amersham Biosciences) or 30µl ANTI-FLAG® M2 Affinity Gel (Sigma) and mixed at 4°C for 2h with constant rotation. The beads were washed thrice with GST purification buffer and the bound protein was eluted in SDS sample buffer by heating at 100°C for 10min. The eluted sample was subjected to SDS-PAGE and Western blotting.

2.2.11 Time-lapse imaging of mCherry-LIC2

NIH3T3 cells were transfected with mCherry-LIC2^{WT}, LIC2^{S194A} or LIC2^{S194D}. Cells were imaged using the Zeiss Plan Neo-fluar 100X/1.3 oil objective on a Carl Zeiss axiovert microscope equipped with a humid chamber at 37°C and 5% CO_2. Images were captured with Axiovision software using a Roper Scientific CoolSNAP CCD camera. Cells were imaged at 3s/frame for a total of 2 minutes, mCherry-LIC2 particles that could be clearly observed were tracked using ImageJ. At least 100 vesicles were tracked across 2 independent experiments and used for analysis. The error bars represent SEM.

3. Results

3.1 The role of POPX2 in centrosome positioning

3.1.1 POPX2 overexpression results in a loss of directional migration

The level of POPX2 expression is positively correlated with the rate of cell migration and cancer cell invasiveness (Singh et al., 2011; Susila et al., 2010; Zhang et al., 2013). Analyzing the paths taken by control (Ctrl), POPX2-overexpressing (X2) and POPX2 phosphatase-dead mutant-overexpressing (X2m) NIH3T3 fibroblasts shows that in addition to the rate of migration, POPX2 overexpression also affects the migratory patterns of fibroblasts. Ctrl and X2m fibroblasts tend to migrate more perpendicularly across the wound, while X2 fibroblasts tend to migrate in a more random and less directional manner as they close the wound, as shown by the greater spread in their migratory paths when they are overlaid with their start points at the origin (Figure 11). This suggests that the phosphatase activity of POPX2 plays a role in the control of directional migration.

In fibroblasts, the direction of migration is largely determined by the position of the centrosome. Upon cell polarization, the centrosome orients itself such that it lies between the nucleus and the leading edge, and the cell moves in the direction where the centrosome is oriented towards. Since X2 cells are defective in the directionality of migration, we postulate that centrosome orientation is affected upon overexpression of POPX2.

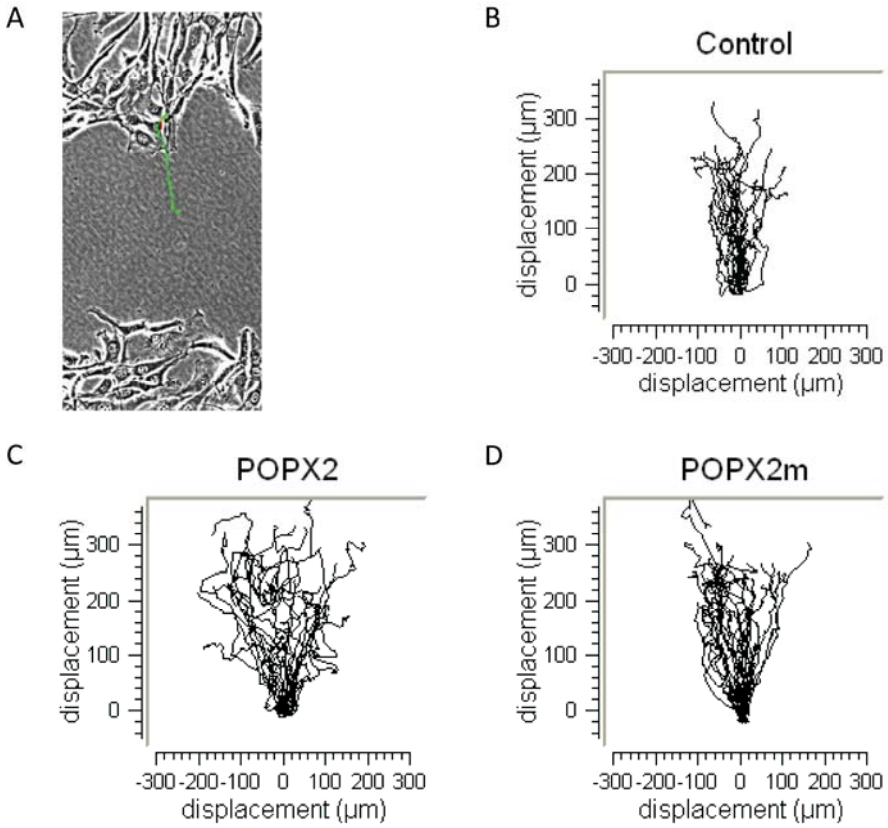

Figure 11. POPX2-overexpressing fibroblasts move less perpendicularly across scratch wounds
(A) Representative path taken by a NIH3T3 Ctrl fibroblast across a scratch wound. (B) Paths taken by Ctrl cells (n=40). (C) Paths taken by X2 cells (n=42). (D) Paths taken by X2m cells (n=46). All paths are oriented such that the start point is normalized to the origin and overlaid on the same graph.

3.1.2 POPX2-overexpressing cells are defective in centrosome orientation

We next analyzed the centrosome orientation status in Ctrl and X2 fibroblasts using a wound-induced centrosome orientation assay. Confluent fibroblast monolayers were scratch-wounded and stained for γ-tubulin to show the position of the centrosome. Cells were determined to have correctly oriented centrosomes if the centrosome was located in a 120˚ sector defined by the wound edge and the center of the cell (Figure 12A). A 120˚ sector was chosen as this approximately covers the region of the cell that is exposed to the wound and later forms the leading edge as the cell migrates. Based on this method of classification, random centrosome orientation occurs in a population of cells if only 33.3% of cells show proper centrosome orientation upon scratch wounding, suggesting that there are defects in centrosome positioning.

Most Ctrl cells were able to orient their centrosomes towards the wound edge upon scratch wounding; however, X2 cells showed consistently reduced centrosome orientation at 2, 4 and 6 hours post-wounding (Figure 12B). Since both Ctrl and X2 cells showed consistent trends in centrosome orientation from 2 to 6 hours post-wounding, all future analyses were carried out on cells fixed 4 hours post-wounding. Proper centrosome orientation could be partially restored in X2 cells by treating them with a siRNA against both endogenous and exogenous POPX2 (Figure 12C,D), indicating that high levels of POPX2 negatively impacts centrosome orientation. The phosphatase activity of POPX2 appears to be essential in the regulation of centrosome orientation, as overexpression of the phosphatase-dead mutant of POPX2, POPX2m, did not affect centrosome orientation (Figure 13).

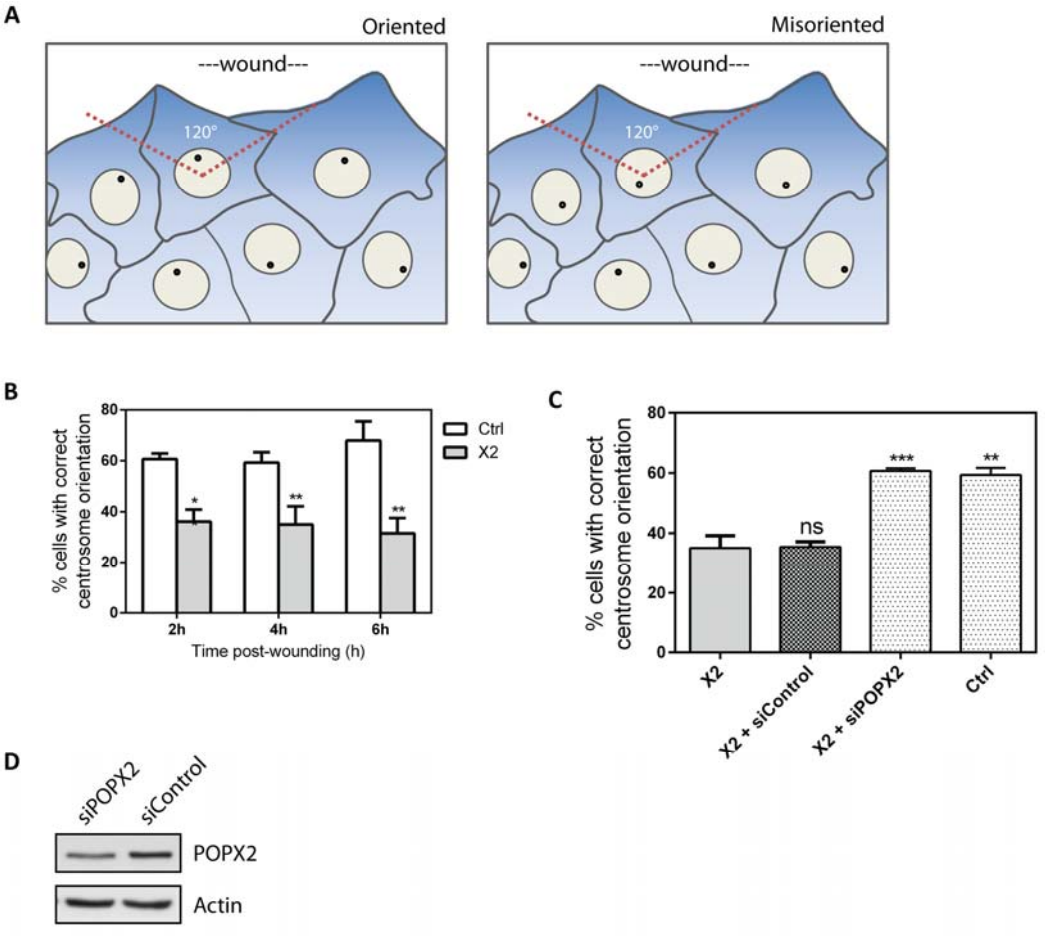

Figure 12. POPX2-overexpressing cells are defective in centrosome orientation
(A) Diagram showing assessment of centrosome orientation in NIH3T3 cells. Centrosomes were classified as correctly oriented if they were positioned in a 120˚ sector facing the wound edge, and misoriented if not. (B) Histogram showing percentage of Ctrl and X2 cells with correctly oriented centrosomes at 2, 4 and 6h post-wounding. Results are shown as means of 3 independent experiments with errors bars representing standard deviation (Student's T test, n=100; *P<0.5, **P<0.01). (C) Histogram showing percentage of cells with proper centrosome orientation upon treatment with control or POPX2 siRNA targeting both endogenous and exogenous POPX2. Results are shown as means of 3 independent experiments with errors bars representing standard deviation (Student's T test, n=100; **P<0.01, ***P<0.001). (D) Western blot showing knockdown of POPX2 in X2 cells treated with POPX2 and control siRNAs. Actin was used as a loading control.

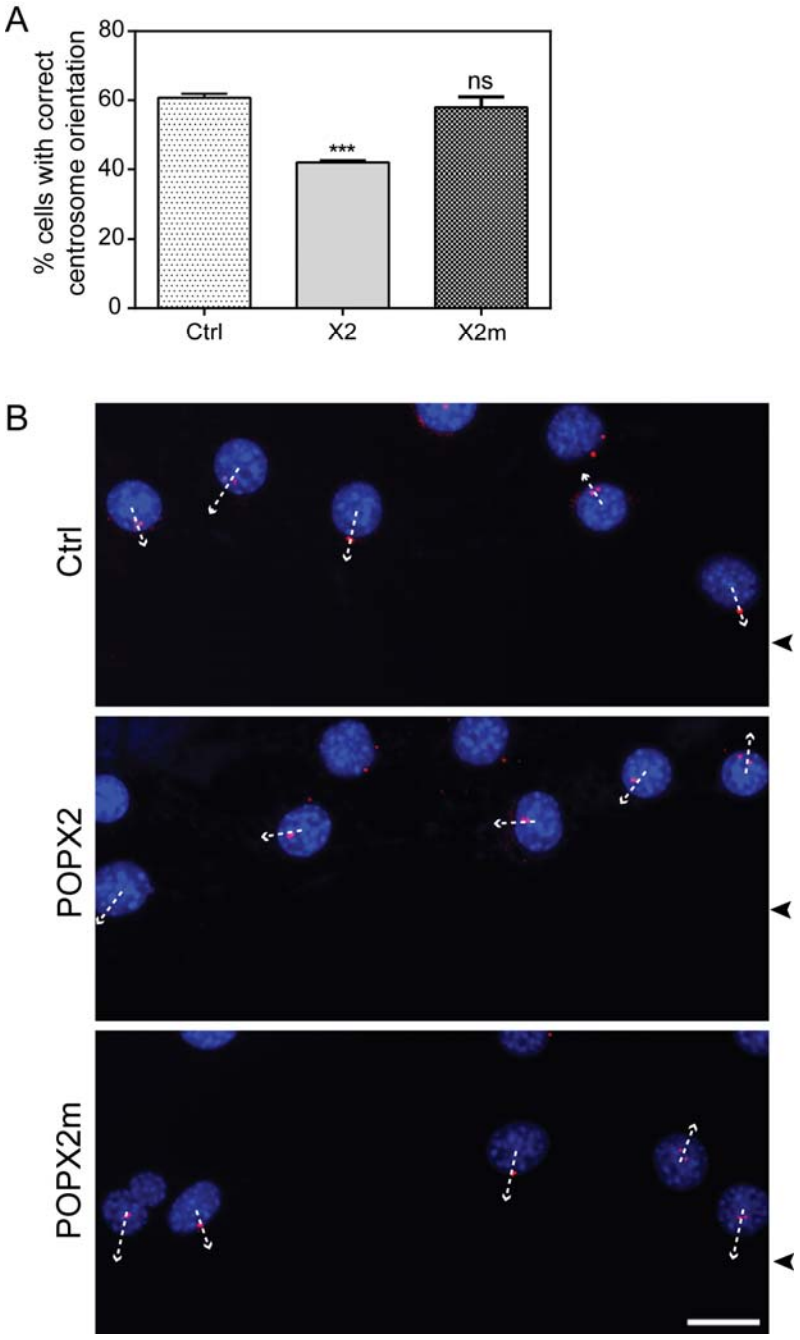

Figure 13. Phosphatase activity of POPX2 plays a role in centrosome orientation
(A) Histogram showing percentage of Ctrl fibroblasts and fibroblasts overexpressing POPX2 or POPX2m with correctly oriented centrosomes. Results are shown as means of 3 independent experiments with errors bars representing standard deviation (Student's T test, n=100; ***P<0.001). (B) Representative images showing immunostaining of gamma-Tubulin and DAPI in Ctrl, X2 and X2m cells 4h post-wounding. Gamma-Tubulin is a centrosomal marker. Arrows indicate the direction of the nuclear-centrosomal axis and arrowheads indicate the position of the wound. Scale bar: 20µm.

Centrosome reorientation occurs in response to scratch-wounding of confluent cell monolayers. In cells such as fibroblasts and astrocytes, the nucleus moves towards the rear of the cell while the centrosome remains at the cell centroid, and both of these events are separately controlled. In order to determine whether overexpression of POPX2 affects nuclear movement and/or centrosome positioning, we compared the positions of both the nucleus and centrosome relative to the cell centroid in Ctrl and X2 cells. We did not observe any significant difference in the position of the nucleus in both cell types, and both the nuclei in Ctrl and X2 cells are positioned at a similar distance towards the rear of the cell. However, the centrosome was positioned closer to the rear in X2 cells as compared to Ctrl cells, where it is much closer to the cell centroid (Figure 14). This indicates that POPX2 affects the process of centrosome orientation by influencing centrosome positioning rather than nuclear movement.

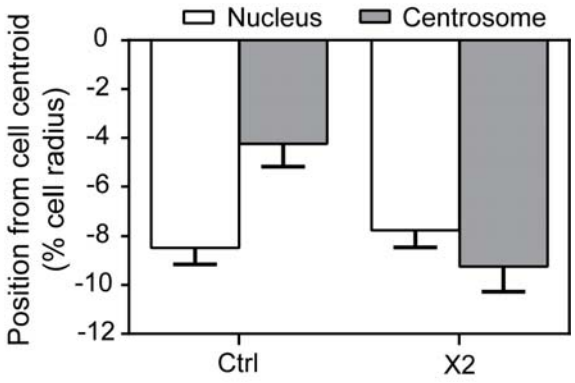

Figure 14. POPX2 affects centrosome orientation by affecting centrosome positioning, and not rearward nucleus movement

Quantification of the position of the nucleus and centrosome along the axis of the cell perpendicular to the wound. The nucleus is similarly positioned towards the rear in both Ctrl and X2 cells while the centrosome is positioned closer to the cell centroid in Ctrl cells as compared to X2 cells. The cell centroid is defined as “0”. Positive values are towards the leading edge and negative values are towards the rear of the cell. Error bars represent SEM.

3.1.3 N-cadherin is required for centrosome positioning and its localization is affected in X2 cells

Having established that POPX2 affects the process of centrosome orientation by controlling centrosome positioning rather than nuclear movement, we next investigate how POPX2 regulates centrosome positioning.

N-cadherin is one of the players involved in centrosome positioning (Dupin et al., 2009). N-cadherin, β-catenin and other proteins involved in cell polarity have been reported to be cargoes of the Kinesin-2 motor, which consists of the KIF3A and B motor subunits and the non-motor KAP3 subunit (Yamazaki et al., 1995). It has been recently reported that POPX2 negatively regulates N-cadherin transport by inhibiting the Kinesin-2 heterotrimeric motor, specifically through precluding phosphorylation or directly dephosphorylating serine-690 on KIF3A (Phang et al., 2014). Consistent with this, X2 cells show reduced peripheral N-cadherin localization as compared to Ctrl and X2m cells. Knockdown of POPX2 in X2 cells restored the peripheral localization of N-cadherin (Figure 15).

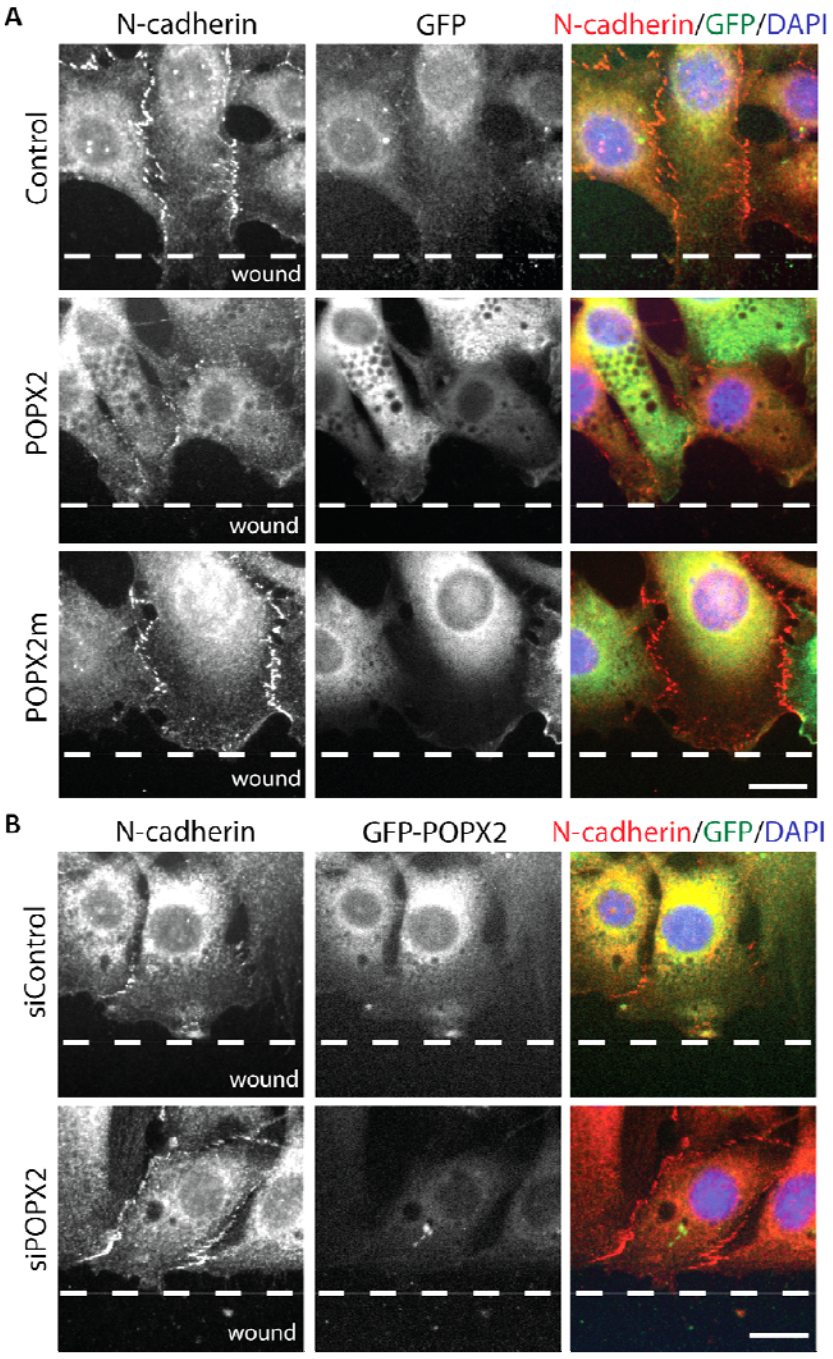

Figure 15. N-cadherin localization in Ctrl, X2 and X2m cells
(A) Immunostaining of N-cadherin in Ctrl, X2 and X2m cells and (B) X2 cells transfected with either control or POPX2 siRNA. Scale bar: 20µm.

Since N-cadherin has been shown to control centrosome positioning by regulating cell-ECM interactions (Dupin et al., 2009), we next determined whether POPX2 inhibits proper centrosome positioning through perturbing Kinein-2-mediated N-cadherin transport. We first confirmed the requirement of N-cadherin for proper centrosome orientation by treating Ctrl and X2 cells with siRNAs against N-cadherin. Reduction of N-cadherin expression in Ctrl cells resulted in a reduced number of cells with proper centrosome orientation (Figure 16A, B). Overexpression of POPX2 does not affect N-cadherin protein expression in cells as Western blot analysis showed that endogenous N-cadherin expression was similar in both Ctrl and X2 cells (Figure 16C).

Overexpression of N-cadherin failed to restore proper centrosome orientation in X2 cells (Figure 16D,E), suggesting that it is a defect in Kinesin-2 motor transport, rather than a lack of N-cadherin expression, that is inhibiting proper centrosome orientation in X2 cells. We also verified that the microtubule network appears to be normal in both Ctrl and X2 cells by immunoflurorescence staining with anti-tubulin antibody (Figure 16F). This suggests that the defect in Kinesin-2 motor transport is due to a defective Kinesin-2 motor and not a defect with the microtubule network.

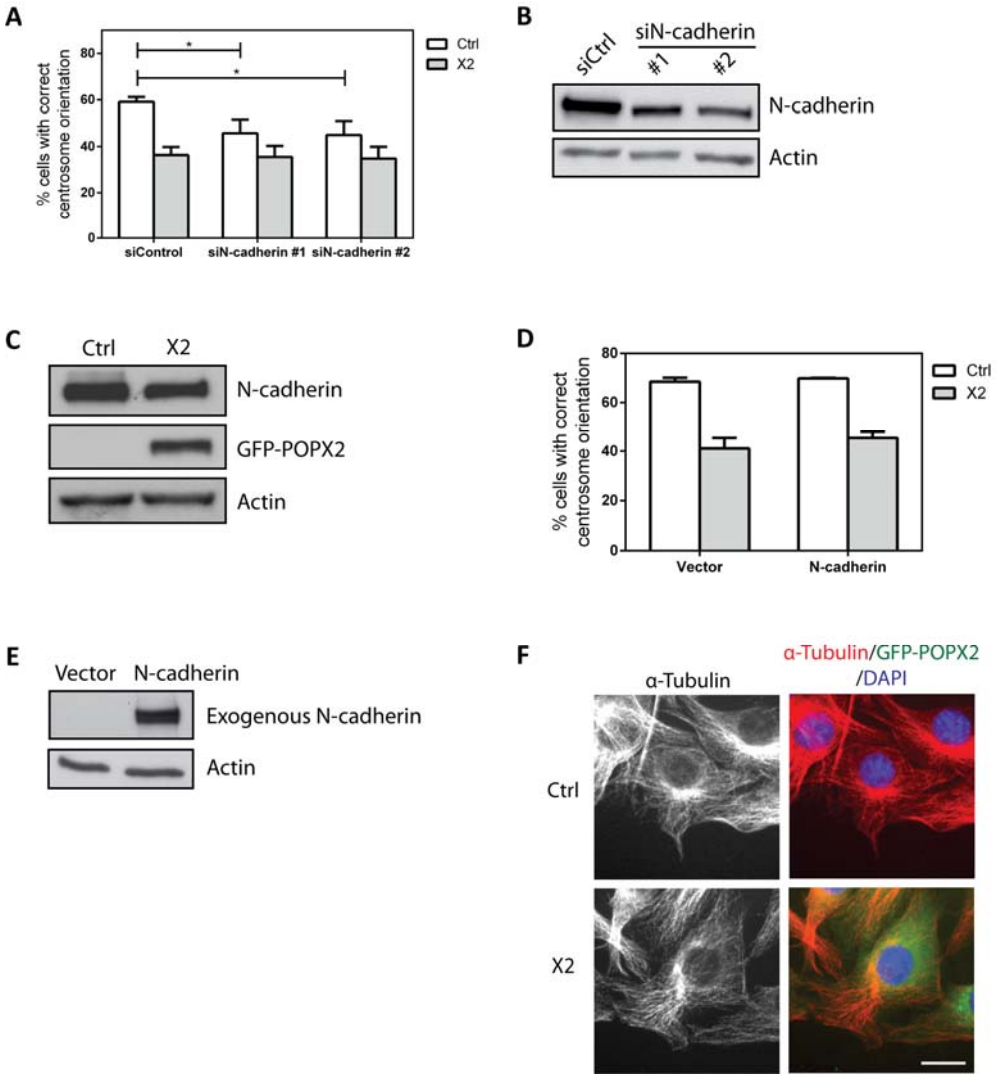

Figure 16. N-cadherin is required for proper centrosome positioning
(A) Histogram showing percentage of Ctrl and X2 fibroblasts transfected with control or N-cadherin siRNA with correctly oriented centrosomes 4 hours after wounding. Results are shown as means +/- standard deviation of 3 independent experiments (N=100, Student's T test, *P<0.05). (B) Western blot showing knockdown of N-cadherin in NIH3T3 fibroblasts transfected with N-cadherin siRNA. Actin was used as a loading control. (C) Western blot showing expression of N-cadherin in Ctrl and X2 fibroblasts. Actin was used as a loading control. (D) Histogram showing percentage of Ctrl and X2 fibroblasts overexpressing N-cadherin with correctly oriented centrosomes 4 hours after wounding. Results are shown as means +/- standard deviation of 3 independent experiments (N=100, Student's T test). (E) Western blot showing expression of exogenous N-cadherin in Ctrl cells. Actin was used as a loading control. (F) Immunostaining of α-Tubulin in Ctrl and X2 cells. Scale bar: 20µm.

In order to demonstrate that Kinesin-2 transport is implicated in the process of centrosome orientation, we overexpressed the KIF3A tail domain in Ctrl cells. When introduced into cells, the tail domain competes with endogenous KIF3A for cargoes, but is unable to transport them, thus acting in a dominant-negative manner. Overexpression of the KIF3A tail in Ctrl cells inhibits centrosome orientation, confirming that proper KIF3A motor activity is required to position the centrosome (Figure 17A). The motility of the KIF3A motor can be controlled by phosphorylation on serine-690, and this affects the distribution of N-cadherin(Phang et al., 2014). We observe that cells overexpressing GFP-WT KIF3A and the phospho-mimic GFP-KIF3A S690D showed normal N-cadherin localization to regions of cell-cell contact, while those overexpressing GFP-KIF3A S690A, which precludes serine-690 phosphorylation, lacked N-cadherin localization to cell-cell contacts (Figure 17B). We next overexpressed wild-type (WT) KIF3A, KIF3A S690D and KIF3A S690A in X2 cells to observe how they affect centrosome orientation. Overexpression of WT KIF3A and KIF3A S690D, but not KIF3A S690A, partially rescued the centrosome orientation defect (Figure 17C).

KIF3A is phosphorylated on serine-690 by CaMKII (Phang et al., 2014), and inhibition of CaMKII activity should thus result in a loss of proper centrosome orientation. Indeed, treatment of Ctrl cells with small molecule inhibitors of CaMKII, KN-93 and KN-62, resulted in a loss of N-cadherin localization to cell-cell contacts (Figure 18A,B) as well as impairment of centrosome orientation (Figure 18C,D). Thus, the motor activity of KIF3A, which is controlled by phosphorylation of serine-690, is required for proper positioning of the centrosome.

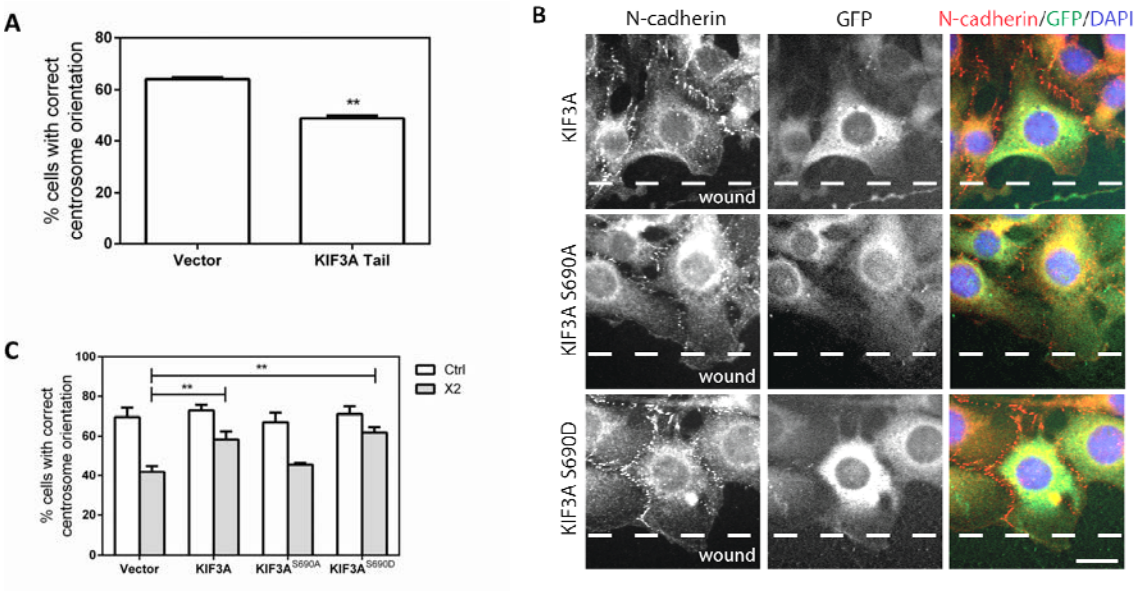

Figure 17. Phosphorylation status of KIF3A affects centrosome orientation
(A) Histogram showing percentage of NIH3T3 fibroblasts overexpressing KIF3A tail with correctly oriented centrosomes 4 hours after wounding. Results are shown as means +/- standard deviation of 3 independent experiments (n=100; Student's T-test, **P<0.01). (B) Immunostaining of N-cadherin in NIH3T3 fibroblasts overexpressing GFP-KIF3A, GFP-KIF3A S690A or GFP-KIF3A S690D. Scale bar: 20µm. (C) Histogram showing percentage of NIH3T3 fibroblasts overexpressing KIF3A, KIF3A S690A or KIF3A S690D with correctly oriented centrosomes 4 hours after wounding. Results are shown as means +/- standard deviation of 3 independent experiments (n=100; Student's T test, **P<0.01).

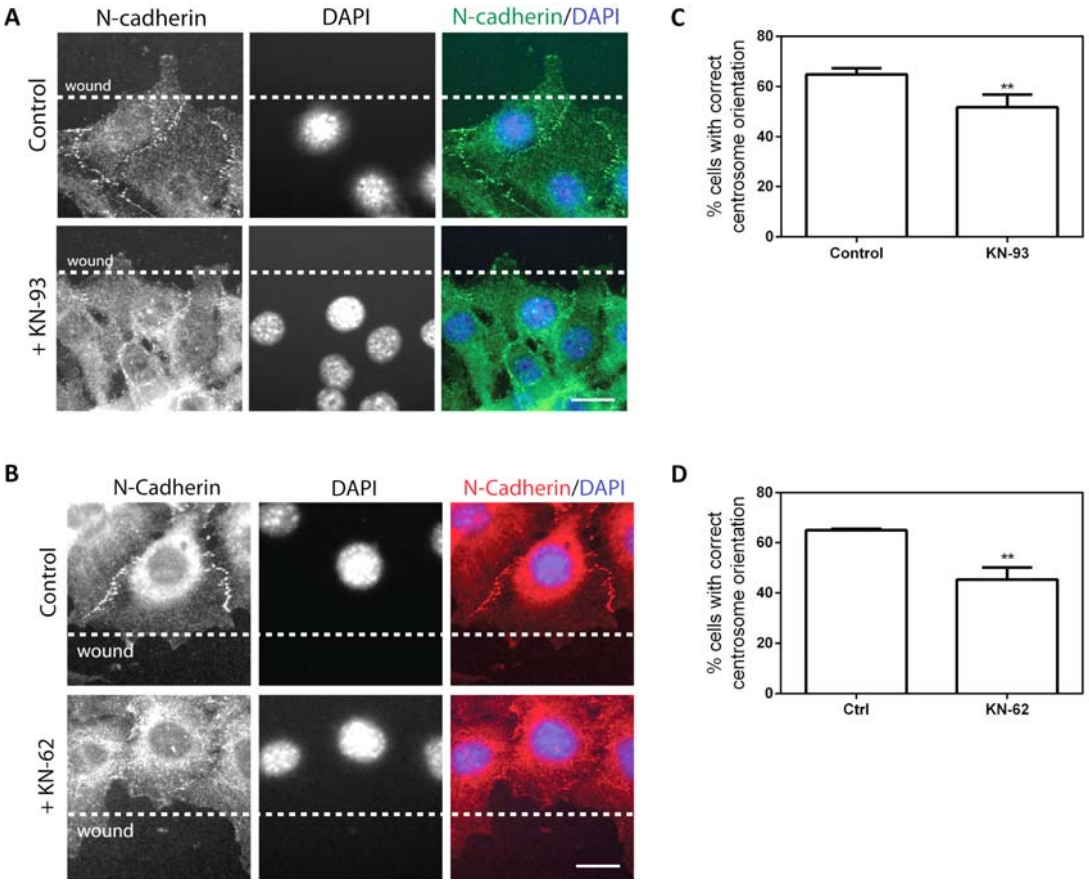

Figure 18. Inhibition of CaMKII by small molecule inhibitors prevents peripheral N-cadherin localisation and inhibits proper centrosome orientation in Ctrl cells

(A) Immunostaining of N-cadherin in Ctrl cells treated with water (Control) or KN-93. Scale bar: 20µm. (B) Immunostaining of N-cadherin in Ctrl cells treated with DMSO (Control) or KN-62. Scale bar: 20µm. (C) Histogram showing percentage of NIH3T3 fibroblasts treated with 10µM KN-93 with correctly oriented centrosomes 4 hours after wounding. Results are shown as means +/- standard deviation of 3 independent experiments (n=100; Student's T-test, **P<0.01). (D) Histogram showing percentage of NIH3T3 fibroblasts treated with 15µM KN-62 with correctly oriented centrosomes 4 hours after wounding. Results are shown as means +/- standard deviation of 3 independent experiments (n=100; Student's T-test, **P<0.01).

3.1.4 X2 cells show defects in focal adhesion localization and βPIX recruitment to the leading edge

Spatial segregation occurs between cell-cell and cell-matrix adhesions as a result of negative feedback between both systems. As a result, N-cadherin and focal adhesions localize in a pattern exclusive to each other (Burute and Thery, 2012; Dupin et al., 2009). N-cadherin localizes to cell-cell contacts while focal adhesions are found at the free edge of scratch-wounded fibroblasts. Focal adhesions are able to recruit βPIX, a guanine nucleotide exchange factor (GEF) of Cdc42 and Rac, resulting in the activation of Cdc42 signaling. Cdc42 signaling in turn affects centrosome positioning through Par6 and PKCζ (Etienne-Manneville and Hall, 2001; Gomes et al., 2005).

Since X2 cells have reduced localization of N-cadherin to cell-cell contacts, they are also likely to have defects in the localization of focal adhesions and βPIX recruitment. We confirmed this by immunostaining of paxillin and βPIX. Paxillin, a component of focal adhesions, was generally localized to the free edge in scratch-wounded Ctrl and X2m cells, but found throughout X2 cells (Figure 19A). Similarly, βPIX was localized to the free edge in scratched Ctrl and X2m cells but not X2 cells (Figure 19B). Since βPIX recruitment to the free edge is required to activate Cdc42-Par6/PKCζ signaling, it is likely that activation of this signaling pathway is perturbed in X2 cells, thus preventing proper centrosome orientation.

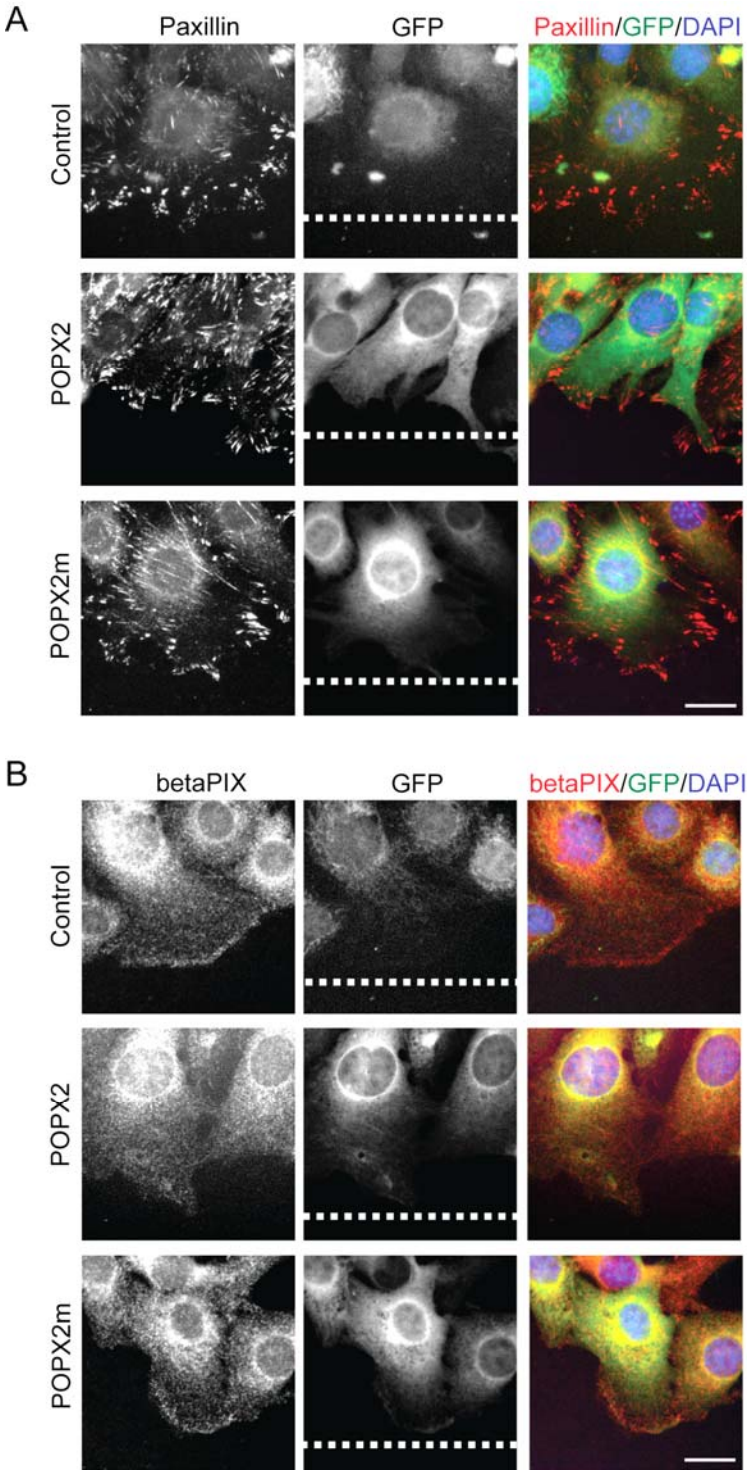

Figure 19. POPX2-overexpressing cells show loss of focal adhesion localization and βPIX recruitment to the leading edge

Immunostaining of (A) paxillin or (B) βPIX in cells infected with retroviral vector encoding GFP, GFP-POPX2 or GFP-POPX2m. Scale bar: 20 μm. Dashed lines indicate the position of the wound.

3.1.5 POPX2 does not affect centrosome positioning through upstream components of the Cdc42-Par6/PKCζ signaling pathway

Our observations thus far indicate that the localized activation of Cdc42-Par6/PKCζ signaling at the free edge is perturbed in X2 cells as a result of defective Kinesin-2-mediated N-cadherin transport, and this could affect proper positioning of the centrosome. We also wanted to determine whether overexpression of POPX2 had any additional effects on Cdc42-Par6/PKCζ signaling – for example, inhibiting the expression or activity of one or more proteins that function in this pathway. If overexpression of POPX2 also affects the expression or activity of proteins that function in the Cdc42-Par6/PKCζ signaling pathway, then overexpression of that protein should be able to at least partially restore proper centrosome orientation in X2 cells.

We first confirm the requirement of Cdc42 signaling in the control of centrosome orientation by depleting Cdc42 in Ctrl and X2 cells. Consistent with published data, loss of Cdc42 inhibited proper centrosome polarization in Ctrl cells (Figure 20A,B). Overexpression of a dominant negative mutant of Cdc42, Cdc42N17, resulted in a loss of centrosome orientation in Ctrl cells (Figure 20C), indicating that that activation of Cdc42 signaling is required for centrosome orientation. However, overexpression of Cdc42N17 and the constitutively active Cdc42V12 had no effect on centrosome orientation in X2 cells (Figure 20C). Overexpression of Cdc42N17 is not expected to have any effect in X2 cells, since X2 cells already show an almost complete loss of proper centrosome orientation. On the other hand, the failure of Cdc42V12 to restore proper centrosome orientation in X2 cells suggests that Cdc42 can be properly activated in X2 cells. Thus, POPX2 does not affect the process of Cdc42 activation itself, but instead affects the *localized* activation of Cdc42 in the control of centrosome orientation.

Overexpression of Par6, which is activated by Cdc42, resulted in a loss of centrosome orientation in Ctrl cells, Overexpression of Par6 has been shown to sequester PKCζ from the cell edge in MDCK cells (Joberty et al., 2000), and this might result in a loss of centrosome orientation as less PKCζ is present at the free cell edge to activate downstream signaling pathways required for proper centrosome orientation. However, overexpression of the protein did not have any effect in X2 cells (Figure 20D). Similarly, overexpression of PKCζ

failed to restore proper centrosome orientation in X2 cells (Figure 20E), suggesting that POPX2 overexpression does not have any direct effect on these 2 proteins.

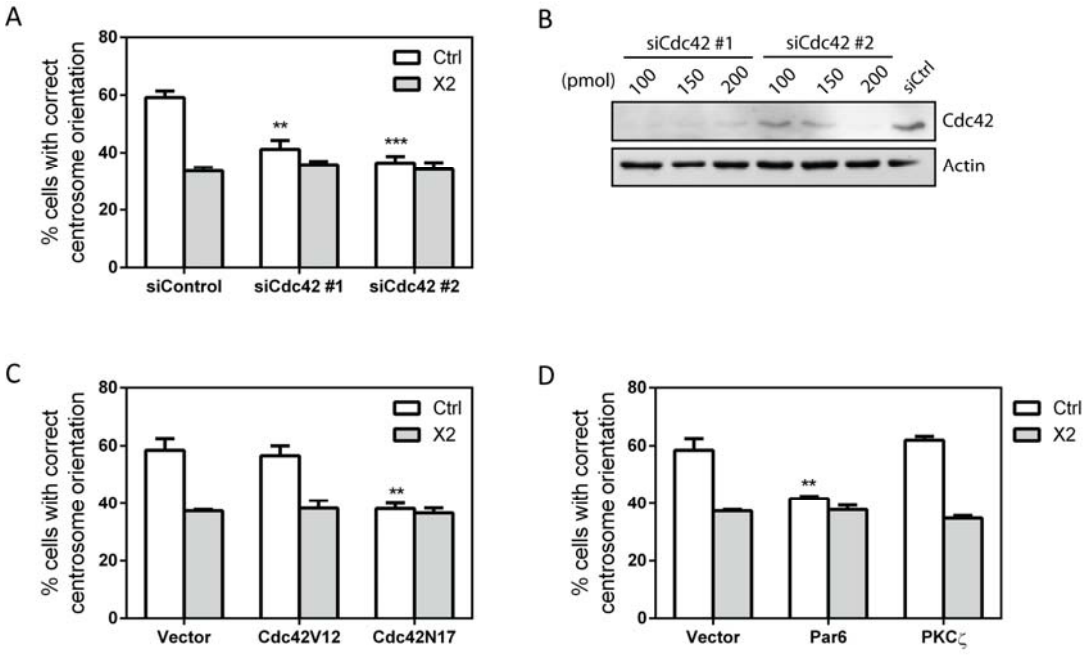

Figure 20. POPX2 does not affect centrosome orientation through Cdc42, Par6 or PKCζ
(A) Histogram showing percentage of Ctrl and X2 fibroblasts transfected with control or Cdc42 siRNA with correctly oriented centrosomes 4 hours after wounding. Results are shown as means +/- standard deviation of 3 independent experiments (N=100, Student's T test, **P<0.01, ***P<0.001). (B) Western blot showing knockdown of Cdc42 in cells treated with Cdc42 siRNA. Actin was used a s a loading control. (C) Histogram showing percentage of Ctrl and X2 fibroblasts transfected with empty vector or vector containing Cdc42V12 or N17 with correctly oriented centrosomes 4 hours after wounding. Results are shown as means +/- standard deviation of 3 independent experiments (N=100, Student's T test, **P<0.01). (D) Histogram showing percentage of Ctrl and X2 fibroblasts transfected with empty vector or vector containing Par6 or PKCζ with correctly oriented centrosomes 4 hours after wounding. Results are shown as means +/- standard deviation of 3 independent experiments (N=100, Student's T test, **P<0.01).

3.1.6 Par3 is required for centrosome positioning and its localization is affected in X2 cells

Two other proteins functioning downstream of the Cdc42-Par6/PKCζ signaling pathway are Par3 and LIC2 (Schmoranzer et al., 2009). Since POPX2 inhibits the motor activity of KIF3A, transport of all Kinesin-2 cargoes are expected to be inhibited in X2 cells. Thus, in addition to N-cadherin, we also decided to investigate whether another cargo of Kinesin-2, Par3 (Nishimura et al., 2004), is mislocalized in X2 cells. We first confirmed that Par3 is required for proper centrosome orientation by depleting Par3 in Ctrl and X2 cells. Loss of Par3 resulted in a loss of proper centrosome orientation in Ctrl cells, but had no effect in X2 cells (Figure 21A,B). Immunostaining of Par3 showed that the protein localized to cell-cell contacts in Ctrl and X2m, but not X2 cells (Figure 21C).

Overexpression of Par3 in X2 cells failed to restore proper centrosome orientation (Figure 21D), and western blot analysis showed that endogenous Par3 expression was similar in both Ctrl and X2 cells (Figure 21E). This suggests that the defects in Par3 localization observed in X2 cells were due to impaired Par3 transport. We confirmed this by immunostaining of Par3 in NIH3T3 fibroblasts overexpressing GFP-KIF3A WT, GFP-KIF3A S690A or GFP-KIF3A S690D. Par3 localised to cell-cell contacts in KIF3A- and KIF3A S690D- but not KIF3A S690A-overexpressing cells (Figure 21F).

Additionally, treatment of Ctrl cells with small molecule inhibitors of CaMKII, KN-93 and KN-62, resulted in a loss of Par3 localization to cell-cell contacts (Figure 22). This implies that (1) the phosphorylation status of KIF3A S690, which is affected by POPX2, is important for proper Par3 transport and localization, and (2) POPX2 affects centrosome orientation through its effects on Kinesin-2-mediated Par3 transport.

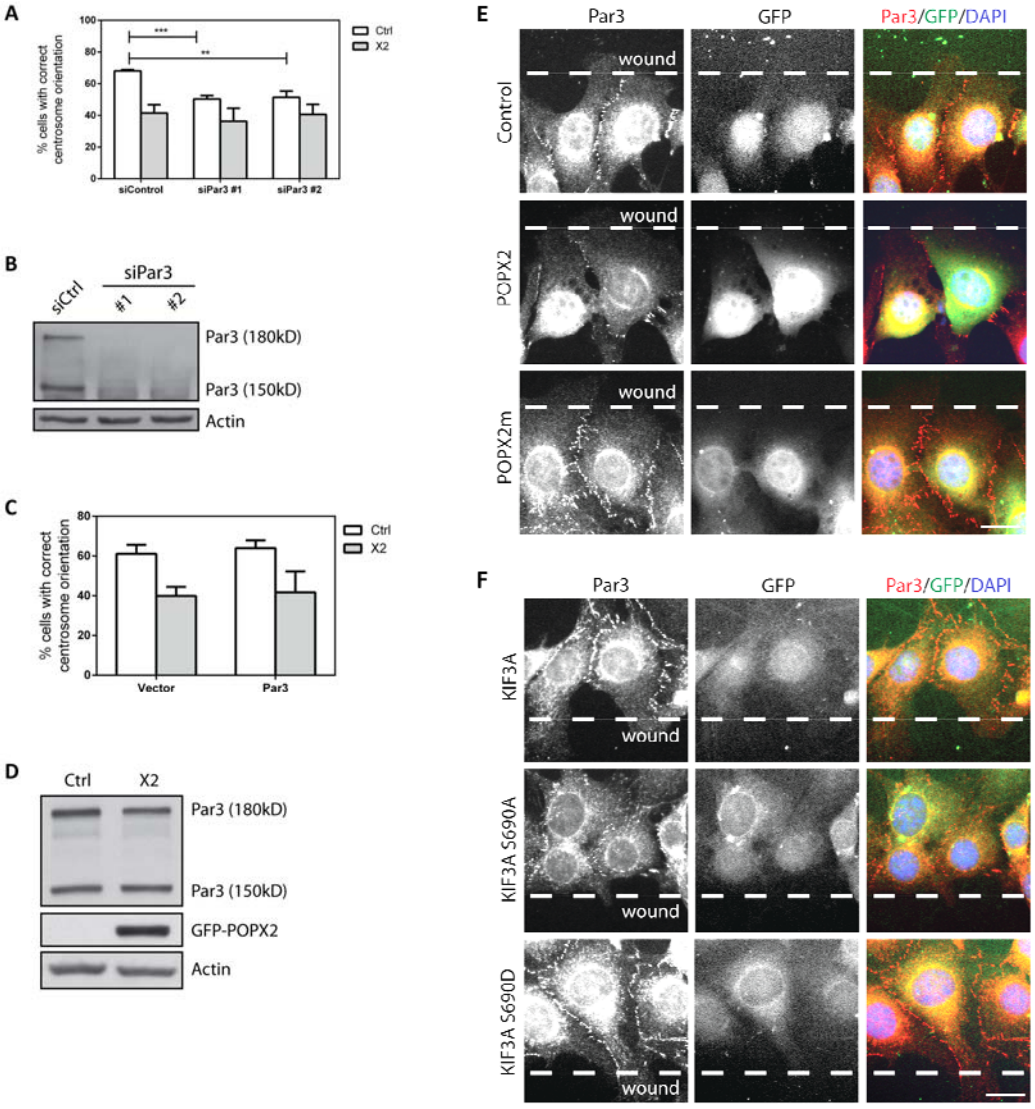

Figure 21. Par3 is required for centrosome positioning and its localization is affected in POPX2-overexpressing cells

(A) Histogram showing percentage of Ctrl and X2 fibroblasts transfected with control or Par3 siRNAs with correctly oriented centrosomes 4 hours after wounding. Results are shown as means +/- standard deviation of 3 independent experiments (n=100; Student's T test, **P<0.01, ***P<0.001). (B) Western blot showing knockdown efficiency in NIH3T3 fibroblasts transfected with Par3 siRNA. Actin was used as a loading control. (C) Histogram showing percentage of Ctrl and X2 fibroblasts overexpressing Par3 with correctly oriented centrosome 4 hours after wounding. Results are shown as means +/- standard deviation of 3 independent experiments (n=100; Student's T test). (D) Western blot showing that the levels of endogenous Par3 are similar in Ctrl and X2 fibroblasts. Actin was used as a loading control. (E) Immunostaining of Par3 in NIH3T3 fibroblasts infected with retroviral vector encoding GFP, GFP-POPX2 or GFP-POPX2m. Scale bar: 20 μm. (F) Immunostaining of Par3 in NIH3T3 fibroblasts infected with retroviral vector encoding GFP-KIF3A, GFP-KIF3A S690A or GFP-KIF3A S690D. Scale bar: 20 μm.

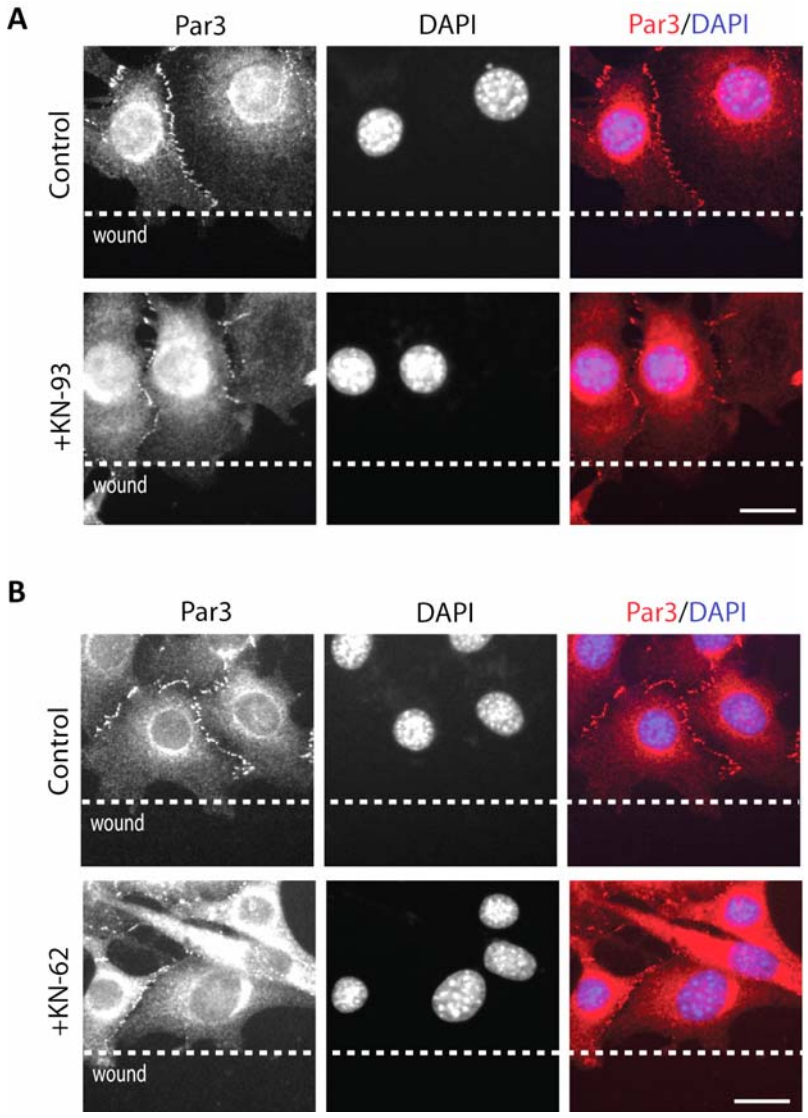

Figure 22. Inhibition of CaMKII by small molecule inhibitors prevents peripheral Par3 localisation and inhibits proper centrosome orientation in Ctrl cells

(A) Immunostaining of Par3 in Ctrl cells treated with water (Control) or KN-93. Scale bar: 20µm. (B) Immunostaining of Par3 in Ctrl cells treated with DMSO (Control) or KN-62. Scale bar: 20µm.

3.1.7 POPX2 affects LIC2 expression, which controls centrosome position and orientation

Par3 functions together with cytoplasmic Dynein light intermediate chain 2 (LIC2) in the regulation of centrosome positioning. Par3 interacts with LIC2, and serves as a cortical factor that tethers microtubules via LIC2, thus controlling centrosome positioning (Schmoranzer et al., 2009). Since Par3 localization to cell-cell contacts is lost in X2 cells, we also wanted to investigate whether POPX2 overexpression might affect the interacting partner of Par3, LIC2.

Treatment of cells with siRNAs targeting LIC2 resulted in a loss of proper centrosome orientation in Ctrl cells, while there was no effect in X2 cells (Figure 23A,B). Western blot analysis revealed that X2 cells expressed lower amounts of LIC2, but not LIC1 as compared to Ctrl (Figure 23C). LIC2 expression could be increased in X2 cells that were treated with a siRNA targeting POPX2 (Figure 23D), suggesting that POPX2 negatively regulates the amount of LIC2 protein.

Since X2 cells have lower levels of LIC2, and LIC2 is required for proper centrosome orientation, then increasing the amount of LIC2 in X2 cells should restore proper centrosome orientation. Indeed, overexpression of LIC2, but not LIC1, restored proper centrosome orientation in X2 cells (Figure 23E). We also measured the positions of the centrosome and nucleus relative to the cell centroid in cells overexpressing LIC1 and LIC2, and observed that only overexpression of LIC2 in X2 cells restored centrosome positioning such that it is closer to the cell centroid (Figure 23F). Thus, POPX2 is able to regulate both components of the Par3-LIC2 complex.

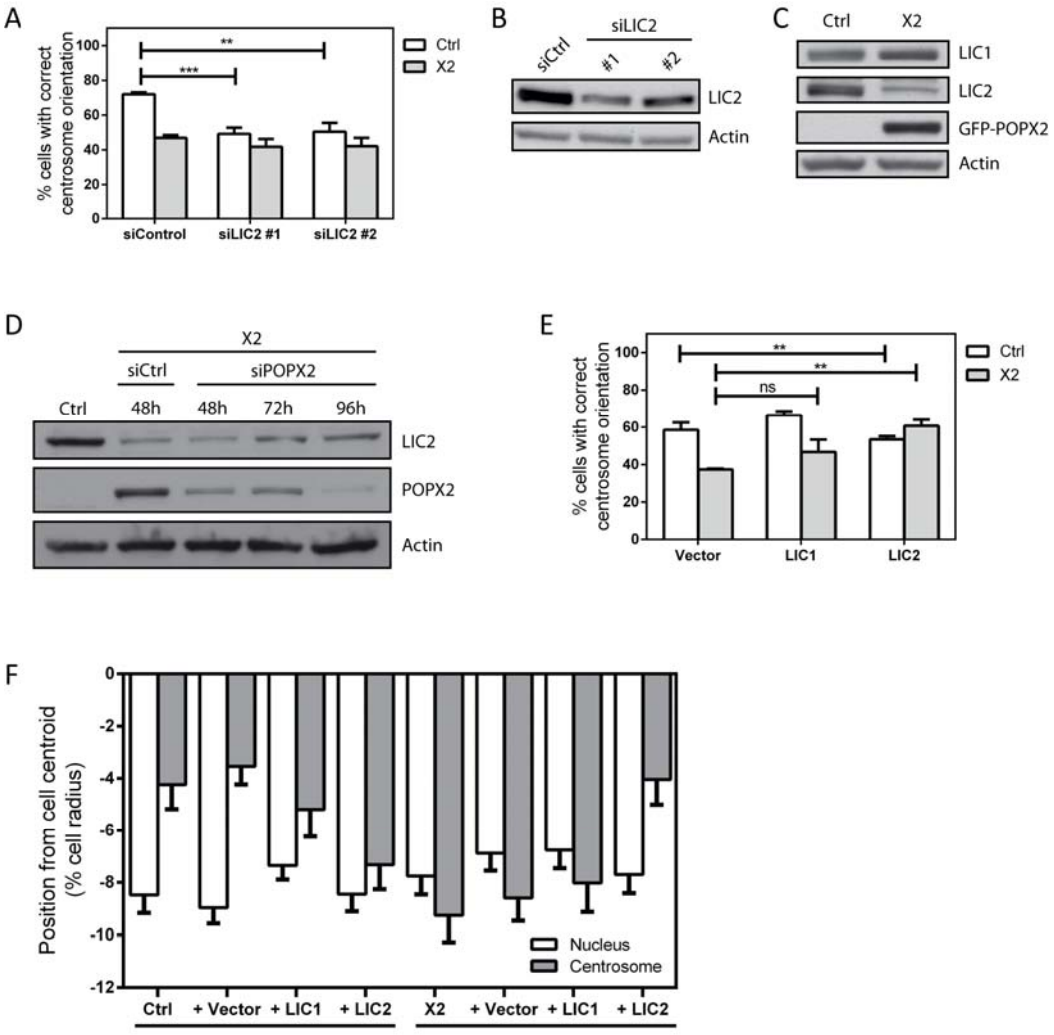

Figure 23. X2 cells are impaired in LIC2 expression, which controls centrosome position and orientation

(A) Histogram showing percentage of Ctrl and X2 fibroblasts transfected with control or LIC2 siRNA with correctly oriented centrosomes 4 hours after wounding. Results are shown as means +/- standard deviation of 3 independent experiments (n=100; Student's T test, **P<0.01, ***P<0.001). (B) Western blot showing knockdown efficiency of LIC2 in NIH3T3 fibroblasts transfected with LIC2 siRNA. Actin was used as a loading control. (C) Western blot showing endogenous levels of LIC1 and LIC2 in Ctrl and X2 fibroblasts. Actin was used as a loading control. (D) Western blot showing increase in LIC2 levels in X2 fibroblasts treated with POPX2 siRNA. Actin was used as a loading control. (E) Histogram showing percentage of Ctrl and X2 fibroblasts transfected with LIC1 or LIC2 with correctly oriented centrosomes 4 hours after wounding. Results are shown as means +/- standard deviation of 3 independent experiments (n=100; Student's T test, **P<0.01). (F) Overexpression of LIC2 is able to rescue the loss of centrosome positioning in X2 cells. Quantification of the position of the nucleus and centrosome along the axis of the cell perpendicular to the wound in Ctrl and X2 cells overexpressing LIC1 or LIC2. The cell centroid is defined as "0". Positive values are towards the leading edge and negative values are towards the rear of the cell. Error bars represent SEM (n=100).

3.1.8 POPX2 affects LIC2 expression at the transcriptional level

The lower LIC2 protein levels observed in X2 cells could be due to a reduction in LIC2 transcription or an increase in LIC2 protein degradation. We next carried out a qPCR to detect mRNA levels of *dync1li2*, which encodes the LIC2 protein. RNA was extracted from Ctrl and X2 cells, and *dync1li2* expression was detected using 2 different primer sets recognizing different regions of the *dync1li2*. We observed lower expression of dync1li2 in X2 cells with both qPCR primers recognizing *dync1li2* (Figure 24A,B), and this suggests that overexpression of POPX2 negatively affects *dync1li2* transcription, resulting in lower LIC2 protein expression.

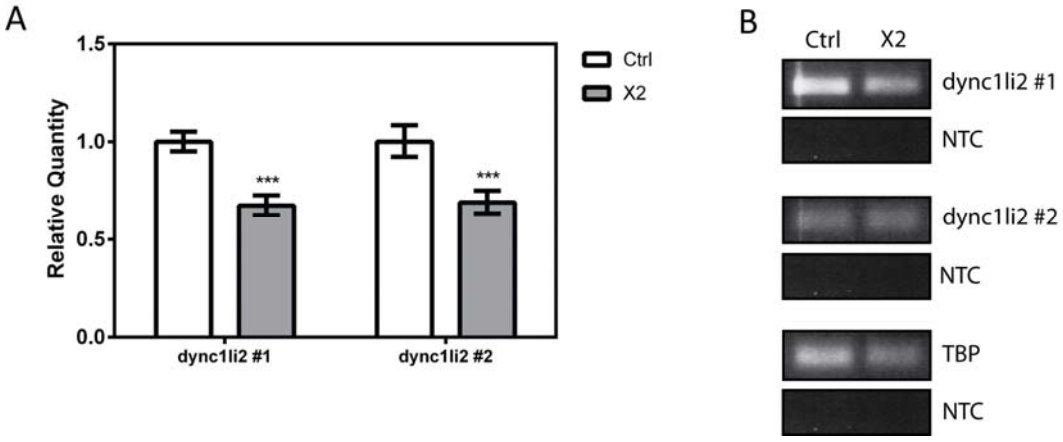

Figure 24. POPX2 affects *dync1li2* mRNA expression
(A) Bar chart showing relative expression of *dync1li2* as detected by 2 different primer sets in Ctrl and X2 cells (Student's T test, **P<0.01). TATA-binding protein (TBP) expression was used as an endogenous control. (B) Agarose gel image showing amplification of cDNA regions recognized by dync1li2 #1, dync1li2 #2 and TBP primer sets. NTC: no template control.

3.1.9 Loss of LIC2 expression and peripheral Par3 localization affects MT pausing at cell-cell contacts

Dynein at the cell cortex, also known as cortical dynein, plays an important role in positioning the mitotic spindle in dividing cells, and positioning the centrosome in migrating fibroblasts. This is carried out through the dynein-mediated regulation of microtubule dynamics and generation of pulling forces that act on the spindle and centrosome (Laan et al., 2012).

Both Par3 and LIC2 contribute to the regulation of microtubule dynamics at cell-cell contacts. Cortical dynein stabilizes microtubule plus ends, and both Par3 and LIC2 are required for microtubule tethering at the cell cortex (Hendricks et al., 2012; Laan et al., 2012; Schmoranzer et al., 2009). We thus went on to monitor microtubule dynamics at cell-cell contacts to observe how overexpression of POPX2 could affect microtubules. NIH3T3 cells were transfected with mCherry-β-tubulin, and microtubules present at cell-cell contacts were imaged and measured (Figure 25A). Various dynamic parameters such as the growth rate, % time growth, shrink rate, % time shrink, pausing and dynamicity were calculated from these measurements (Table 2).

Ctrl cells depleted of LIC2 or Par3 showed a decrease in microtubule pausing time and increase microtubule dynamics while treatment with control siRNA had no effect (Figure 25B). POPX2-overexpression resulted in the same phenotype as loss of LIC2 or Par3, where there was a decrease in microtubule pausing time and an increase in dynamicity (Figure 25, Table 2). Our observations suggest that POPX2 might regulate microtubule dynamics by modulating Par3 and LIC2 in addition to regulating centrosome orientation by affecting Par3 localization and LIC2 levels.

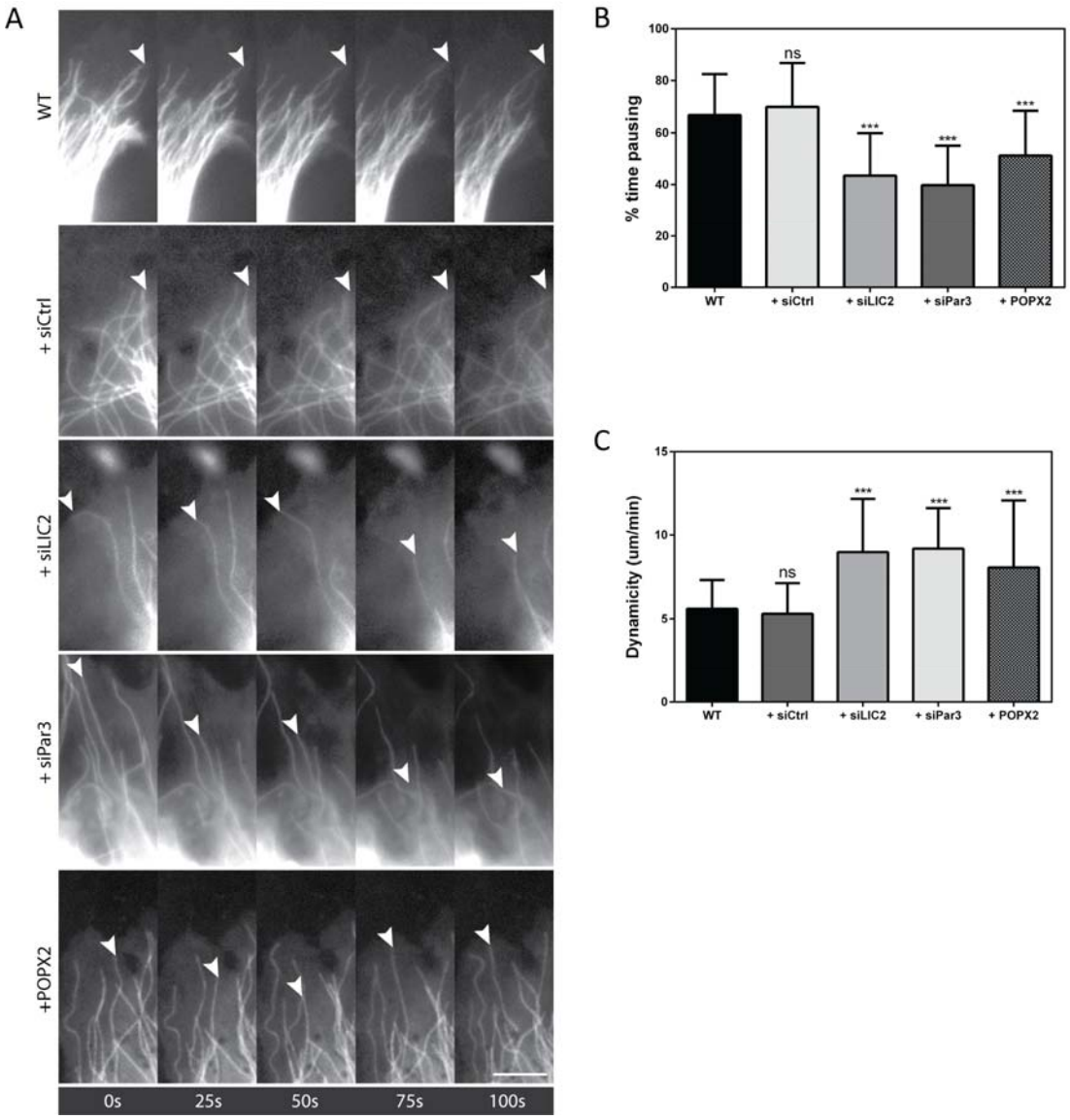

Figure 25. Loss of LIC2 expression and peripheral Par3 localisation affects MT pausing at cell-cell contacts

(A) Frames of movies of NIH3T3 fibroblasts showing MT dynamics at cell-cell contacts under the indicated conditions. Arrowheads indicate dynamic MT ends. Scale bar: 5µm. (B, C) Quantification of (B) % time MTs spent pausing and (C) MT dynamicity at cell-cell contacts in NIH3T3 fibroblasts treated as indicated. Data for each condition are from at least 2 independent experiments and 95-100 MTs. Error bars show SEM (Student's T test, ***P<0.001).

Dynamic parameters	WT (n=100)	+ siCtrl (n=95)		+ siLIC2 (n=95)		+ siPar3 (n=95)		+ POPX2 (n=100)	
Growth rate (μm/min)	8.12 +/- 3.20	7.92 +/- 3.61	(ns)	10.17 +/- 4.10	(***)	11.48 +/- 3.610	(***)	10.09 +/- 2.46	(***)
% time growth	14.48 +/- 10.80	13.70 +/- 10.78	(ns)	24.99 +/- 15.17	(***)	24.73 +/- 10.91	(***)	23.02 +/- 11.06	(***)
Shrink rate (μm/min)	10.43 +/- 3.30	9.49 +/- 4.05	(ns)	14.27 +/- 4.52	(***)	13.67 +/- 3.90	(***)	13.77 +/- 5.54	(***)
% time shrink	19.24 +/- 10.69	16.45 +/- 11.19	(ns)	30.91 +/- 16.07	(***)	35.43 +/- 14.36	(***)	25.51 +/- 13.36	(***)
% time pause	66.60 +/- 15.80	69.80 +/- 16.90	(ns)	43.50 +/- 16.40	(***)	39.80 +/- 15.30	(***)	51.20 +/- 17.10	(***)
Dynamicity (μm/min)	5.61 +/- 1.72	5.31 +/- 1.84	(ns)	8.97 +/- 3.20	(***)	9.18 +/- 2.44	(***)	8.09+/- 3.99	(***)

Table 2. Microtubule dynamics at cell-cell contacts
Stastistically significant differences refer to values within the same parameter that are compared to the values in WT cells (Student's T test, ***P<0.001, ns: not significant).

3.2 Additional studies on LIC2

3.2.1 LIC2 localizes to punctuate structures within the cytoplasm

While the cytoplasmic dynein complex plays an important role in intracellular transport, and multiple studies have been carried out on the dynein heavy, intermediate and light chains, not much is known about the light intermediate chains. We have thus carried out a few additional experiments with the aim to learn more about LIC2.

Immunostaining of LIC1 and 2 in Ctrl cells shows that LIC1 localizes to punctuate, vesicular structures within the cytoplasm as well as the centrosomal region, while LIC2 only localizes to vesicular structures within the cytoplasm (Figure 26A). This observation is consistent with the finding that LIC1, but not LIC2, is able to interact with pericentrin, a component of the pericentriolar material (Tynan et al., 2000b). Immunostaining of LIC2 in both Ctrl and X2 cells show no distinct differences in the localization of vesicles containing LIC2 (Figure 26B), suggesting that overexpression of POPX2 does not affect the distribution of cytoplasmic dynein complexes containing LIC2.

Dynein has been shown to accumulate at the leading edge of migrating cells (Dujardin et al., 2003; Levy and Holzbaur, 2008). To determine whether LIC2 also shows this leading edge accumulation, we stained for LIC2 in wound edge cells fixed 4 hours post-wounding. We observed slight accumulation of LIC2 to the free cell edge of Ctrl cells lining the wound edge (Figure 26C), suggesting that at least some of the dynein vesicles that accumulate at the leading edge during cell migration contain LIC2.

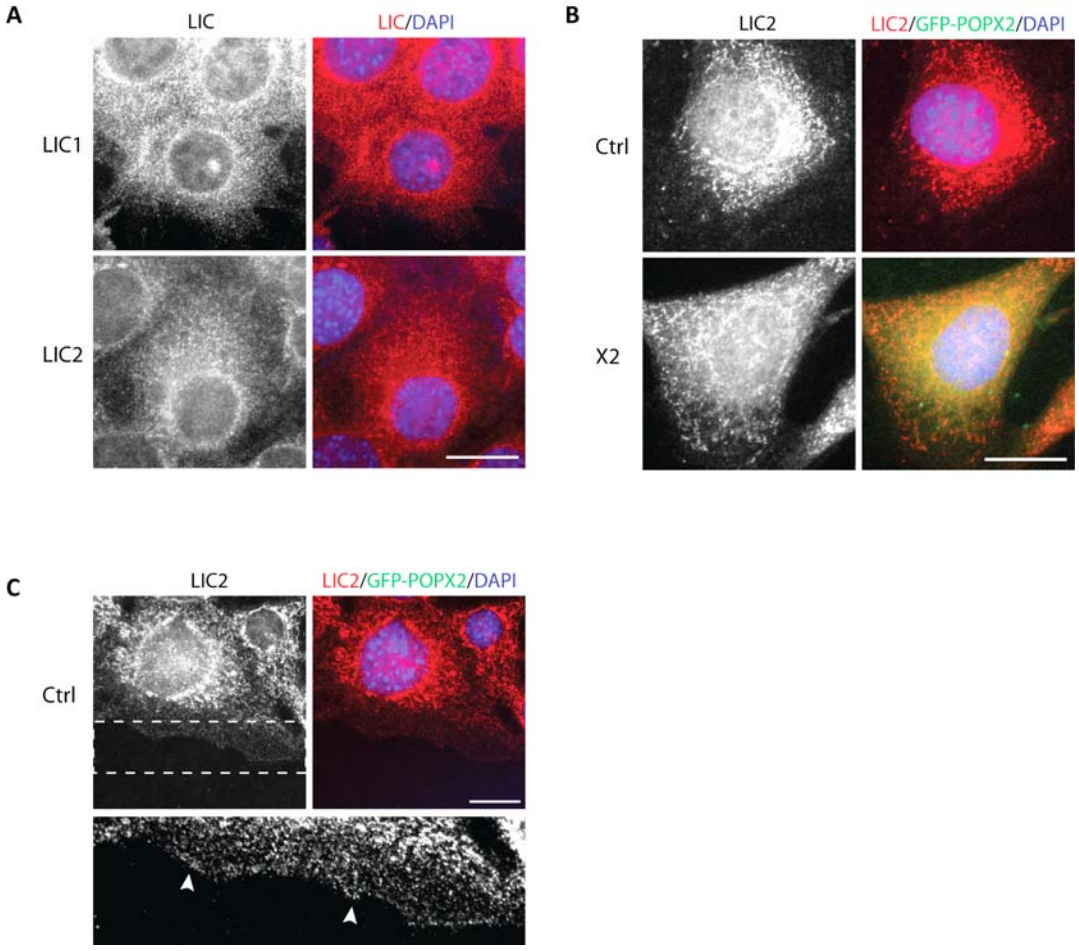

Figure 26. LIC2 localization in NIH3T3 cells
(A) Immunostaining of LIC1 and LIC2 in Ctrl cells. (B) Immunostaining of LIC2 in Ctrl and X2 cells. (C) Immunostaining of LIC2 in Ctrl cells along the wound edge. Boxed area is enlarged below. Arrowheads show accumulation of LIC2 at the leading edge. Scale bar: 20 μm.

3.2.2 Phosphorylation status of LIC2 affects centrosome positioning

Multiple, independent mass spectrometry analyses have indicated that LIC2 is phosphorylated on multiple residues, with S194 being the major site of phosphorylation (Choudhary et al., 2009; Huttlin et al., 2010; Tweedie-Cullen et al., 2012). To determine if phosphorylation controls the activity of LIC2, we generated the phosphomimic (S194D) and phospho-dead (S194A) mutants of LIC2 and overexpressed them in Ctrl and X2 cells. Overexpression of $LIC2^{S194A}$ could not restore proper centrosome orientation in X2 cells; however, overexpression of $LIC2^{S194D}$ had a similar effect as $LIC2^{WT}$ overexpression, and partially restored proper centrosome orientation in X2 cells (Figure 27A). This was confirmed by comparison of the relative positions of the nucleus and centrosome. Overexpression of $LIC2^{S194D}$, but not $LIC2^{S194A}$, brought the centrosome in X2 cells closer to the cell centroid (Figure 27B). This suggests that the activity of LIC2 can be controlled by phosphorylation, and phosphorylation on S194 is required for the activity of LIC2.

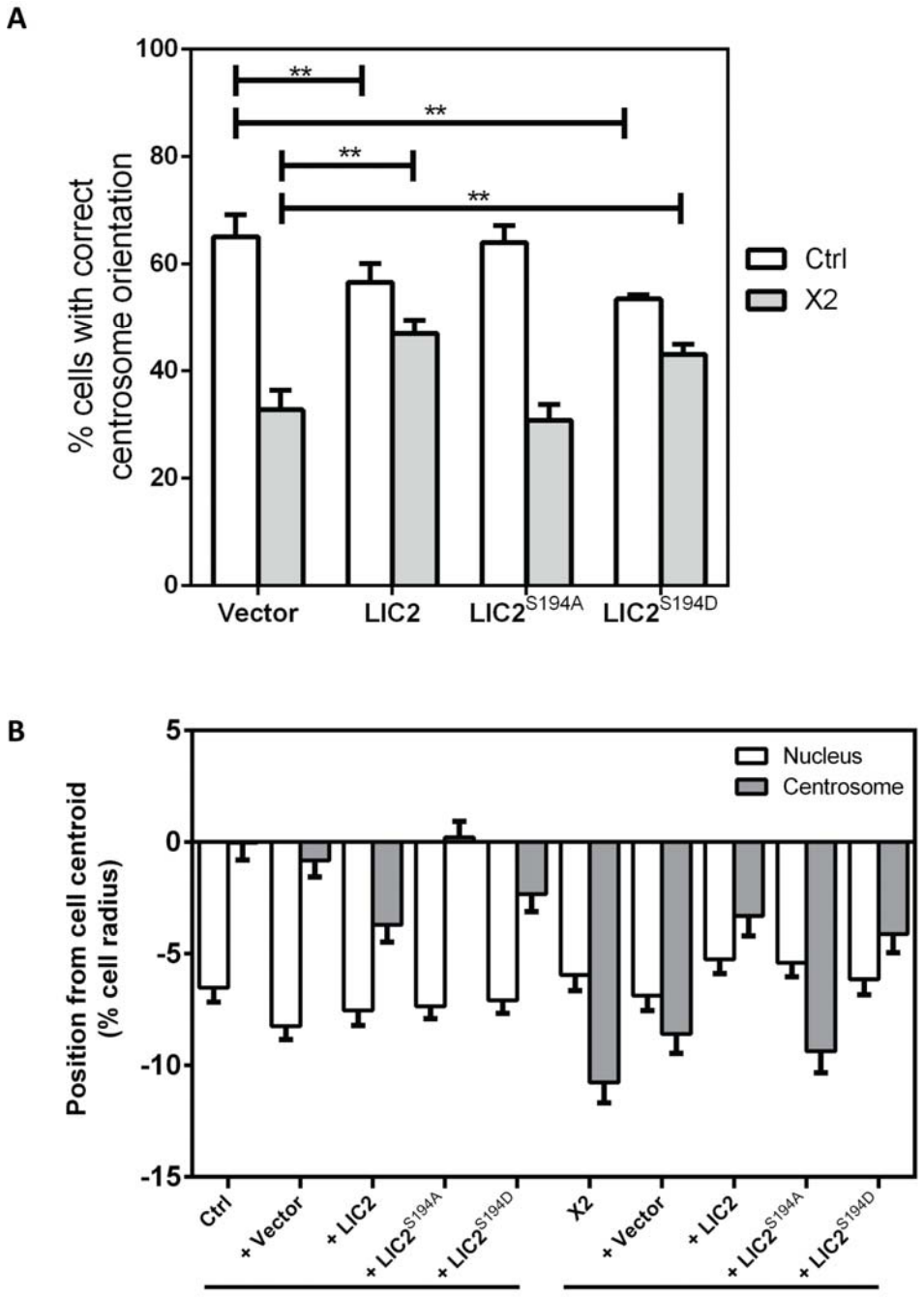

Figure 27. Phosphorylation status of LIC2 affects centrosome positioning

(A) Histogram showing percentage of Ctrl and X2 fibroblasts transfected with empty vector, $LIC2^{WT}$, $LIC2^{S194A}$ or $LIC2^{S194D}$ with correctly oriented centrosomes 4 hours after wounding. Results are shown as means +/- standard deviation of 3 independent experiments (n=100; Student's T test, **P<0.01). (B) Overexpression of $LIC2^{WT}$ and $LIC2^{S194D}$ are able to rescue the loss of centrosome positioning in X2 cells. Quantification of the position of the nucleus and centrosome along the axis of the cell perpendicular to the wound in Ctrl and X2 cells overexpressing empty vector, $LIC2^{WT}$, $LIC2^{S194A}$ or $LIC2^{S194D}$. The cell centroid is defined as "0". Positive values are towards the leading edge and negative values are towards the rear of the cell. Error bars represent SEM (Student's T test, n=100).

3.2.3 Phosphorylation status of LIC2 affects motility of LIC2-containing intracellular structures

Since LIC2 is part of the cytoplasmic dyenin 1 motor complex, and phosphorylation of LIC2 on serine-194 appears to influence centrosome positioning, we wanted to determine whether phosphorylation on serine-194 had other effects on LIC2-containing dynein complexes. We decided to track LIC2-containing intracellular structures to determine their intracellular behavior.

mCherry-tagged $LIC2^{WT}$, $LIC2^{S194A}$ or $LIC2^{S194D}$ were transfected into Ctrl cells, imaged, and the paths of taken by individual LIC2-containing intracellular structures were tracked. The speed of these structures were calculated and presented as a histogram (Figure 28). mCherry-$LIC2^{WT}$ and mCherry-$LIC2^{S194D}$-containing intracellular structures moved at comparable speeds, while mCherry-$LIC2^{S194A}$-containing intracellular structures migrated at a slower rate (Figure 28B,D,E; Figure 29A). Comparison of mCherry-$LIC2^{WT}$-containing intracellular structures transfected into Ctrl and X2 cells showed that these structures migrated at significantly higher speeds in Ctrl as compared to X2 cells (Figure 28B,H; Figure 29B).

Taken together, the above results suggest that phosphorylation could affect the motility of LIC2-containing intracellular structures. However, LIC2 itself does not have any motor activity, and the intracellular movement of cytoplasmic dynein complexes is generated by the motor domain of the heavy chain instead. Thus, the above observations cannot be attributed to changes in the motor activity of the dynein complex. Moreover, since only LIC2 was tagged with a flurorescent tag, it is impossible to tell whether the LIC2 imaged was interacting with the dynein heavy chain.

A more plausible explanation would be that phosphorylation on serine-194 could affect the binding of LIC2 to the dynein heavy chain. A loss of phosphorylation on this residue might reduce the affinity of LIC2 for the heavy chain. As a result, a portion of the LIC2-containing intracellular structures imaged were actually free LIC2 proteins in the cytoplasm that were not functioning as part of an active dynein complex, resulting in the decreased motility observed.

It is also interesting to note that the LIC2-containing intracellular structures imaged in X2 cells migrated at a slower rate as compared to LIC2^{S194A}-containing intracellular structures imaged in Ctrl cells (Figure 28D,G). This suggests that (1) serine-194 might not be the only point of regulation within the LIC2 protein, and/or (2) overexpression of POPX2 is able to affect the motility of LIC2-containing intracellular structures through other means, for example, affecting the motor activity of the dynein heavy chain.

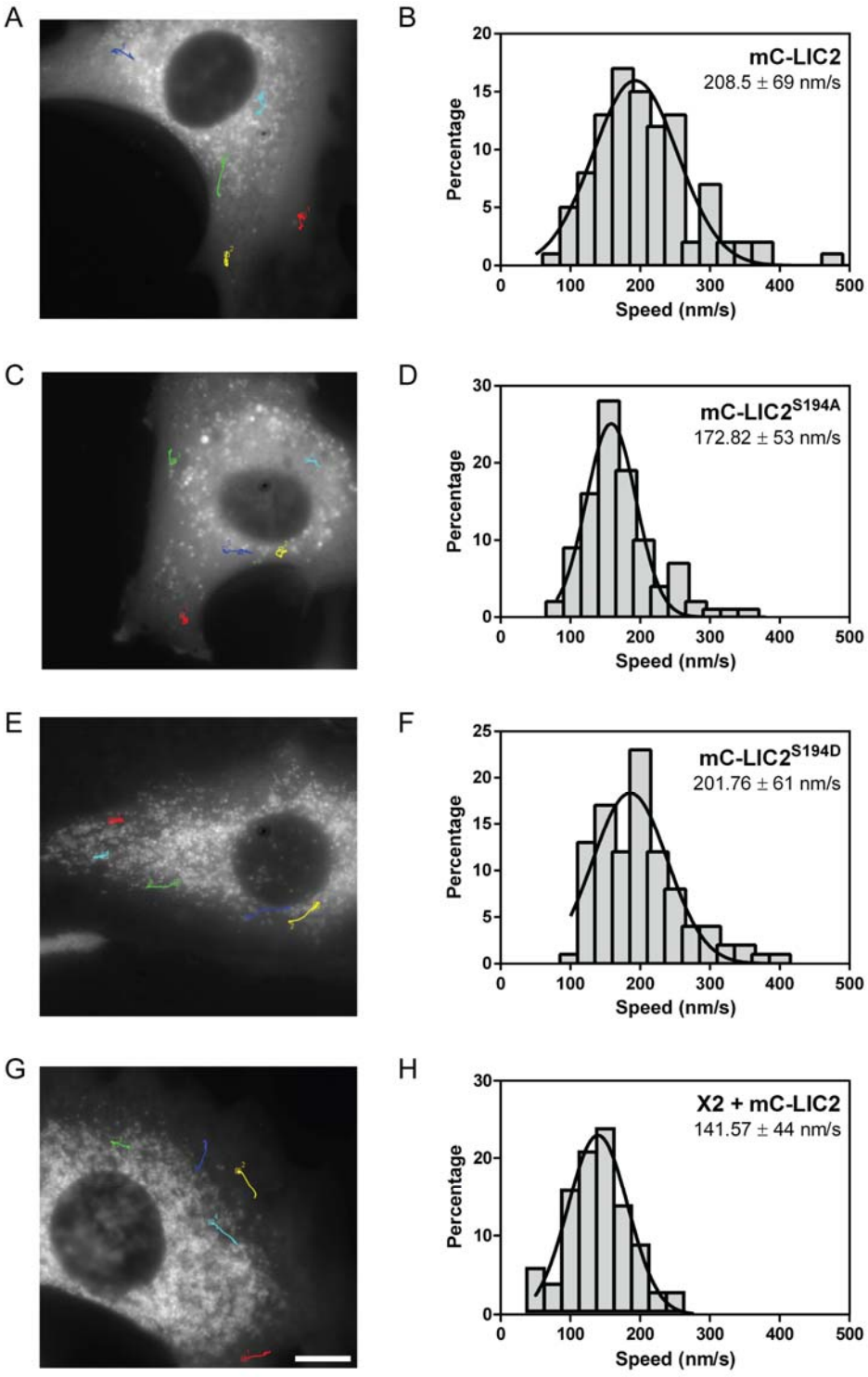

Figure 28. LIC2-containing intracellular structures move at different speeds depending on their phosphorylation status

Representative images of mCherry-tagged (A) $LIC2^{WT}$, (C) $LIC2^{S194A}$ or (E) $LIC2^{S194D}$ tracked in Ctrl and (G) X2 cells, as well as histograms depicting the speed distribution of (B) $LIC2^{WT}$, (D) $LIC2^{S194A}$ or (F) $LIC2^{S194D}$ tracked in Ctrl and (H) X2 cells. 100 vesicles were tracked in multiple cells across at least 2 independent experiments. Scale bar: 10µm.

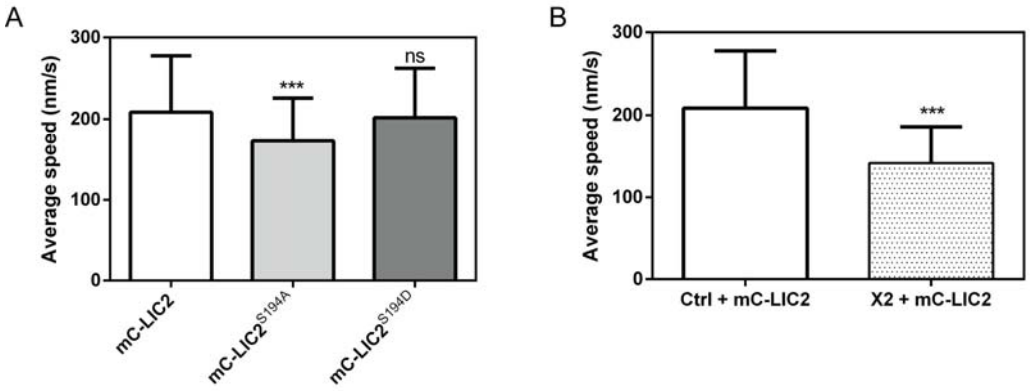

Figure 29. Comparison of motility of LIC2-containing intracellular structures

(A) Comparison of average speed of $LIC2^{WT}$, $LIC2^{S194A}$ and $LIC2^{S194D}$-containing intracellular structures in Ctrl cells (n=100; Student's T test, ***P<0.001, ns: not significant). (B) Comparison of average speed of $LIC2^{WT}$-containing intracellular structures in Ctrl and X2 cells. Results are shown as means +/- standard deviation of 3 independent experiments (n=100; Student's T test, ***P<0.001).

3.2.4 ATM and Aurora kinases are predicted to phosphorylate LIC2 on serine-194

Having determined that phosphorylation of LIC2 on serine-194 affects its ability to regulate centrosome positioning, we wanted to find out which kinase(s) is/are responsible for phosphorylating LIC2 on this residue. Since the kinases involved in phosphorylating LIC2 have yet to be experimentally determined, we made use KinasePhos 2.0 (Wong et al., 2007), an online server for identifying protein kinase-specific phosphorylation sites, to predict which kinase(s) might phosphorylate LIC2 on serine-194. KinasePhos 2.0 predicted ATM and Aurora as the kinases that are likely to phosphorylate LIC2 on serine-194 (Table 3, Figure 30). Whether these kinases are indeed responsible for phosphorylating LIC2, however, still needs to be experimentally proven.

Location (AA)	Phosphorylated site	SVM score	Catalytic kinase
194	GCQG**S**PQRR	0.932154	ATM
194	GCQG**S**PQRR	0.943217	Aurora

Table 3. Kinases predicted to phosohorylate LIC2 on serine-194
ATM and Aurora kinase were predicted to phosphorylate LIC2 on serine-194 using KinasePhos 2.0 (Wong et al., 2007). SVM (support vector machine) score indicates how accurate the prediction is likely to be.

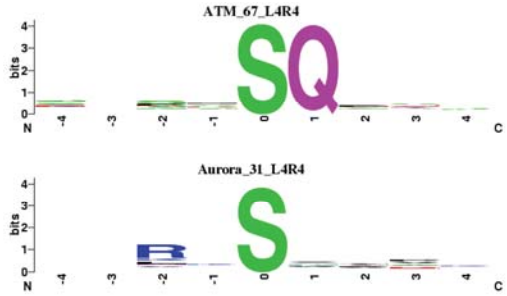

Figure 30. Motif logo showing sequence recognition by ATM and Aurora kinases

3.2.5 LIC2 does not interact with POPX2 or POPX2m

We have shown that POPX2 overexpression affects LIC2 on a transcriptional level by negatively impacting on dync1li2 transcription. However, it is unknown whether POPX2 could affect LIC2 on a protein level as well. Since POPX2 is able to interact with the Kinesin-2 heterodimeric motor (Phang et al., 2014), we wanted to determine whether POPX2 is able to interact with the cytoplasmic dynein complex as well. To determine whether POPX2 is able to interact with LIC2, we overexpressed GST-POPX2, GST-POPX2m and Flag-LIC2 in COS-7 cells and carried out a pull-down assay using GST beads. Pull-down of both POPX2 and POPX2m failed to bring down LIC2 (Figure 31), indicating that POPX2 and LIC2 are not able to interact with one another.

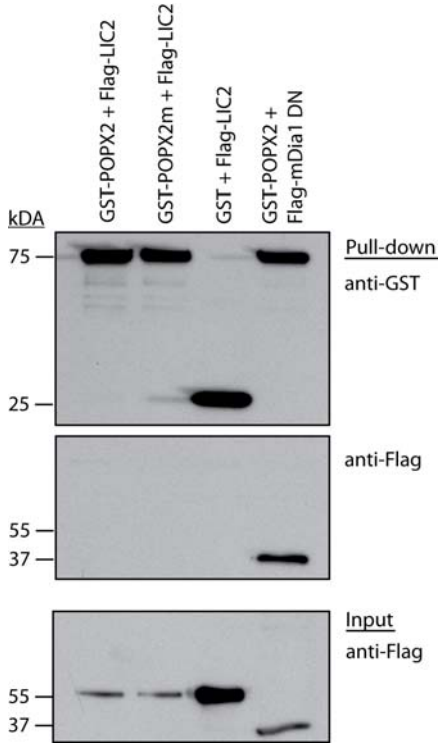

Figure 31. LIC2 does not interact with POPX2 or POPX2m
(A) Western blot showing pull-down of POPX2, POPX2m and LIC2. Both POPX2 and POPX2m fail to interact with LIC2. GST + Flag-LIC2 was used as a negative control, while GST-POPX2 + Flag-mDia1 DN was used as a positive control.

4. Discussion

4.1 POPX2 acts as a regulator of centrosome positioning

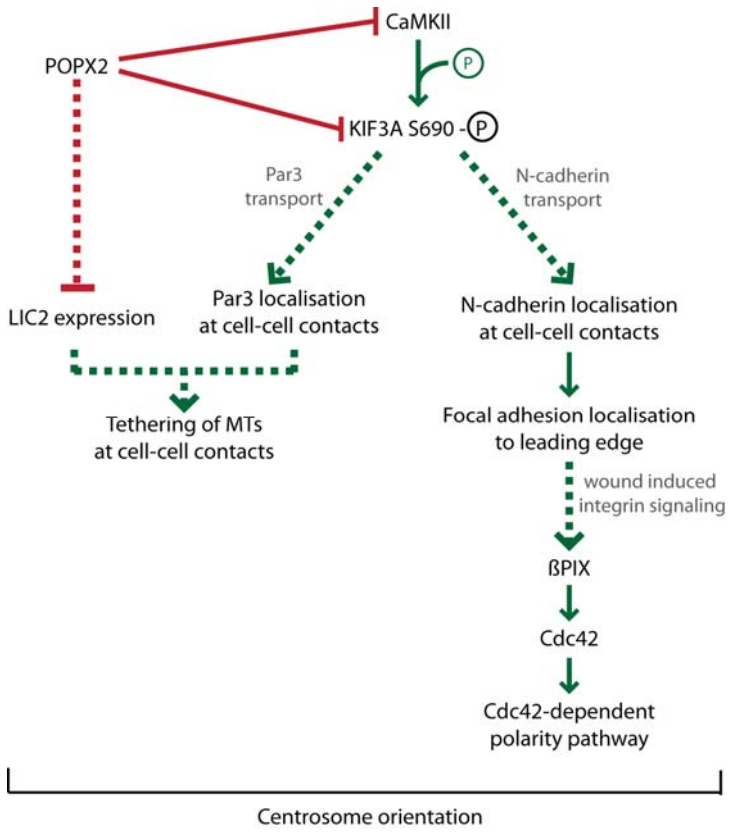

Figure 32. POPX2 inhibits centrosome orientation by affecting LIC2 expression and Kinesin-2 motor transport

POPX2 dephosphorylates KIF3A on S690 either directly or through inhibition of CaMKII activity. This results in a reduction of KIF3A motility, inhibiting the transport of Kinesin-2 cargoes such as N-cadherin and Par3. Due to the loss of N-cadherin localization at cell-cell contacts, focal adhesions are no longer restricted to the leading edge, and instead localize throughout the cell periphery (Dupin et al., 2009). Activation of the Cdc42-dependent polarity pathway as a result of βPIX recruitment to focal adhesions is no longer spatially restricted (Etienne-Manneville and Hall, 2003a; Osmani et al., 2010). Loss of Par3 localization to cell-cell contacts, as well as the inhibition of LIC2 expression as a result of POPX2 activity results in a loss of tethering of MTs at cell-cell contacts (Schmoranzer et al., 2009). The combined effect of POPX2 on these different pathways results in the loss of proper centrosome orientation upon wounding.

Centrosome positioning involves multiple proteins that act in multiple pathways, and is affected by factors such as cell shape and confluence. The process of centrosome positioning is controlled differently in single and confluent cells, and involves different proteins – centrosome positioning in single cells is regulated by EB1 and LIC1, while the same process is regulated by Par3 and LIC2 in confluent monolayers (Hale et al., 2011). We have chosen to focus on centrosome positioning in confluent fibroblast monolayers in this study due to its relevance in cellular processes such as development and wound healing. Many proteins that play a role in centrosome positioning have already been identified, and the pathways they function in elucidated; however, it remains unclear if these different pathways are regulated collectively or independently. Our work shows that POPX2 affects centrosome orientation through inhibiting centrosome centration and not nuclear movement (Figure 12C, Figure 14), and indicates that POPX2 is able to affect multiple proteins that regulate centrosome positioning, and thus acts as a regulator of centrosome orientation (Figure 32).

Cdc42 is well-accepted to be the Rho-GTPase that controls centrosome positioning. When Cdc42 is activated at the free cell edge, it recruits and activates the Par6/PKCζ complex (Etienne-Manneville and Hall, 2001; Gomes et al., 2005; Palazzo et al., 2001; Tzima et al., 2003). The localized activation of Cdc42 requires integrin activation at the free cell edge, and is achieved through crosstalk as well as spatial segregation between cell-cell and cell-matrix adhesions. Local negative feedback between both systems is thought to result in their spatial segregation through a process that involves actin. Formation of cell-cell contacts triggers assembly of the actin cytoskeleton, and this process generates a tugging force at cell-cell contacts, resulting in the local disassembly of cell-matrix adhesions (Burute and Thery, 2012; McCain et al., 2012; Vasioukhin et al., 2000). The involvement of cell-cell and cell-matrix adhesions in centrosome positioning thus implicates focal adhesion distribution and signaling, as well as N-cadherin transport and expression in the process.

Our results confirm the requirement of Cdc42 and N-cadherin in centrosome positioning, as loss or inhibition of either protein inhibits proper centrosome orientation (Figure 16A; Figure 20A,C). We also show that proper localization of N-cadherin and focal adhesions, which is dependent on Kinesin-2-mediated transport, is required for proper centrosome

orientation (Figure 15, Figure 17, Figure 19), which is consistent with what has been established in earlier studies.

Centrosome positioning also involves the dynein-dynactin complex. The complex acts downstream of Par6/PKCζ (Etienne-Manneville and Hall, 2001; Gomes et al., 2005; Palazzo et al., 2001; Tzima et al., 2003), but how Par6/PKCζ affects the dynein-dynactin complex remains unknown. What is known, however, is that dynein complexes containing LIC2 are able to interact with Par3 that is present at the cell periphery. This tethers the microtubule ends to the cell cortex and stabilizes them, thus resulting in decreased microtubule dynamicity and increased microtubule pausing time. The interaction between LIC2 and Par3 also results in the generation of a pulling force on the centrosome, thus allowing it to be positioned close to the cell center (Hendricks et al., 2012; Laan et al., 2012; Schmoranzer et al., 2009). Loss of Par3 or LIC2 would thus impair centrosome orientation, and this was confirmed in our study (Figure 21A, Figure 23A,F). This impairment of proper centrosome orientation is caused by a decrease in microtubule pausing at cell-cell contacts (Figure 25), which affects the pulling force generated on the centrosome.

Overexpression of POPX2 results in a reduction in LIC2 expression and a loss of Par3 localization to the cell periphery. As a result, fewer microtubule ends are able to tether to the cell cortex, resulting in a reduction in microtubule stability. Thus, POPX2-overexpressing cells show an increase in microtubule dynamicity and a reduction in microtubule pausing time, and this translates to an impairment in proper centrosome positioning.

Our results show that centrosome orientation is controlled by multiple pathways which have been identified in previous studies. They also suggest that the currently known pathways regulating centrosome positioning function cooperatively, as disruption of a single pathway results in a loss of proper centrosome positioning (Figure 16, Figure 17, Figure 21, Figure 23). If the pathways were to function independently, then disruption of one pathway should not have a great effect on centrosome positioning, since the other pathway(s) will be able to compensate for it.

Our work implicates POPX2 as a negative regulator of centrosome orientation through 2 means: (1) impairing transport of N-cadherin and Par3 to cell-cell contacts and (2) inhibiting LIC2 protein expression. Overexpression of POPX2 impairs Kinesin-2-mediated transport of

N-cadherin and Par3 by keeping the KIF3A subunit of the Kinesin-2 complex in a dephosphorylated state. This is achieved through (1) dephosphorylating KIF3A on serine-690 and/or (2) inhibition of CaMKII, which phosphorylates KIF3A on serine-690 (Figure 17 **Figure 17**) (Phang et al., 2014). Overexpression of POPX2 results in a loss of LIC2 protein expression by resulting in a decrease in *dync1li2* transcription (Figure 23, Figure 24, Figure 32).

The limitation of our work, however, is that is heavily relies on the overexpression of transgenes. We have been unable to study the effects of endogenous POPX2 knockdown in NIH3T3 cells due to the lack of a good antibody that is able to detect mouse POPX2 protein, thus limiting our work to studying the overexpression of human POPX2 in NIH3T3 cells by using a stable cell line expressing GFP-POPX2. There are limitations to this approach, one of which is the difficulty in controlling transgene expression. A high level of transgene expression might lead to perturbation of other signaling pathways or cellular processes. Also, insertion of the transgene during the generation of the stable cell line might result in the disruption of other genes, thus affecting non-target signaling pathways. We have tried to prevent this problem by not carrying out clonal selection while generating the POPX2 stable cell line, as well as confirming that NIH3T3 cells transiently overexpressing POPX2 also show the same defects in centrosome orientation.

Should a good antibody against mouse POPX2 protein become available, it would be very useful to repeat these experiments using RNAi or other loss-of-function approaches to study the effect of the loss of endogenous POPX2 on centrosome orientation and wound healing. Performing such experiments would further support our hypothesis if the results agree with those obtained in this study, and can also provide some clues as to whether POPX2 protein expression needs to exceed a certain threshold before its effects on centrosome orientation can be observed, allowing for a better understanding of POPX2's function in centrosome positioning.

In addition to the above, our findings also highlight the importance of regulating POPX2, either through controlling its expression or modulating its activity. Since POPX2 is implicated in Kinesin-2-mediated transport, modulating the activity of POPX2 will affect the speed and amount of Kinesin-2 cargoes being transported intracellularly, which in turn affects

numerous cellular processes including, but not limited to, cell-cell adhesion, endocytic protein recycling and insulin signaling (Imamura et al., 2003; Schonteich et al., 2008; Teng et al., 2005). POPX2 expression levels could also influence cytoplamic dynein 1 function by affecting LIC2 expression. The heavy chain of cytoplasmic dynein 1 binds to either LIC1 or LIC2 in a mutually exclusive manner (Palmer et al., 2009; Tynan et al., 2000b), and this influences the function of the resulting dynein complex. LIC1 is involved in centrosome assembly, organization and function, and is also required at the Golgi (Palmer et al., 2009; Purohit et al., 1999; Tynan et al., 2000a), while LIC2 is required for centrosome orientation and at recycling endosomes (Palmer et al., 2009; Schmoranzer et al., 2009). Since high levels of POPX2 inhibits LIC2 expression, it is likely to shift the balance of heavy chain binding towards LIC1, while low levels of POPX2 expression could promote LIC2 binding. This balance between binding of LIC1 or LIC2 to the heavy chain could in turn target the cytoplasmic dynein 1 complex towards different functions.

The amount of POPX2 expression also affects directional cell migration. Directional cell migration is essential in cellular processes such as the immune response, embryogenesis and wound healing, and the orientation of the centrosome determines the direction of cell migration in multiple cell types.

By maintaining tight control over the expression of POPX2, cells are able to ensure that their centrosomes can be correctly oriented, and thus migrate in the right direction. Loss of regulation of POPX2 expression, on the other hand, results in defects in cell migration, which on a larger scale, could lead to developmental defects. Loss of cell polarity is also associated with tumorigenesis and cancer cell invasion. Consistent with this, POPX2 levels have been found to be higher in more invasive breast cancer cells as compared to non-invasive ones (Susila et al., 2010). Thus, POPX2 could act as a major regulator of cell polarity by integrating both cell-cell- and cell-matrix-dependent signaling pathways through regulating kinesin-2-N-cadherin and the βPIX-Cdc42-Par3/LIC2 pathway respectively, as well as through controlling the localization of polarity proteins such as Par3.

4.2 Transcriptional regulation of *dync1li2*

Our results show that LIC2 protein expression is decreased in X2 cells, and this decrease is due to a reduction of *dync1li2* transcription. Thus, it would be of interest to investigate how overexpression of POPX2 might inhibit the transcription of *dync1li2*.

Transcriptome analysis carried out in POPX2 knockdown cells have suggested that a number of transcription factors are differentially regulated in a manner dependent on POPX2 levels (Zhang et al., 2013), and it is likely that one or more of these transcription factors is/are responsible for controlling transcription of *dync1li2*. However, the exact transcription factor(s) that is/are responsible for controlling *dync1li2* expression is currently unknown.

Prediction of transcription factors that might bind to the *dync1li2* promoter was carried out using TFSEARCH (Appendix A) (Heinemeyer et al., 1998), and the potential transcription factors produced was compared to the list of transcription factors that are regulated by POPX2 (Zhang et al., 2013). Transcription factors found in both the list of transcription factors likely to be regulated by POPX2 and also predicted by bind to the *dync1li2* promoter are listed in Table 4.

Transcription factor	No. of binding sites	Phosphorylating kinase(s) as predicted by	
		PhosphoSite	NetworKIN kinase family
C/EBP	1	MAPK1/3	-
GATA1	2	AKT1	EGFR, RSK, PKC, PKB
HFH-1	2	-	-
HSF	17	MAPK1/3, GSK3B, PLK1, CK2-A1, CK-A2, PKACa	p38MAPK, MAPK1/3, GSK3, CDK5, PKA, RSK
MZF1	5	-	PKA
S8	1	-	-
SRY	5	-	-
TATA	2	-	-
YY1	3	CK2-A1	CKII, PKC, EGFR, INSR

Table 4. Transcription factors predicted to bind to *dync1li2* promoter which are also downregulated with increasing POPX2 expression

Since reduction of *dync1li2* expression is dependent on the phosphatase activity of POPX2, it is likely that the transcription factor involved in *dync1li2* expression is controlled by phosphorylation, reducing the potential hits to C/EBP, GATA1, HSF and YY1. Of these, C/EBP (CCAAT/enhancer binding protein) and HSF (heat shock factor) are of particular interest, as they are phosphorylated by MAP Kinases, whose phosphorylation status and activities are affected by POPX2 levels. High levels of POPX2 are correlated with increasing phosphorylation, and hence activity, of MAP Kinases (Singh et al., 2011; Zhang et al., 2013). Phosphorylation of C/EBP by MAPK1/3 on T188 activates it, allowing activation of transcription (Piwien-Pilipuk et al., 2002; Tang et al., 2005); on the other hand, phosphorylation of HSF-1 by MAPK1/3 results in repression of transcription (Chu et al., 1996; He et al., 1998). Phosphorylation of HSF-1 by other kinases, on the other hand, is able to activate transcription (Guettouche et al., 2005; Holmberg et al., 2001). This makes HSF a plausible candidate that regulates *dync1li2* transcription. Interestingly, HSF-1 is phosphorylated on Ser^{230} by CaMKII, which results in its activation (Holmberg et al., 2001). CaMKII is a substrate of POPX2, and inactivation of CaMKII by POPX2 could be another way in which HSF-1 transcriptional activity is inhibited in POPX2 cells.

DYNC1LI2 transcript expression is down-regulated in HeLa cells in response to heat shock, and HSF motifs have been detected in Alu repeats both in the upstream and genic regions of the *DYNC1LI2* transcript (Pandey et al., 2011), suggesting that HSF regulates transcription of *DYNC1LI2*. In further support of this, *DYNC1LI2* expression has also been shown to be different in mammary epithelial cells and breast cancer cells subjected to hypothermia (Amaya et al., 2014).

To confirm whether HSF is indeed the transcription factor regulating *dync1li2* expression, a luciferase assay can be carried out. The promoter of *dync1li2* can be cloned into a luciferase reporter vector, and binding of the appropriate transcription factor will result in transcription of the luciferase gene, which codes for the luciferase enzyme that can act on its substrate to give off bioluminescence. Electrophoretic mobility shift assays (EMSA) can also be carried out for further confirmation. Purified HSF protein can be added to a DNA fragment containing the *dync1li2* promoter to see if the protein is able to bind to it.

4.3 Localization of LIC2

Immunostaining of LIC2 in Ctrl and X2 cells did not show significant differences in localization of this protein in both cell types (Figure 26B). While this suggests that overexpression of the phosphatase does not affect localization of LIC2, it does not rule out the possibility that overexpression of POPX2 has other effects on LIC2 in addition to affecting its transcription. Since POPX2 is a phosphatase, its overexpression might also affect LIC2 phosphorylation, and this is worth investigating. Changes in LIC2 phosphorylation might affect the activity of the protein or its interaction with other binding partners without affecting localization of the protein.

Dynein has been observed to localize at the leading edge of migrating cells (Dujardin et al., 2003; Levy and Holzbaur, 2008), and this is thought to result in a increase in the dynein force-producing capacity at the leading edge. This pulling force generated at the leading edge could serve to balance the rearward actomyosin-mediated forces to keep the centrosome at the cell center (Vallee and Stehman, 2005). The dynein heavy chain, intermediate chains and p150 are known to localize to the leading edge, and LIC2, being a component of the cytoplasmic dynein complex, would thus be expected to localize to the leading edge as well. However, we only observed a slight localization of LIC2 to the leading edge of our scratch-wounded cells (Figure 26C). There are a few reasons that could explain this: firstly, our cells were fixed for immunostaining at 4 hours post-wounding. Not all the cells might already be migrating to close the wound at this time point, and it is difficult to distinguish migrating cells from non-migrating ones during the imaging of our fixed cells. The cells could be fixed at a longer time post-wounding so that more cells are in the stage of migration to see if there is more LIC2 localization to the leading edge. Should there still be little LIC2 localized to this region, it could suggest that the subset of dynein that localizes to the leading edge might not preferentially contain LIC2, or that LIC2 is not specifically involved in the increased force generation at the leading edge of migrating cells.

4.4 Phosphorylation status of LIC2 affects its ability to regulate centrosome orientation

Phosphorylation of the cytoplasmic dynein complex has been shown to regulate its motor activity, intracellular targeting and binding to cargoes or accessory proteins. Phosphorylation of the cytoplasmic dynein complex is likely to be regulated by multiple kinases and phosphatases, and variable phosphorylation of the different subunits may help to independently regulate specific steps of dynein-mediated transport.

The dynein heavy chain appears to be less phosphorylated in the anterograde pool, which contains inactive dynein, as compared to the intracellular pool, which contains both active and inactive dynein (Dillman and Pfister, 1994). Phosphorylation of the intermediate chains, on the other hand, regulates its binding to proteins such as dynactin and zw10, and in turn affects its binding to its cargoes as well as its intracellular targeting (Vaughan et al., 2001; Whyte et al., 2008). Phosphorylation on serine-88 of dynein light chain 1 affects the dimerization status of the light chain and affects its interaction with substrates (Song et al., 2008).

Mass spectrometry has identified multiple phosphorylation sites on LIC2 (Choudhary et al., 2009; Huttlin et al., 2010; Tweedie-Cullen et al., 2012), and this has been experimentally proven by alkaline phosphatase treatment of LIC2 (Gill et al., 1994; Hughes et al., 1995). Treatment with alkaline phosphatase results in a reduction in molecular mass of the protein, leading to a band shift when the protein is run on a polyacrylamide gel. However, other biochemical work has yet to be done to provide further insight into the phosphorylation status of LIC2 and how it could control LIC2 activity.

Serine-194 has been identified as the major phosphorylation site in LIC2 by multiple mass spectrometry analyses (Choudhary et al., 2009; Huttlin et al., 2010; Tweedie-Cullen et al., 2012); however, no molecular work has been done to determine the effect of LIC2 phosphorylation on this residue. In this work, we have shown that phosphorylation on LIC2 on this reside is required for proper centrosome positioning (Figure 27), suggesting that phosphorylation on LIC2 affects its activity. Additionally, phosphorylation on serine-194 appears to affect the motility of LIC2-containing structures (Figure 28, Figure 29). Since LIC2 has no known motor activity, we propose that phosphorylation on serine-194 affects the

binding of LIC2 to the heavy chain. Binding of LIC2 to the heavy chain might be reduced in the absence of phosphorylation on serine-194, resulting in the lower motility observed. This reduced binding between LIC2 and the heavy chain would also prevent the generation of a sufficient, balanced pulling force that is required to position the centrosome at the cell center, as this is dependent on the motor activity of the cytoplasmic dynein complex, thus preventing proper centrosome positioning. Further experiments are needed to support this hypothesis.

Our results thus far suggest that POPX2 affects centrosome positioning through affecting LIC2 expression. Since POPX2 is a phosphatase, there is also a possibility that POPX2 might affect the phosphorylation of LIC2. POPX2 might be able to dephosphorylate LIC2 directly, or inactivate the kinases that phosphorylate LIC2. To study this, it would be useful to first determine whether LIC2 is differentially phosphorylated in Ctrl, X2 and X2m cells. A difference in phosphorylation levels would suggest that overexpression of POPX2 affects phosphorylation of LIC2, and a phosphatase assay can be carried out to determine whether POPX2 is capable of directly dephosphorylating LIC2.

If LIC2 is differentially phosphorylated in Ctrl and X2 cells, yet POPX2 does not directly dephosphorylate LIC2, then it is possible that POPX2 regulates the activity of the kinase that phosphorylates LIC2 instead. Prediction of the kinases responsible for phosphorylating LIC2 have suggested that ATM and Aurora kinase are responsible for phosphorylating LIC2 on serine-194 (Table 3). However, such prediction models are not always accurate, and *in vitro* kinase assays need to be carried out in future to determine if either kinase can actually phosphorylate LIC2. After the kinase involved is identified, a phosphatase assay can be carried out to determine whether POPX2 is able to dephosphorylate the kinase to regulate the phosphorylation of LIC2.

5. Conclusion

Scratch wounding of fibroblasts results in the loss of N-cadherin at what becomes the free edge of the cell facing the wound. Focal adhesions, which are excluded from regions of cell-cell contact, later form at the free edge of the cell. They are able to recruit βPIX, which activates Cdc42-Par6/PKCζ signaling to position the centrosome at the cell center. At the microtubule ends present at cell-cell contacts, LIC2-containing dynein complexes interact with Par3 to tether microtubules to the cell cortex, generating a pulling force that also helps to position the centrosome. In this study, we found that overexpression of POPX2 perturbs the localized activation of Cdc42-Par6/PKCζ signaling and microtubule tethering to inhibit proper centrosome positioning. This is achieved through inhibition of N-cadherin and Par3 transport to the cell periphery by Kinesin-2, as well as inhibition of *dync1li2* transcription. Thus, POPX2 acts as a negative regulator of centrosome positioning.

LIC2 plays an important role in controlling centrosome orientation. In addition to LIC2 protein levels, the phosphorylation status of LIC2 also appears to influence the centrosome orientation process. However, only preliminary work has been done in this area, and more experiments have to be carried out in the future to better understand how phosphorylation affects the activity of LIC2 and LIC2-containing dynein complexes.

6. References

Amaya, C., Kurisetty, V., Stiles, J., Nyakeriga, A.M., Arumugam, A., Lakshmanaswamy, R., Botez, C.E., Mitchell, D.C., and Bryan, B.A. (2014). A genomics approach to identify susceptibilities of breast cancer cells to "fever-range" hyperthermia. BMC Cancer *14*, 81.

Bananis, E., Nath, S., Gordon, K., Satir, P., Stockert, R.J., Murray, J.W., and Wolkoff, A.W. (2004). Microtubule-dependent movement of late endocytic vesicles in vitro: requirements for Dynein and Kinesin. Mol Biol Cell *15*, 3688-3697.

Bielli, A., Thörnqvist, P.-O., Hendrick, A.G., Finn, R., Fitzgerald, K., and McCaffrey, M.W. (2001). The Small GTPase Rab4A Interacts with the Central Region of Cytoplasmic Dynein Light Intermediate Chain-1. Biochemical and Biophysical Research Communications *281*, 1141-1153.

Burgess, S.A., Walker, M.L., Sakakibara, H., Knight, P.J., and Oiwa, K. (2003). Dynein structure and power stroke. Nature *421*, 715-718.

Burute, M., and Thery, M. (2012). Spatial segregation between cell-cell and cell-matrix adhesions. Curr Opin Cell Biol *24*, 628-636.

Carter, A.P., Cho, C., Jin, L., and Vale, R.D. (2011). Crystal structure of the dynein motor domain. Science *331*, 1159-1165.

Chen, C.P., Posy, S., Ben-Shaul, A., Shapiro, L., and Honig, B.H. (2005). Specificity of cell–cell adhesion by classical cadherins: Critical role for low-affinity dimerization through β-strand swapping. Proceedings of the National Academy of Sciences of the United States of America *102*, 8531-8536.

Choudhary, C., Olsen, J.V., Brandts, C., Cox, J., Reddy, P.N., Bohmer, F.D., Gerke, V., Schmidt-Arras, D.E., Berdel, W.E., Muller-Tidow, C*., et al.* (2009). Mislocalized activation of oncogenic RTKs switches downstream signaling outcomes. Mol Cell *36*, 326-339.

Chu, B., Soncin, F., Price, B.D., Stevenson, M.A., and Calderwood, S.K. (1996). Sequential Phosphorylation by Mitogen-activated Protein Kinase and Glycogen Synthase Kinase 3 Represses Transcriptional Activation by Heat Shock Factor-1. Journal of Biological Chemistry *271*, 30847-30857.

Cole, D.G., Diener, D.R., Himelblau, A.L., Beech, P.L., Fuster, J.C., and Rosenbaum, J.L. (1998). Chlamydomonas kinesin-II-dependent intraflagellar transport (IFT): IFT particles contain proteins required for ciliary assembly in Caenorhabditis elegans sensory neurons. J Cell Biol *141*, 993-1008.

Desai, R.A., Gao, L., Raghavan, S., Liu, W.F., and Chen, C.S. (2009). Cell polarity triggered by cell-cell adhesion via E-cadherin. J Cell Sci *122*, 905-911.

Dillman, J.F., 3rd, and Pfister, K.K. (1994). Differential phosphorylation in vivo of cytoplasmic dynein associated with anterogradely moving organelles. J Cell Biol *127*, 1671-1681.

Dujardin, D.L., Barnhart, L.E., Stehman, S.A., Gomes, E.R., Gundersen, G.G., and Vallee, R.B. (2003). A role for cytoplasmic dynein and LIS1 in directed cell movement. The Journal of Cell Biology *163*, 1205-1211.

Dupin, I., Camand, E., and Etienne-Manneville, S. (2009). Classical cadherins control nucleus and centrosome position and cell polarity. J Cell Biol *185*, 779-786.

Eng, C.H., Huckaba, T.M., and Gundersen, G.G. (2006). The Formin mDia Regulates GSK3beta through Novel PKCs to Promote Microtubule Stabilization but Not MTOC Reorientation in Migrating Fibroblasts. Mol Biol Cell *17*, 5004-5016.

Etienne-Manneville, S., and Hall, A. (2001). Integrin-mediated activation of Cdc42 controls cell polarity in migrating astrocytes through PKCzeta. Cell *106*, 489-498.

Etienne-Manneville, S., and Hall, A. (2003a). Cdc42 regulates GSK-3[beta] and adenomatous polyposis coli to control cell polarity. Nature *421*, 753-756.

Etienne-Manneville, S., and Hall, A. (2003b). Cell polarity: Par6, aPKC and cytoskeletal crosstalk. Curr Opin Cell Biol *15*, 67-72.

Geneste, O., Copeland, J.W., and Treisman, R. (2002). LIM kinase and Diaphanous cooperate to regulate serum response factor and actin dynamics. J Cell Biol *157*, 831-838.

Gill, S.R., Cleveland, D.W., and Schroer, T.A. (1994). Characterization of DLC-A and DLC-B, two families of cytoplasmic dynein light chain subunits. Mol Biol Cell *5*, 645-654.

Gomes, E.R., Jani, S., and Gundersen, G.G. (2005). Nuclear movement regulated by Cdc42, MRCK, myosin, and actin flow establishes MTOC polarization in migrating cells. Cell *121*, 451-463.

Grunwald, G.B., Pratt, R.S., and Lilien, J. (1982). Enzymic dissection of embryonic cell adhesive mechanisms. III. Immunological identification of a component of the calcium-dependent adhesive system of embryonic chick neural retina cells. J Cell Sci *55*, 69-83.

Guettouche, T., Boellmann, F., Lane, W., and Voellmy, R. (2005). Analysis of phosphorylation of human heat shock factor 1 in cells experiencing a stress. BMC Biochem *6*, 1-14.

Gumbiner, B.M. (1996). Cell adhesion: the molecular basis of tissue architecture and morphogenesis. Cell *84*, 345-357.

Halbleib, J.M., and Nelson, W.J. (2006). Cadherins in development: cell adhesion, sorting, and tissue morphogenesis. Genes & Development *20*, 3199-3214.

Hale, C.M., Chen, W.C., Khatau, S.B., Daniels, B.R., Lee, J.S., and Wirtz, D. (2011). SMRT analysis of MTOC and nuclear positioning reveals the role of EB1 and LIC1 in single-cell polarization. J Cell Sci *124*, 4267-4285.

Harvey, B.P., Banga, S.S., and Ozer, H.L. (2004). Regulation of the Multifunctional Ca2+/Calmodulin-dependent Protein Kinase II by the PP2C Phosphatase PPM1F in Fibroblasts. Journal of Biological Chemistry *279*, 24889-24898.

Hatta, K., and Takeichi, M. (1986). Expression of N-cadherin adhesion molecules associated with early morphogenetic events in chick development. Nature *320*, 447-449.

He, B., Meng, Y.-H., and Mivechi, N.F. (1998). Glycogen Synthase Kinase 3β and Extracellular Signal-Regulated Kinase Inactivate Heat Shock Transcription Factor 1 by Facilitating the Disappearance of Transcriptionally Active Granules after Heat Shock. Molecular and Cellular Biology *18*, 6624-6633.

Heinemeyer, T., Wingender, E., Reuter, I., Hermjakob, H., Kel, A.E., Kel, O.V., Ignatieva, E.V., Ananko, E.A., Podkolodnaya, O.A., Kolpakov, F.A.*, et al.* (1998). Databases on transcriptional regulation: TRANSFAC, TRRD and COMPEL. Nucleic Acids Res *26*, 362-367.

Hendricks, A.G., Lazarus, J.E., Perlson, E., Gardner, M.K., Odde, D.J., Goldman, Y.E., and Holzbaur, E.L. (2012). Dynein tethers and stabilizes dynamic microtubule plus ends. Curr Biol *22*, 632-637.

Hoeng, J.C., Dawson, S.C., House, S.A., Sagolla, M.S., Pham, J.K., Mancuso, J.J., Löwe, J., and Cande, W.Z. (2008). High-Resolution Crystal Structure and In Vivo Function of a Kinesin-2 Homologue in Giardia intestinalis. Molecular Biology of the Cell *19*, 3124-3137.

Holmberg, C.I., Hietakangas, V., Mikhailov, A., Rantanen, J.O., Kallio, M., Meinander, A., Hellman, J., Morrice, N., MacKintosh, C., Morimoto, R.I.*, et al.* (2001). Phosphorylation of serine 230 promotes inducible transcriptional activity of heat shock factor 1. The EMBO Journal *20*, 3800-3810.

Höök, P., and Vallee, R.B. (2006). The dynein family at a glance. Journal of Cell Science *119*, 4369-4371.

Horgan, C.P., Hanscom, S.R., Jolly, R.S., Futter, C.E., and McCaffrey, M.W. (2010). Rab11-FIP3 binds dynein light intermediate chain 2 and its overexpression fragments the Golgi complex. Biochemical and Biophysical Research Communications *394*, 387-392.

Hughes, S.M., Vaughan, K.T., Herskovits, J.S., and Vallee, R.B. (1995). Molecular analysis of a cytoplasmic dynein light intermediate chain reveals homology to a family of ATPases. J Cell Sci *108 (Pt 1)*, 17-24.

Huttlin, E.L., Jedrychowski, M.P., Elias, J.E., Goswami, T., Rad, R., Beausoleil, S.A., Villen, J., Haas, W., Sowa, M.E., and Gygi, S.P. (2010). A tissue-specific atlas of mouse protein phosphorylation and expression. Cell *143*, 1174-1189.

Iden, S., and Collard, J.G. (2008). Crosstalk between small GTPases and polarity proteins in cell polarization. Nat Rev Mol Cell Biol *9*, 846-859.

Imamura, T., Huang, J., Usui, I., Satoh, H., Bever, J., and Olefsky, J.M. (2003). Insulin-induced GLUT4 translocation involves protein kinase C-lambda-mediated functional coupling between Rab4 and the motor protein kinesin. Mol Cell Biol *23*, 4892-4900.

Joberty, G., Petersen, C., Gao, L., and Macara, I.G. (2000). The cell-polarity protein Par6 links Par3 and atypical protein kinase C to Cdc42. Nat Cell Biol *2*, 531-539.

Kardon, J.R., and Vale, R.D. (2009). Regulators of the cytoplasmic dynein motor. Nat Rev Mol Cell Biol *10*, 854-865.

Koh, C.G., Tan, E.J., Manser, E., and Lim, L. (2002). The p21-activated kinase PAK is negatively regulated by POPX1 and POPX2, a pair of serine/threonine phosphatases of the PP2C family. Curr Biol *12*, 317-321.

Laan, L., Pavin, N., Husson, J., Romet-Lemonne, G., van Duijn, M., López, Magdalena P., Vale, Ronald D., Jülicher, F., Reck-Peterson, Samara L., and Dogterom, M. (2012). Cortical Dynein Controls Microtubule Dynamics to Generate Pulling Forces that Position Microtubule Asters. Cell *148*, 502-514.

Legate, K.R., Wickstrom, S.A., and Fassler, R. (2009). Genetic and cell biological analysis of integrin outside-in signaling. Genes Dev *23*, 397-418.

Leung, T., Chen, X.Q., Tan, I., Manser, E., and Lim, L. (1998). Myotonic dystrophy kinase-related Cdc42-binding kinase acts as a Cdc42 effector in promoting cytoskeletal reorganization. Mol Cell Biol *18*, 130-140.

Levy, J.R., and Holzbaur, E.L.F. (2008). Dynein drives nuclear rotation during forward progression of motile fibroblasts. Journal of Cell Science *121*, 3187-3195.

Lupas, A., Van Dyke, M., and Stock, J. (1991). Predicting coiled coils from protein sequences. Science *252*, 1162-1164.

McCain, M.L., Lee, H., Aratyn-Schaus, Y., Kleber, A.G., and Parker, K.K. (2012). Cooperative coupling of cell-matrix and cell-cell adhesions in cardiac muscle. Proc Natl Acad Sci U S A *109*, 9881-9886.

Mikami, A., Tynan, S.H., Hama, T., Luby-Phelps, K., Saito, T., Crandall, J.E., Besharse, J.C., and Vallee, R.B. (2002). Molecular structure of cytoplasmic dynein 2 and its distribution in neuronal and ciliated cells. Journal of Cell Science *115*, 4801-4808.

Muresan, V., Abramson, T., Lyass, A., Winter, D., Porro, E., Hong, F., Chamberlin, N.L., and Schnapp, B.J. (1998). KIF3C and KIF3A form a novel neuronal heteromeric kinesin that associates with membrane vesicles. Mol Biol Cell *9*, 637-652.

Nishimura, T., Kato, K., Yamaguchi, T., Fukata, Y., Ohno, S., and Kaibuchi, K. (2004). Role of the PAR-3-KIF3 complex in the establishment of neuronal polarity. Nat Cell Biol *6*, 328-334.

Nose, A., Nagafuchi, A., and Takeichi, M. (1988). Expressed recombinant cadherins mediate cell sorting in model systems. Cell *54*, 993-1001.

Osmani, N., Peglion, F., Chavrier, P., and Etienne-Manneville, S. (2010). Cdc42 localization and cell polarity depend on membrane traffic. J Cell Biol *191*, 1261-1269.

Osmani, N., Vitale, N., Borg, J.P., and Etienne-Manneville, S. (2006). Scrib controls Cdc42 localization and activity to promote cell polarization during astrocyte migration. Curr Biol *16*, 2395-2405.

Ou, G., Blacque, O.E., Snow, J.J., Leroux, M.R., and Scholey, J.M. (2005). Functional coordination of intraflagellar transport motors. Nature *436*, 583-587.

Palazzo, A.F., Joseph, H.L., Chen, Y.J., Dujardin, D.L., Alberts, A.S., Pfister, K.K., Vallee, R.B., and Gundersen, G.G. (2001). Cdc42, dynein, and dynactin regulate MTOC reorientation independent of Rho-regulated microtubule stabilization. Curr Biol *11*, 1536-1541.

Palmer, K.J., Hughes, H., and Stephens, D.J. (2009). Specificity of Cytoplasmic Dynein Subunits in Discrete Membrane-trafficking Steps. Molecular Biology of the Cell *20*, 2885-2899.

Pandey, R., Mandal, A.K., Jha, V., and Mukerji, M. (2011). Heat shock factor binding in Alu repeats expands its involvement in stress through an antisense mechanism. Genome Biol *12*, R117.

Paschal, B.M., and Vallee, R.B. (1987). Retrograde transport by the microtubule-associated protein MAP 1C. Nature *330*, 181-183.

Patel, S.D., Ciatto, C., Chen, C.P., Bahna, F., Rajebhosale, M., Arkus, N., Schieren, I., Jessell, T.M., Honig, B., Price, S.R.*, et al.* (2006). Type II Cadherin Ectodomain Structures: Implications for Classical Cadherin Specificity. Cell *124*, 1255-1268.

Petit, V., and Thiery, J.P. (2000). Focal adhesions: structure and dynamics. Biol Cell *92*, 477-494.

Pfister, K.K., Shah, P.R., Hummerich, H., Russ, A., Cotton, J., Annuar, A.A., King, S.M., and Fisher, E.M. (2006). Genetic analysis of the cytoplasmic dynein subunit families. PLoS Genet *2*, e1.

Phang, H.-Q., Hoon, J.-L., Lai, S.K., Zeng, Y., Chiam, K.-H., Li, H.Y., and Koh, C.-G. (2014). POPX2 phosphatase regulates the KIF3 kinesin motor complex. Journal of Cell Science, 727-739.

Piwien-Pilipuk, G., MacDougald, O., and Schwartz, J. (2002). Dual regulation of phosphorylation and dephosphorylation of C/EBPbeta modulate its transcriptional activation and DNA binding in response to growth hormone. J Biol Chem *277*, 44557-44565.

Purohit, A., Tynan, S.H., Vallee, R., and Doxsey, S.J. (1999). Direct Interaction of Pericentrin with Cytoplasmic Dynein Light Intermediate Chain Contributes to Mitotic Spindle Organization. The Journal of Cell Biology *147*, 481-492.

Raftopoulou, M., and Hall, A. (2004). Cell migration: Rho GTPases lead the way. Dev Biol *265*, 23-32.

Rashid, D.J., Wedaman, K.P., and Scholey, J.M. (1995). Heterodimerization of the Two Motor Subunits of the Heterotrimeric Kinesin, KRP85/95. Journal of Molecular Biology *252*, 157-162.

Ridley, A.J., Schwartz, M.A., Burridge, K., Firtel, R.A., Ginsberg, M.H., Borisy, G., Parsons, J.T., and Horwitz, A.R. (2003). Cell migration: integrating signals from front to back. Science *302*, 1704-1709.

Schmoranzer, J., Fawcett, J.P., Segura, M., Tan, S., Vallee, R.B., Pawson, T., and Gundersen, G.G. (2009). Par3 and dynein associate to regulate local microtubule dynamics and centrosome orientation during migration. Curr Biol *19*, 1065-1074.

Scholey, J.M. (2013). Kinesin-2: a family of heterotrimeric and homodimeric motors with diverse intracellular transport functions. Annu Rev Cell Dev Biol *29*, 443-469.

Schonteich, E., Wilson, G.M., Burden, J., Hopkins, C.R., Anderson, K., Goldenring, J.R., and Prekeris, R. (2008). The Rip11/Rab11-FIP5 and kinesin II complex regulates endocytic protein recycling. J Cell Sci *121*, 3824-3833.

Setou, M., Nakagawa, T., Seog, D.H., and Hirokawa, N. (2000). Kinesin superfamily motor protein KIF17 and mLin-10 in NMDA receptor-containing vesicle transport. Science *288*, 1796-1802.

Shi, S.H., Cheng, T., Jan, L.Y., and Jan, Y.N. (2004). APC and GSK-3beta are involved in mPar3 targeting to the nascent axon and establishment of neuronal polarity. Curr Biol *14*, 2025-2032.

Singh, P., Gan, C.S., Guo, T., Phang, H.Q., Sze, S.K., and Koh, C.G. (2011). Investigation of POPX2 phosphatase functions by comparative phosphoproteomic analysis. Proteomics *11*, 2891-2900.

Smilenov, L.B., Mikhailov, A., Pelham, R.J., Marcantonio, E.E., and Gundersen, G.G. (1999). Focal adhesion motility revealed in stationary fibroblasts. Science *286*, 1172-1174.

Song, C., Wen, W., Rayala, S.K., Chen, M., Ma, J., Zhang, M., and Kumar, R. (2008). Serine 88 Phosphorylation of the 8-kDa Dynein Light Chain 1 Is a Molecular Switch for Its Dimerization Status and Functions. Journal of Biological Chemistry *283*, 4004-4013.

Sotiropoulos, A., Gineitis, D., Copeland, J., and Treisman, R. (1999). Signal-regulated activation of serum response factor is mediated by changes in actin dynamics. Cell *98*, 159-169.

Stauber, T., Simpson, J.C., Pepperkok, R., and Vernos, I. (2006). A role for kinesin-2 in COPI-dependent recycling between the ER and the Golgi complex. Curr Biol *16*, 2245-2251.

Susalka, S.J., and Pfister, K.K. (2000). Cytoplasmic dynein subunit heterogeneity: implications for axonal transport. Journal of Neurocytology *29*, 819-829.

Susila, A., Chan, H., Loh, A.X., Phang, H.Q., Wong, E.T., Tergaonkar, V., and Koh, C.G. (2010). The POPX2 phosphatase regulates cancer cell motility and invasiveness. Cell Cycle *9*, 179-187.

Takeda, S., Yamazaki, H., Seog, D.H., Kanai, Y., Terada, S., and Hirokawa, N. (2000). Kinesin superfamily protein 3 (KIF3) motor transports fodrin-associating vesicles important for neurite building. J Cell Biol *148*, 1255-1265.

Takeichi, M. (1991). Cadherin cell adhesion receptors as a morphogenetic regulator. Science *251*, 1451-1455.

Tamura, K., Shan, W.S., Hendrickson, W.A., Colman, D.R., and Shapiro, L. (1998). Structure-function analysis of cell adhesion by neural (N-) cadherin. Neuron *20*, 1153-1163.

Tang, Q.Q., Gronborg, M., Huang, H., Kim, J.W., Otto, T.C., Pandey, A., and Lane, M.D. (2005). Sequential phosphorylation of CCAAT enhancer-binding protein beta by MAPK and glycogen synthase kinase 3beta is required for adipogenesis. Proc Natl Acad Sci U S A *102*, 9766-9771.

Teng, J., Rai, T., Tanaka, Y., Takei, Y., Nakata, T., Hirasawa, M., Kulkarni, A.B., and Hirokawa, N. (2005). The KIF3 motor transports N-cadherin and organizes the developing neuroepithelium. Nat Cell Biol *7*, 474-482.

Tominaga, T., Sahai, E., Chardin, P., McCormick, F., Courtneidge, S.A., and Alberts, A.S. (2000). Diaphanous-related formins bridge Rho GTPase and Src tyrosine kinase signaling. Mol Cell *5*, 13-25.

Trokter, M., Mücke, N., and Surrey, T. (2012). Reconstitution of the human cytoplasmic dynein complex. Proceedings of the National Academy of Sciences *109*, 20895-20900.

Tweedie-Cullen, R.Y., Brunner, A.M., Grossmann, J., Mohanna, S., Sichau, D., Nanni, P., Panse, C., and Mansuy, I.M. (2012). Identification of Combinatorial Patterns of Post-Translational Modifications on Individual Histones in the Mouse Brain. PLoS ONE *7*, e36980.

Tynan, S.H., Gee, M.A., and Vallee, R.B. (2000a). Distinct but overlapping sites within the cytoplasmic dynein heavy chain for dimerization and for intermediate chain and light intermediate chain binding. J Biol Chem *275*, 32769-32774.

Tynan, S.H., Purohit, A., Doxsey, S.J., and Vallee, R.B. (2000b). Light Intermediate Chain 1 Defines a Functional Subfraction of Cytoplasmic Dynein Which Binds to Pericentrin. Journal of Biological Chemistry *275*, 32763-32768.

Tzima, E., Kiosses, W.B., del Pozo, M.A., and Schwartz, M.A. (2003). Localized cdc42 activation, detected using a novel assay, mediates microtubule organizing center positioning in endothelial cells in response to fluid shear stress. J Biol Chem *278*, 31020-31023.

Vallee, R.B., and Stehman, S.A. (2005). How dynein helps the cell find its center: a servomechanical model. Trends in Cell Biology *15*, 288-294.

Vasioukhin, V., Bauer, C., Yin, M., and Fuchs, E. (2000). Directed actin polymerization is the driving force for epithelial cell-cell adhesion. Cell *100*, 209-219.

Vaughan, P.S., Leszyk, J.D., and Vaughan, K.T. (2001). Cytoplasmic Dynein Intermediate Chain Phosphorylation Regulates Binding to Dynactin. Journal of Biological Chemistry *276*, 26171-26179.

Wang, N., and Suo, Z. (2005). Long-distance propagation of forces in a cell. Biochem Biophys Res Commun *328*, 1133-1138.

Watanabe, N., Madaule, P., Reid, T., Ishizaki, T., Watanabe, G., Kakizuka, A., Saito, Y., Nakao, K., Jockusch, B.M., and Narumiya, S. (1997). p140mDia, a mammalian homolog of Drosophila diaphanous, is a target protein for Rho small GTPase and is a ligand for profilin. EMBO J *16*, 3044-3056.

Wedaman, K.P., Meyer, D.W., Rashid, D.J., Cole, D.G., and Scholey, J.M. (1996). Sequence and submolecular localization of the 115-kD accessory subunit of the heterotrimeric kinesin-II (KRP85/95) complex. J Cell Biol *132*, 371-380.

Wen, Y., Eng, C.H., Schmoranzer, J., Cabrera-Poch, N., Morris, E.J., Chen, M., Wallar, B.J., Alberts, A.S., and Gundersen, G.G. (2004). EB1 and APC bind to mDia to stabilize microtubules downstream of Rho and promote cell migration. Nat Cell Biol *6*, 820-830.

Whyte, J., Bader, J.R., Tauhata, S.B., Raycroft, M., Hornick, J., Pfister, K.K., Lane, W.S., Chan, G.K., Hinchcliffe, E.H., Vaughan, P.S.*, et al.* (2008). Phosphorylation regulates targeting of cytoplasmic dynein to kinetochores during mitosis. J Cell Biol *183*, 819-834.

Wong, Y.H., Lee, T.Y., Liang, H.K., Huang, C.M., Wang, T.Y., Yang, Y.H., Chu, C.H., Huang, H.D., Ko, M.T., and Hwang, J.K. (2007). KinasePhos 2.0: a web server for identifying protein kinase-specific phosphorylation sites based on sequences and coupling patterns. Nucleic Acids Res *35*, W588-594.

Xie, Y., Tan, E.J., Wee, S., Manser, E., Lim, L., and Koh, C.G. (2008). Functional interactions between phosphatase POPX2 and mDia modulate RhoA pathways. J Cell Sci *121*, 514-521.

Yamanaka, T., Horikoshi, Y., Suzuki, A., Sugiyama, Y., Kitamura, K., Maniwa, R., Nagai, Y., Yamashita, A., Hirose, T., Ishikawa, H.*, et al.* (2001). PAR-6 regulates aPKC activity in a novel way and mediates cell-cell contact-induced formation of the epithelial junctional complex. Genes Cells *6*, 721-731.

Yamazaki, H., Nakata, T., Okada, Y., and Hirokawa, N. (1995). KIF3A/B: a heterodimeric kinesin superfamily protein that works as a microtubule plus end-directed motor for membrane organelle transport. J Cell Biol *130*, 1387-1399.

Yap, A.S., Brieher, W.M., and Gumbiner, B.M. (1997). Molecular and functional analysis of cadherin-based adherens junctions. Annu Rev Cell Dev Biol *13*, 119-146.

Zaidel-Bar, R., Cohen, M., Addadi, L., and Geiger, B. (2004). Hierarchical assembly of cell-matrix adhesion complexes. Biochem Soc Trans *32*, 416-420.

Zhang, S., Guo, T., Chan, H., Sze, S.K., and Koh, C.G. (2013). Integrative transcriptome and proteome study to identify the signaling network regulated by POPX2 phosphatase. J Proteome Res *12*, 2525-2536.

7. Appendix

A. TFSEARCH results for prediction of transcription factors binding to dync1li2 promoter

```
** TFSEARCH  ver.1.3 **         (c)1995 Yutaka Akiyama (Kyoto Univ.)

 This simple routine searches highly correlated sequence fragments
 versus TFMATRIX transcription factor binding site profile database
 by E.Wingender, R.Knueppel, P.Dietze, H.Karas (GBF-Braunschweig).

  <Warning> Scoring scheme is so straightforward in this version.
            score = 100.0 * ('weighted sum' - min) / (max - min)
            The score does not properly reflect statistical significance!

 Database:  TRANSFAC MATRIX TABLE, Rel.3.3 06-01-1998
 Query:     untitled (520 bases)
 Taxonomy:  ALL
 Threshold: 85.0 point


 TFMATRIX entries with High-scoring:

   1 ENSMTSGNCG CACACAGGGT CTCACTATGT AGCCCTGGCT ACCCTCGAAC entry        score
                            ------->                      M00253 cap    87.9
                                                   ----> M00029 HSF    87.4

  51 TTGCTATGTA GACCAGGATG GCTTCAAATG TATAGAGTTC CTCCCGCCTC entry        score
                   ---------->                            M00076 GATA-2 90.9
                                          <-----          M00029 HSF    90.9
                   ---------->                            M00075 GATA-1 90.2
                                             <------      M00048 ADR1   86.2

 101 TGCCTCCTGA ATGCTGGGAT TAAAGGCGTG TGACACCATG TGCAACCATT entry        score
                     -------->                            M00140 Bcd    100.0
                                                        - M00019 Dfd    91.0
                                <--------                 M00253 cap    88.8
       <-----                                           M00048 ADR1   87.7
                  ----------------->                    M00019 Dfd    86.9
                                               ---------- M00059 YY1    86.5
                                          -------->       M00217 USF    86.5

 151 TTAAAATTAA TTTTTTTGAA GTAGGCTCTC ACATAGCTCA TGCTCAACTT entry        score
      <----------------                                   M00019 Dfd    92.0
     ---------------->                                   M00019 Dfd    91.0
         <-------                                        M00101 CdxA   90.0
          ------->                                       M00101 CdxA   90.0
     ------>                                             M00059 YY1    86.5
              <----------                                M00022 Hb     85.7
        <----------------                                M00099 S8     85.5

 201 AAACTTACCA AGTAGTCTAA GACTTCTGAT CCCTCCCCCT CCCCCCCTCC entry        score
                                                    <-- M00008 Sp1    95.9
                            <----                       M00028 HSF    95.3
                                              <-------- M00083 MZF1   94.8
                                        <-----          M00048 ADR1   93.8
                                                 <-----  M00048 ADR1   93.8
                            <----                       M00029 HSF    93.7
                                                  <-- M00083 MZF1   93.0
                                               <-----    M00048 ADR1   92.3
                                                <-----   M00048 ADR1   92.3
```

```
                                                  <-- M00048 ADR1   92.3
                                        <-------------      M00084 MZF1   91.9
                                                     <---  M00196 Sp1    91.8
                                                    <----  M00255 GC box 89.4
     <-------------                                       M00159 C/EBP  89.2
                                         <--------          M00083 MZF1   88.7
                           <-------                        M00253 cap    87.8
                                         <-----             M00048 ADR1   87.7
                                               <------      M00048 ADR1   87.7
                                         <-------------     M00196 Sp1    86.2
                                       <-----               M00048 ADR1   86.2
                                            <------         M00048 ADR1   86.2
                                                    <----  M00048 ADR1   86.2
                                          <--------         M00154 STRE   85.8
                                                   <-------  M00154 STRE   85.8
    ------>                                               M00148 SRY    85.5

251 CCGCCCCCAC CAGCTGCCCA TTGCTGGTAT GACAGGACAT GCAAATATCT entry        score
                                                    -----  M00142 NIT2   100.0
       <-----                                             M00048 ADR1   98.5
    -------                                               M00008 Sp1    95.9
            <----------                                   M00175 AP-4   95.8
            ---------->                                   M00184 MyoD   93.6
    -----                                                 M00083 MZF1   93.0
    ---                                                   M00048 ADR1   92.3
            <----------                                   M00176 AP-4   91.9
    ---------                                             M00196 Sp1    91.8
    ---------                                             M00255 GC box 89.4
      <-----                                              M00048 ADR1   89.2
                                          ---------------> M00195 Oct-1  88.4
           <------------                                  M00001 MyoD   88.4
                                 <----------              M00031 MATalp 87.3
    -                                                     M00048 ADR1   86.2
                                       <--------------    M00162 Oct-1  85.7
                             <--------                    M00253 cap    85.5
            <----------                                   M00184 MyoD   85.1

301 ATGTCCAGTC ATTTTTTTGT GGATCTTCGT TCATGTTTGG CCCATTTTCT entry        score
    >                                                     M00142 NIT2   100.0
                                                    <---- M00028 HSF    100.0
                                                    <---- M00029 HSF    96.0
                 <----------                              M00022 Hb     92.9
            -------->                                     M00253 cap    92.4
                                                    <---- M00148 SRY    90.0
        -------->                                         M00253 cap    86.7
                <----------                               M00022 Hb     86.6
                             <----                        M00028 HSF    86.5
                                 <-----                   M00029 HSF    86.3
                                          -------->       M00050 E2F    86.2
                                                    <-    M00216 TATA   85.6
             <-------                                     M00101 CdxA   85.0

351 TTTAAACTTC TGAGCTGTAG TTTCCTCACC TCACTTATTA AGAATTAAAC entry        score
                                                 ---->    M00029 HSF    95.4
          <-----                                         M00028 HSF    95.3
                                                 ---->    M00028 HSF    94.3
          <-----                                         M00029 HSF    93.7
                    <-------                             M00148 SRY    90.9
                                                  ----   M00148 SRY    90.9
                              ----------->               M00073 deltaE 90.5
    --                                                  M00148 SRY    90.0
                                <------                 M00271 AML-1a 88.7
                                     <------            M00240 Nkx-2. 88.4
                                      <----------       M00145 Brn-2  88.1
                                         <-------       M00101 CdxA   87.9
         <--------                                      M00253 cap    87.8
                                    ------->            M00253 cap    87.4
                          <----                         M00029 HSF    86.9
```

```
                                      <--------------    M00149 SBF-1  86.8
                          <----                          M00028 HSF    85.9
    --------                                             M00216 TATA   85.6
                                                <------- M00129 HFH-1  85.4
                                       <--------         M00241 Nkx-2. 85.3
                                    <-------------       M00137 Oct-1  85.1
                                         ------->        M00101 CdxA   85.0

401 AAGATTCAAT GAGATCGCTT TATAAATATG GTTGTCTAGC TTGAGTTCAT entry        score
                          <------                        M00101 CdxA   100.0
                          <------                        M00100 CdxA   96.2
                       ------->                          M00100 CdxA   92.3
    -->                                                  M00148 SRY    90.9
                                                   ---- M00253 cap    90.5
                       ------->                          M00101 CdxA   87.9
                            ------>                      M00101 CdxA   87.1
                                                 <----   M00029 HSF    86.3
                                                     <-  M00029 HSF    86.3
              ---------->                                M00076 GATA-2 85.8
                          --------------->               M00268 XFD-2  85.7
                           <-------------------          M00059 YY1    85.7
    ----                                                 M00129 HFH-1  85.4
                              ------>                    M00101 CdxA   85.0

451 TCCAAAGCTT GGACTTGCCG CATCAGAGGC TGCCCTGCAG GGGTCGCCAG entry        score
                                             ------>     M00048 ADR1   95.4
    --->                                                 M00253 cap    90.5
                                <--------                M00253 cap    89.9
                       <----------                       M00075 GATA-1 88.2
                                          --------->     M00111 CF1 /  86.8
    ---                                                  M00029 HSF    86.3
                                       -------->         M00154 STRE   85.8
                                ------->                 M00253 cap    85.4

501 CGCGCTCTCG GTCTGGTGGC                                entry        score


Total 105 high-scoring sites found.
Max score: 100.0 point, Min score: 85.0 point
```

8. Author's publications

Hoon, J.L., Wong, W.K., and Koh, C.G. (2012). Functions and regulation of circular dorsal ruffles. Mol Cell Biol 32, 4246-4257.

Phang, H.-Q.*, Hoon, J.-L.*, Lai, S.K.*, Zeng, Y., Chiam, K.-H., Li, H.Y., and Koh, C.-G. (2014). POPX2 phosphatase regulates the KIF3 kinesin motor complex. Journal of Cell Science 127, 727-739. *Joint first author.

Hoon, J. L., H. Y. Li, et al. (2014). "POPX2 phosphatase regulates cell polarity and centrosome placement." Cell Cycle 13(15): 2459-2468.

9. Posters

Title: POPX2 Phosphatase Regulates the KIF3 Kinesin Motor Complex

Conference: Annual meeting of the American Society for Cell Biology, New Orleans, USA (2013)